Erich Sackmann: Lecture Notes on Biological Physics

Physics of cell adhesion

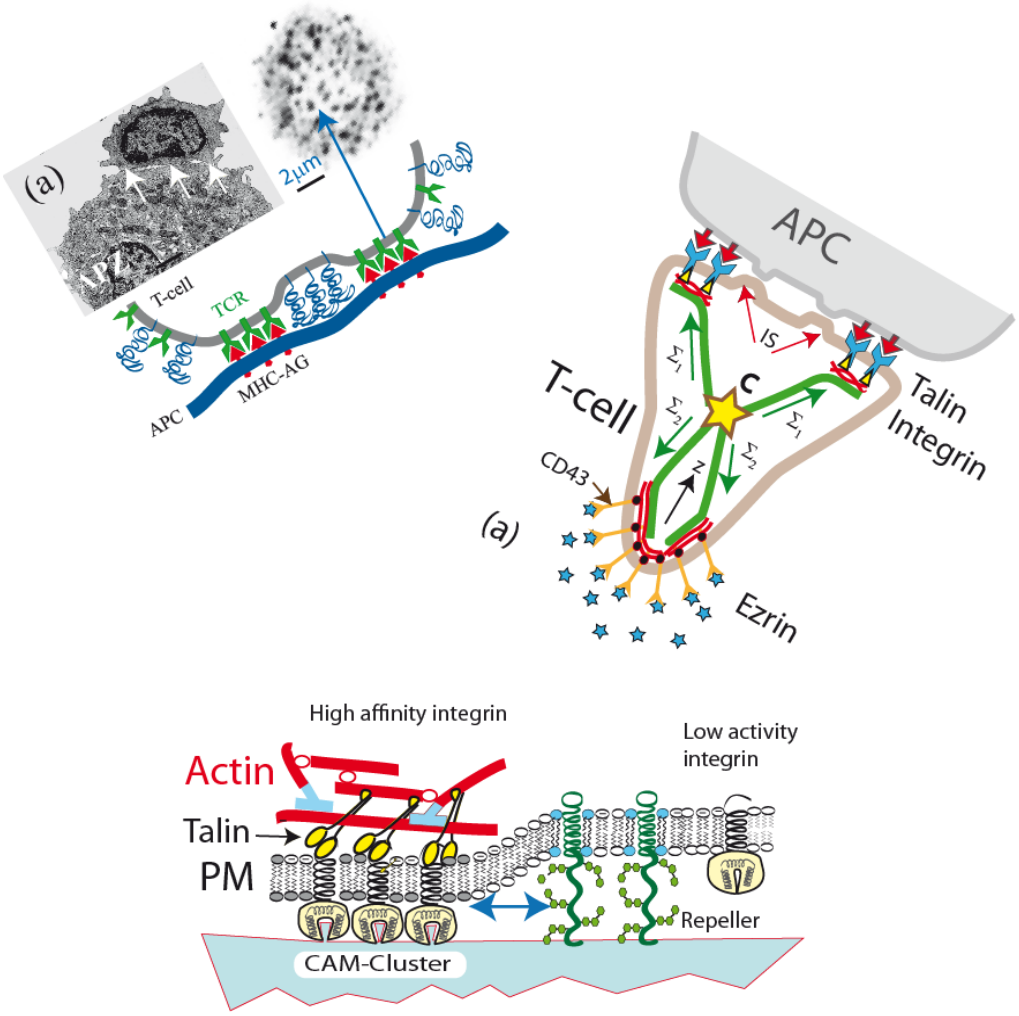

Accessible via www.biophy.de.

 E-Mail: sackmann@ph.tum.de

Physics of cell adhesion:

Erich Sackmann Physics Department E22 Technical University Munich* and Lehrstuhl Applied Physics, Sektion Physik LMU Munich.˙ E-mail: sackmann@ph.tum.de

Part I: What biomimetic systems can teach us

Abbreviations Definitions ENC endothelium cells; EM: Extracellular Matrix; HA: hyaluronic acid; APC: antigen presenting cells; DC: dendritic cells ; Eph-X: ephrin signal molecule of type X; Ephr-X ephrin receptor of type X; MT microtubuli; MHC: Major histocompatibility complex
PIP2: phosphoiniositol (3,4) diphosphate ; PIP3: phosphoiniositol (3,4,5) diphosphate
RGD-sequence: linear or cyclic peptides containing the amino acids sequence arginine-glycine-aspartic acid; RTK receptor tyrosin kinase; TCR T-cell receptor; VEGF: vascular endithelial growth factor; ZAP-70 (synonym for zeta-chain-associated protein)

Abstract Part I

Cell adhesion is a paradigm of the ubiquitous interplay of cell signalling, modulation of material properties and biological functions of cells. It is controlled by competition of short range attractive forces, medium range repellant forces and the elastic stresses associated with local and global deformation of the composite cell envelopes.

In the first part we review basic physical rules governing the physics of cell adhesion learned from studying biomimetic systems. Adhesion induced micro-domains couple to the intracellular actin and microtubule networks allowing cells to generate strong forces with a minimum of attractive CAMs and to manipulate other cells through filopodia over mμ distances. The adhesion strength can be adapted to external force fluctuations within seconds by varying the density of attractive and repellant CAMs through exocytosis and endocytosis or protease-mediated dismantling of the CAM-cytoskeleton link. Adhesion domains form local end global biochemical reaction centres enabling the control of enzymes. Actin-microtubule crosstalk at adhesion foci serve the mechanical stabilization of polarized cell shapes. Axon growth in tissue is guided by attractive and repulsive cues controlled by antagonistic signalling pathways. In the last subsection we present a model of adhesion mediated formation of myelin sheaths wrapped around the axon cables by suppression of electrostatic forces. This example shows how nature managed to minimize the electrical loss in axon cables by choosing the right lipid and protein composition

I. Introduction

Cell adhesion plays a vital role for the live of all animals and plants during all stages of their lives. It saves our life when macrophages catch and engulf dangerous bacteria or when cytotoxic lymphocytes destroy cells infected by pathogens (viruses and bacteria). Cell-cell and cell-tissue recognition guides the formation of neural networks and the contact between nerve cells and muscles. Cell adhesion is one of the most challenging questions of life science which involves rich, albeit complex physics. Studying the basic processes of adhesion is an essential step towards our understanding how basic physical concepts guide the self-assembly and function of living matter aspects,

The specificity of cell-cell recognition was impressively demonstrated by experiments with cells of embryos at their early stage of development. If cells of different organs such as the epithelial cells of the outer shell (the ectoderm) and of inner organs (the mesoderm) are homogeneously mixed they reorganize after several hours in such a way that the cells from the ectoderm form an envelope that encloses organ-like assemblies of cells from the mesoderm. [Hofstetter 1995]. We now know that this specificity of cell adhesion is mediated by cell surface proteins, in the following called cell adhesion molecules (CAM's), co-receptors or linkers[1]. The strength of cell adhesion can be roughly quantified in terms of the surfaces tension (Σ) of clusters of cells, which is a measure of the resulting force (per unit area) acting on each cell on the surface [Fotya and Steinberg 2005]. Mixtures of different epithelial cells self-assemble into circular discs, whereby the cells with the lowest surface tension Σ are surrounded by the population with the higher values. This so called principle of differential adhesion hypothesis implies that the cells can be considered as liquid droplets hold together by cohesion forces. Since the cells envelopes are fluid the surface tension is isotropic and it does not matter whether the interaction CAM-CAM-links between the cells are distributed homogeneously or whether they form adhesion microdomains, which is generally the case as we will see below.

Astonishingly, it turned out that the enormous manifold of adhesion processes of eukaryotes is controlled by a few super-families of CAM's. In the resting state of cells only a few 10,000 species of each family are exposed on the surface, while the density of specific CAMs can be drastically increase by external signals (such as cytokines) within the time scales of seconds (see Sub-Chapter on VII. 3). Most CAMs penetrate the cell envelope and mechanically couple with their intracellular domains to the actin cortex and biochemically to intracellular cell signaling and genetic transcription processes. In this way cells can control their adhesion strength by restructuring the actin cortex and the associated MT network as well as by increasing the surface density of specific CAMs. The dissociation constants of CAM-CAM pairs are typically of the order of $K_a \sim 10^{-6}$-$10^{-5}\,M^{-1}$ (1.3 µM for cadherin-cadherin dimers in the presence of Ca^{++}) and are orders of magnitude larger than the characteristic values for hormone-receptor binding ($K_a \sim 10^{-10}\,M^{-1}$ for Insulin). Thus, other factors have to come into play to explain the high degree of selectivity of cell adhesion.

The main purpose of Part I of this review is to show that model membrane studies can provide detailed insight into the physical basis of cell adhesion. First, they teach us how to

[1] Repeller molecules: In the present nomenclature repellers or repellant CAMs are cell surface proteins with long extracellular tails or high negative charges which generate generic repulsion forces and impede short range attractions.

quantify adhesion processes by measuring free adhesion energies ΔG_{ad}.. Second, they show that adhesion domain formation is an inevitable consequence of the interplay of short range attraction forces between CAM-CAM pairs, long range repulsion forces mediated by repeller molecules of the glycocalix and elastic stresses of the lipid protein bilayer (Chapter V). Third, comparative studies of model systems and cells provide insight into the control of cell adhesion by coupling of the actin cortex to the adhesion domains. A second purpose is to show that adhesion domains play a central role for the self-assembly of local and global reaction spaces within membranes exerting specific functions. The adhesion domain formation offers many advantages. First, strong (nano-Newton) forces between moving cells and substrates can be established by commitment of small numbers (typically 10 000) of receptors. Second, the adhesion strength can be rapidly adapted in several ways: (i) by varying the repeller or receptor densities on the cell surface through exocytosis or endocytosis; (ii) by modifying the ligand density of tissue surfaces through removal of ligands (via proteases) or by blocking the binding sites of CAMs through antagonists (see Chapter VI.2); (iii) by decoupling of the actin gel patches from the adhesion domains (see [Simson 1998]).

The most intriguing consequence of adhesion domain formation is the generation of local reaction spaces which can regulate biochemical reactions by controlling the accessibility of inhibitors or activators. Paradigms of such reaction platfoms are the immunological synapses (see Chapter VII). By large scale lateral segregation of CAMs and repellers, mediated by actin-microtubule crosstalk, cells can polarize and exert completely different functions at the front and at rear (Chapter VII.2 and VII.4).

The lecture note is organized as follows: In the first part we describe the biomimetic system and the micro-interferometric method (RICM) which allows us to visualize the adhesion zone between the two surfaces with nm spatial and msec temporal resolution. We then summarize the thermo-mechanical theories of cell adhesion and show that the adhesion strength and the kinetics of adhesion can be evaluated in two ways: first by analyzing the contour of the adhering shell close to the surface in terms of the elastic boundary conditions [Bruinsma et al.2000], [Guttenberg et al 2001] and second by considering the detailed balance between the global deformation of the shell, the gain in adhesion energy and the translational entropy of the of mobile CAMs and repellers [Smith and Seifert 2005], [Smith and Sackmann 2008)]. We next show a fundamental difference between cell-cell adhesion with mobile CAMs on both membranes and cell-tissue adhesion with one linker on the tissue immobilized.

After the introduction of the physical concepts of cell adhesion revealed by the model membrane studies we present two paradigms of cell adhesion: first, the immunological synapses showing the role played by adhesion domains as local and global reaction spaces (platforms) and second, the penetration of lymphocytes through endothelial cell layers by sub-second switching of strong adhesion and adhesion mediated cell polarization. In the last three chapters of Part I we show that the lessons learned from model membrane studies allow us to understand the guidance of growing axons in tissues. In Chapter VIII we show how nature utilized the physics of adhesion to wrap myelin sheath around axons and thus minimizes the electrical losses during action potential propagation by choosing the specific lipid composition.

In Part II we deal with the regulation of cell adhesion by glycoproteins of the glycocalix; a control mechanism which is often underestimated. We first discuss a general mechanism of cell proliferation by adhesion induced clustering of integrins through cell tissue-adhesion mediated by cell surface proteoglycans and by coupling of the attractive and repellant CAMs to actin gel patches. We then discuss the control of cell proliferation by lateral coupling of the multifunctional hyaluronic acid receptor CD44 and growth factor receptors through linkage to the actin cortex by merlin-ezrin complexes. We first describe the down-regulation of cell proliferation by merlin mediated uncoupling of the CD44 actin linkage by phophorylation switches. Finally we show that the growth factor mediated cell proliferation may be impeded by dense layers of hyaluronic acid which may thus provide a mechanism of growth inhibition by lateral inhibition. In the last section we develop some ideas of cancer generation by dysfunctions of cell adhesion or complex formation between CD44 and growth factor receptors.

II. Biomimetic Models of cell adhesion.

Insight into the physical basis of cell adhesion is gained by studying model systems containing the essential ingredients involved [Sackmann 1996], [Sackmann and Tnaka 2000/2005]. Giant vesicles doped with CAMs or ligands of the extracellular matrix (EM) serve as test cells, while solid supported membranes with reconstituted co-receptors (or polymer cushion exposing ligands of the EM) act as target cells (or tissue). To mimic the role of the glycocalix, one of the membranes is doped with lipids exposing polymer head groups which serve as repeller molecules. To mimic the softness of tissue and to avoid artifacts typically caused by solid surfaces (such as the generation of defects and pores in the supported membrane or the denaturing of membrane proteins), the membranes are separated from the solid by ultrathin polymer cushions. Polymer cushions have been designed by surface grafting of hyaluronic acid films or rod-like cellulose molecules exposing (hydrophobic or hydrophilic) flexible segments, called hairy rods (see Figure). Another strategy is to separate the membranes from the solid by hydrophilic polymer head groups attached to lipids, called tethered membranes [Sackmann and Tanaka 2005].

An example of a biomimetic cell-cell adhesion system is shown in Figure 1. In this case the vesicles are doped with lipids exposing arginine-glycine-aspartic acid (RGD) peptide sequences which bind specifically to integrins of the $\alpha IIb3$-family [Hu et al. 2000].These receptors are reconstituted into the supported membranes. Due to the separation of the membrane from the solid by the polymer cushion both linkers are mobile, mimicking the situation of cell-cell adhesion.

.

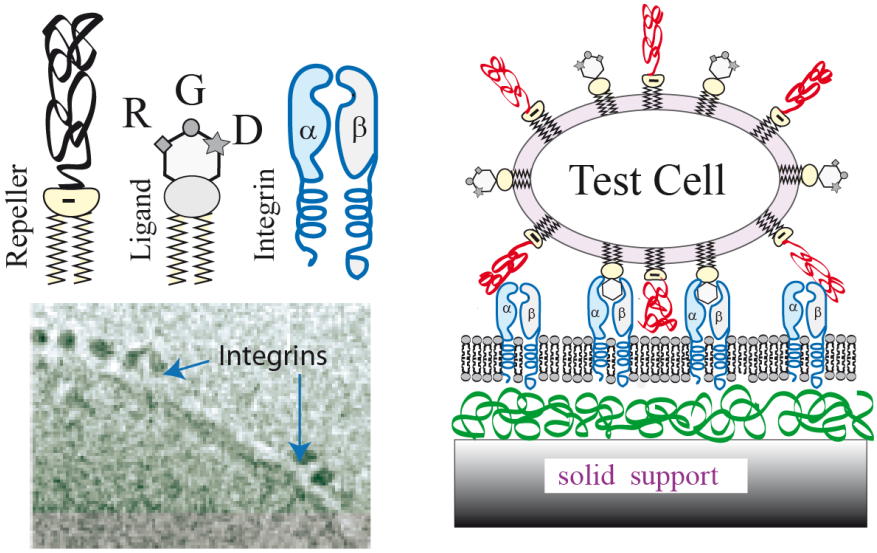

Figure 1 *Model system mimicking cell-cell adhesion containing major ingredients that control the primary process of cell adhesion (prior to coupling of the intracellular receptor domains to the actin cortex). The target cell is generated by fusion of vesicles (harboring reconstituted integrins) on polymer cushions composed of hairy rods, (see [Sackmann and Tanaka 2000]).The cyclic peptides exposing RGD sequences recognize the integrin αIIβ3 more specifically then linear RGD peptides. The EM image of the reconstituted integrins, shown at the bottom left, is reproduced from reference [Hu et al 2000].*

Using supported membranes as test cells or tissue has several advantages. First: by application of micro-interferometry (RICM, see Figure 3), the contour of adhering soft shells close to the surface can be reconstructed with 10 nm height and lateral resolution and with msec time resolution. Second, as shown in figure 2, the position of randomly formed adhesion domains within the adhesion zone can be visualized by application of lift forces. Third, by analyzing the contour of the shells near the solid surface as function of external forces (lift forces or hydrodynamic shear forces) the essential physical parameters can be measured. Observables include: the membrane bending modulus κ, the lateral tensions σ, the work of adhesion ΔG (see Figure 4 below and [Simon 1998]).

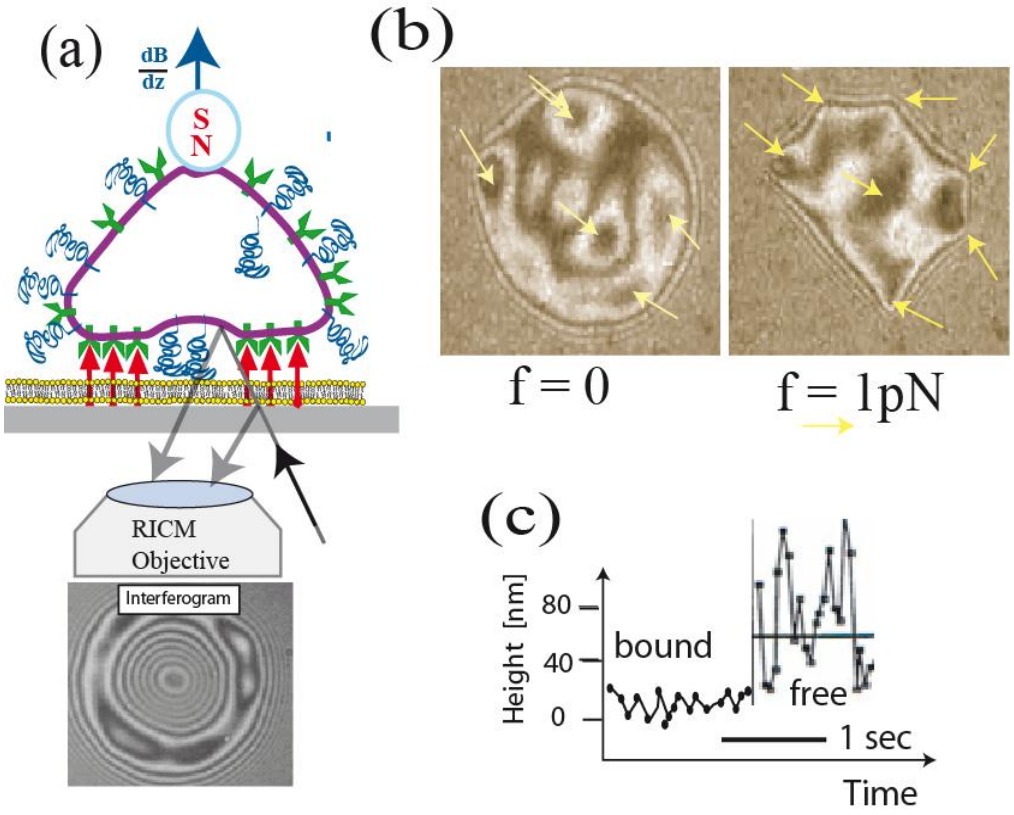

Figure 2*(a) Schematic view of RICM interferogram formation by interference of light reflected from the cell and the substrate surface. Lift forces are applied by magnetic tweezers using super- paramagnetic beads. Forces are generated by inhomogeneous magnetic fields (dB/dz) .*

(b) Interferogram of test cell adhering on immobilized integrin receptors, observed by RICM before (left) and during (right) application of a lift force of 1 pN. Some early visible adhesion domains are indicated by arrow. They are revealed by the formation of dark patches in the absence or by the formation of sharp edges at the contact line L in the presence of lift forces. (c) Direct visualization of transition of membrane from bound to free state, triggered by blocking the CAM binding pocket by incubation with antibodies (reproduced from Barbara Feneberg PHD Thesis TUM 2003).

III. Theory of Soft Shell Adhesion: The Global Adhesion Model

Introductory remarks: The rigorous elasticity theory of elastic shells is very complex and generally described by the non-linear Föppl von Karman theory (see §11 in [Landau /Lifshitz 1978). Fortunately, the adhesion-induced elastic deformation of vesicles and most cells (such as hematopoietic cells), can be described by the simple bending elasticity theory of soft shells [Helfrich 1978], [Lipowsky and Seifert, 1995], [Seifert 1997], [Smith and Seifert 2005]). This model can also be applied to analyse the adhesion of cells with homogeneous soft shells, such as amoeboid Dictyostelia cells [Simson 1998] and macrophages since these cells form small

and short lived adhesion domains but no large stress fibres, even on functionalized solid surfaces [Zidovska 2006], [Pixley 2012].

Fortunately it is frequently possible to evaluate the adhesion strength of vesicles and composite cell envelopes in terms of the elastic theory of shells by considering the elastic deformation close to the surface, while neglecting the global bending deformation of the shell (see [Guttenberg et al 2001] and Appendix B). The situation is much more complex for fibroblasts or nerve cells adhering on solid supports which tend to form large focal contacts connected by stress fibres. In this case more rigorous theories developed by the group of Samuel Safran have to be applied [Zemel et al 2011].

The elastic models neglect a very important aspect of cell adhesion, namely the control of the state and the free energy of adhesion by the lateral osmotic pressure exerted by the receptors and repellers outside of the adhesion zone. This entropic control mechanism can be considered separately as in the heterogeneous wetting model [Bruinsma et al 2000]. However the model cannot account rigorously for the non-equilibrium situation of adhering shells subjected to external lift forces. For this purpose a more general theory has been proposed by Smith and Seifert [Smith and Seifert 2005] [Smith and Sackmann 2009] which accounts simultaneously for the global elastic deformation of the shell and the balance between the gain in binding energy due to the formation of CAM-CAM pairs and the loss of entropic free energy associated with the linker immobilisation.

In the following we consider first the free elastic energy of an adhering soft shell forming a homogeneous contact zone and derive some pertinent physical laws of cell adhesion. In particular we first show how free energies of adhesion and elastic parameters of cells can be measured by the analysing the contour of the adhering shells close to the surface in terms of the balance of elastic boundary forces. We then consider the modulation of the adhesion strength by the lateral osmotic pressure.

The elastic energy functional: The elastic free energy can be expressed as [Lipowsky and Seifert 1995], [Seifert 1997]

$$\Delta G_{adh} = wA_c + \Delta G_{grav} + \frac{1}{2}\kappa \iint_A dO[\Delta h(x,y)]^2 + \frac{1}{2}\sigma \iint_A dO[\nabla h(x,y)]^2 + \frac{1}{2}\iint_O dOV''(h-h_0)^2 \quad (1)$$

The first term accounts for the free energy gain by the specific adhesion and holds for a homogeneous adhesion zone of area A_c with random distribution of CAM-CAM pairs, where w is the specific binding energy per unit area mediated by the CAM-CAM bonds. ΔG_{grav} is the gravitational energy which is considered in [Guttenberg et al 2001]. The third term stands for the bending deformation, the fourth for the membrane tension. The last term accounts for the generic interfacial potential V ($h-h_0$). It is generally approximated by a harmonic potential according to

$$V(h-h_0) = V_o + \frac{1}{2}\frac{\partial^2 V}{\partial h^2}(h-h_0)^2 = V_0 + \frac{1}{2}V''(h-h_0)^2 \quad (2)$$

V'' is the curvature of the potential, measured in units of J/m^4 . With this approximation, the free energy of adhesion is determined by four, a priori unknown, parameters w, κ, σ, V'' which can be determined experimentally as follows. The bending modulus κ is a material constant of the membrane which can be determined in separate micromechanical experiments,

both for vesicles (see [Haeckl 1997] and for cells [Simson 1998]). The bending modulus of soft shells can be related to the usual elastic material parameters: the Young modulus E and the Poisson ratio ν by $\kappa = \mathrm{E}d_m^3/\{12\pi(1-\nu^2)\}$, where d_m is the thickness of the shell. κ and the area compression modulus K are interrelated according to $\kappa d_m^{\ 2} \approx K$.

The strength of the harmonic potential V'' can be related to experimental observables by noticing that the general free energy functional implies two important length scales: the capillary length λ and the persistence length ζ_ρ given by

$$\lambda = \sqrt{\kappa/\sigma} \qquad \text{and} \qquad \zeta_p = \sqrt[4]{\kappa/V''} \quad (3)$$

The capillary length λ is a measure for the distance (in the radial direction) over which the contour of the shell near the surface is dominated by membrane tension, allowing us to define a contact angle θ_c (see Figure 3 below). $2\zeta_p$ is a measure for the lateral extension of a bending deformation evoked by a local point like force. Both lengths can be measured with high accuracy by analyzing the contour of the adhering shell enabling the determination of the curvature V'' of the harmonic potential (see Figure 7 in [Albersdörfer et al 1997]). For fluid vesicles, the capillary length is of the order of $\lambda \approx 1\mu m$, the persistence length is $\zeta_p \approx 50nm$ and the curvature of the potential $V'' \approx (10^{12} - 10^{14})\, Jm^{-4}$.

Measurement of Adhesion Strength by Interferometric Contour Analysis:

The contour of adhering soft shells close to the contact line exhibits the general shape shown in Figure 3a. The membrane is slightly bent at the contact line, characterized by a contact curvature . It goes smoothly over into a linear region, before it is deflected upwards. The contour is thus completely defined by a contact curvature R_c and a contact angle θ_c. The linear regime and the curved regimes are determined by the balance of surface tensions and bending moments at the contact line, respectively. For fluid membranes the balance of tensions is determined by the well-known Young's law (Eq. 4a), which relates the contact angle θ_c to the work of adhesion W. The balance of bending moments yields a relationship between contact curvature R_c and W (for a justification of these relationships see [Albersdörfer) 1997]).

$$W = \sigma(1-\cos\theta_c) \qquad (4a) \qquad\qquad W = \frac{1}{2}\kappa R_c^{-2} \qquad (4b)$$

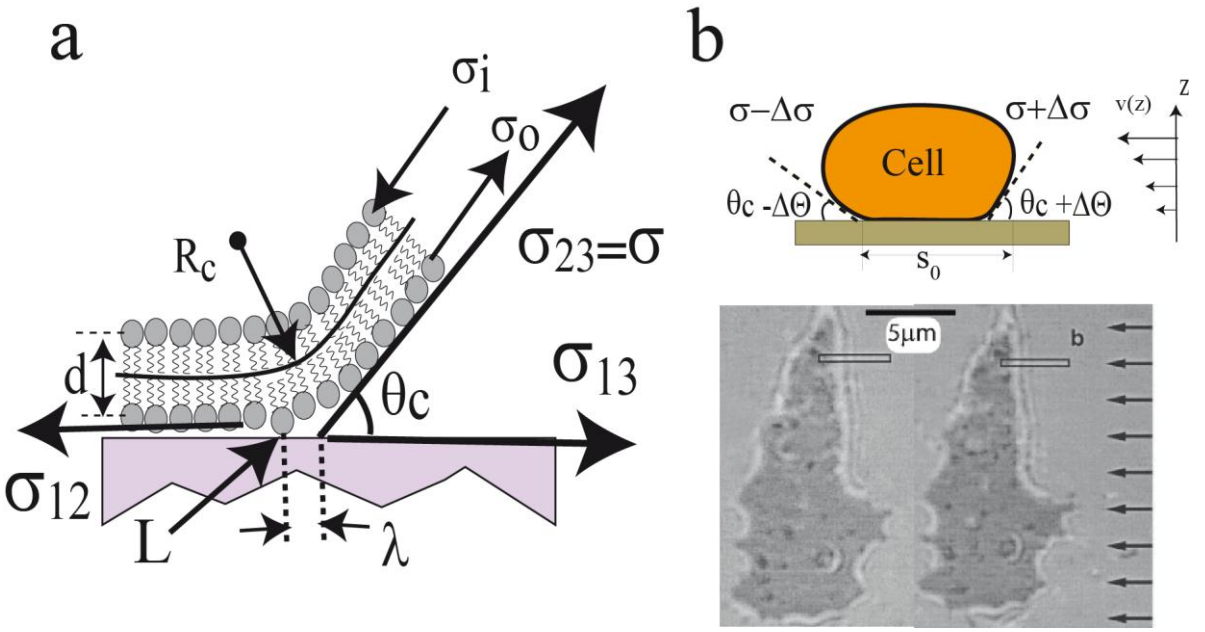

Figure 3*(a) Left side: equilibrium of the line tensions in the radial direction of the adhering shell. The contact Line L marks the transition between the adhering and non-adhering zones of the membrane. The contact tension* σ_{12}, σ_{13} *and* σ_{23} *are measures of the interfacial energies between the supported membrane and the vesicle surface, between the supported membrane and the aqueous phase and the surface tension of the vesicle, respectively. (b) Independent measurement of lateral tension, bending moduli and free adhesion energies of Dictyostelia cell (adhering on collagen covered glass substrate) by contour analysis in the presence and absence of a hydrodynamic flow field. Bottom: RICM image of Dictyostelium cell adhering on collagen covered glass in the absence (left) and presence (right) of hydrodynamic flow field. Image reproduced from PHD thesis of Rudolf Simson.*

The Young equation tells us that the surface tension $\sigma_{23} \equiv \sigma$ is a measure for the free energy gained by partial wetting of the surface by the membrane and is called spreading pressure. By determining the geometric parameters R_c and θ_c through contour analysis, the free adhesion energy W and the surface tension can be measured, provided the bending modulus κ is known. If κ is not known θ_c σ and κ can be determined by measuring the change of contact angle under hydrodynamic shear flow (see Figure 3 and [Simson 1998]). The above method of contour analysis can also be applied to measure the adhesion strength of adhesion domains [Albersdörfer et al. 1997]. In contrast, the measurement of the adhesion strength of sharp edges, formed after application of lift forces, requires a more refined analysis. It allows us to measure the local unbinding forces. An example of such an analysis is presented in reference [Guttenberg et al 2001].

IV. Modulation of Adhesion Strength by Membrane Bending Excitations.

Lipid bilayers and many cell envelopes (such as red blood cells, macrophages or endothelial cells) exhibit pronounced bending excitations and behave as dynamically rough surfaces (exhibiting roughness amplitudes of the order of ~50 nm). If we consider two adjacent positions (with a distance of x ~1μm) on the surface of the shell they do not move synchronically but independently similar to two independent particle performing Brownian motions. As usual, this behavior can be characterized by the correlation function of the amplitudes:

$$C(\Delta x) = < u(x)u(x+\Delta x) > = u_0^2 \exp\{- x / \zeta_p\}.$$

The correlation length ζ_p is determined by Eq (4b) (see [Lipowsky 1995] and and [Raedler et al 1995]).

In summary, fluid membranes can be considered to be composed of cushions of dimension $\zeta_p \, x \zeta_p$ [Helfrich 1973] which perform independent Brownian motions in the normal direction (Figure 4a). Close to surfaces the collisions of the cushions with the wall exert an entropic pressure, very similar to the 3D pressure exerted by molecules of an ideal gas hitting the wall of a piston. Owing to this analogy, the disjoining pressure is of the order

$$p_{disj} = \tfrac{1}{2} k_B T / < h > \zeta_p^2 \qquad (5)$$

which corresponds to the thermal energy stored in the space between the membrane cushion and the surface.

The dynamic roughness can be related to the bending elasticity κ by Fourier analysis of the membrane bending excitations. If we consider a flat membrane of dimension LxL, the mean square amplitudes <u^2> is obtained by the integration over all bending modes (of wavelength Λ_c) excitable under the given boundary conditions, such as the interfacial distance <h> and the membrane tension

$$< u^2 >= (2\pi)^{-2} \int_{q_{min}}^{q_{max}} u(q)^2 q dq$$

For free membranes and zero tensions (or $q_c \Lambda_c << 1$) the dynamic roughness can be calculated by considering a single cushion of dimension $\zeta_p \, x \zeta_p$ and by application of the equipartition theorem yielding

$$< u^2 >= c \frac{k_B T}{8\kappa} \zeta_p^{\,2} \qquad (6a) \qquad p_{disj} \approx c \frac{(k_B T)^2}{\kappa < h >^3} \qquad (6b)$$

Eq (4a) is Monte Carlo simulations yield a pre-factor of c≈ 0.23 (see [Lipowsky 1995] and [Netz 1995]).

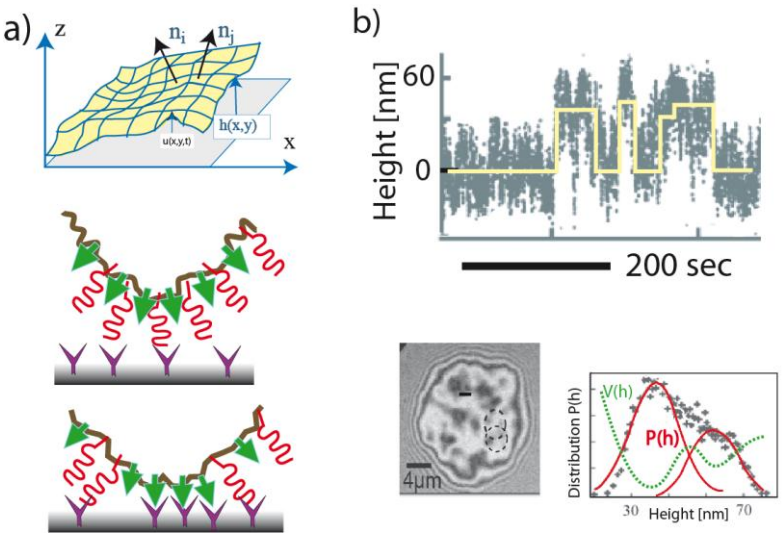

Figure 4*Nucleation of CAM-CAM pairs driven by pushing forces generated by membrane bending excitations. (a) Top: Characterization of roughness by local orientation of membrane normale which are correlated over the coherence length* ζ_p*. Bottom: Illustration of formation of CAM-CAM clusters by transient displacement of repellers from site of CAM-CAM contact. (b) Top: time sequence of fluctuation of distance of membrane from solid surface (measured by RICM at the site marked by circle in interferogram). The yellow line indicates the random transition of the membrane between a bound (<d> ~3 nm) and an unbound state (<d>~100 nm). The bimodal height distribution P(h), shown at the bottom right, defines the double well interfacial interaction potential according to* $V(h) \propto k_B T \ln\{P(d)\}$*. Image reproduced after [Marx et a. 2002].*

The membrane roughness controls cell adhesion in various ways:

- The disjoining pressure prevents adhesion of vesicles and cells by gravitational or Van der Waals forces. It impedes the non-specific attachment of blood cells (erythrocytes and macrophages) to tissue surfaces [Zidovska et al 2006]. In fact, the surface roughness of erythrocytes is enhanced by active forces (see [Auth 2007], [Zilker et al 1992).
- Bending excitations play a key role for the nucleation of adhesion domains by driving the contact formation between CAM-CAM pairs of cells, most likely by transiently pushing aside repeller molecules of the glycocalix [Pierres et al. 2004]. The transient contact formation between membranes and supported membranes can be directly visualized by RICM as shown in Figure 4. The double well surface potential can be reconstructed by measuring the inter-membrane distance distribution P(h).
- The dynamic disjoining pressure attenuates the local interaction potential V_0.

According to Eqs. (2) and (4a) the effective binding energy of the bonds is shifted to higher energies according to (see [Bruisma et al 2000] and [Reister Gottfried 2008]

$$V_{eff} = V_0 + \frac{1}{2}V'' < u^2 > = V_0 + \frac{k_B T}{4\kappa}V''\zeta_p^2$$

The curvature of the harmonic potential for weak adhesion ($V_0 \sim 10^{-6} J/m^2$) is of the order of $V'' \sim 10^{14} Jm^{-4}$ [Bruisma et al. 2000] while $\zeta_p \sim 25nm$ and $\kappa \approx 10^{-19} J$ resulting in a shift of Vo of the order of $10^{-5} J/m^2$. For strong bonds such as biotin-streptavidin (for which $V_0 \sim 10^{-5} Jm^{-2}$) the bending excitation does not play a role. It could however strongly affect the Integrin-RGD bonds for which $V_0 \sim 10^{-7} Jm^{-2}$ (see [Reister Gottfried 2008]).

- If adhering shells are subjected to membrane lateral tensions, the long wavelength excitations of the membranes are suppressed and the roughness is drastically reduced to

$$< u^2 > \approx \frac{k_B T}{4\pi\sigma} \ln\left\{1 + \frac{\sigma L^2}{\pi^2 \kappa}\right\} \qquad (7)$$

The suppression of the dynamic roughness by membrane tension triggers the transition of soft shells from free to adhering states, a process called tension induced switching of adhesion (see Figure 5 [Albersdörfer et al 1997]).

V. Models of cell adhesion

V.1. Cell Adhesion as Heterogeneous Wetting Process

Pure lipid vesicles with excess area adhering on supported membranes often exhibit similar shapes as partially wetting fluid droplets, with the exception of the finite contact curvature R_c (see Figure 3). The shape is determined by the balance of the elastic energy costs due to the deformation of the shells and the gain in adhesion energy wA_C (see Equation 1 and [Seifert and Lipowsky 1995]). The adhesion zone is homogeneous. The situation changes dramatically if the vesicle and the supported membranes are doped with small concentrations of linkers and repellers that control the adhesion strength, thus mimicking biological situations. The adhesion zone decays into domains of strong adhesion formed by segregation of the linker pairs and unbound zones (see Figure 6). Therefore vesicle adhesion is a paradigm of a heterogeneous wetting process.

The decay of the adhesion zone can be understood in terms of the competition of short range attraction forces between CAM-CAM pairs (often called lock-and key forces) and long range repulsion forces mediated by repellers and membrane bending excitations (see Figure 4). A summary of the generic interfacial forces is presented in the Supplemental Section (S1). The situation is depicted in Figure 5a. Due to the different range of interactions of the attractive and the repulsive forces, the formation of a CAM-CAM link is associated with a local deformation of the bilayer (see Figure 5b top), which is associated with an elastic energy cost U . Obviously the elastic energy cost is reduced by the formation of adhesion domains.

Before proceeding it should be noted that the lateral segregation of the CAM-CAM pairs can be driven by several mechanisms, including (i) the lateral attraction between CAMs [Weikl and Lipowsky, 2004]; (ii) the coupling of CAMs to actin patches, the formation of

which is controlled by actin membrane linkers, such as talin (see Figure 7); (iii) the long range attraction between CAM-CAM pairs mediated by bending excitations [Bruisma et al. 1994].

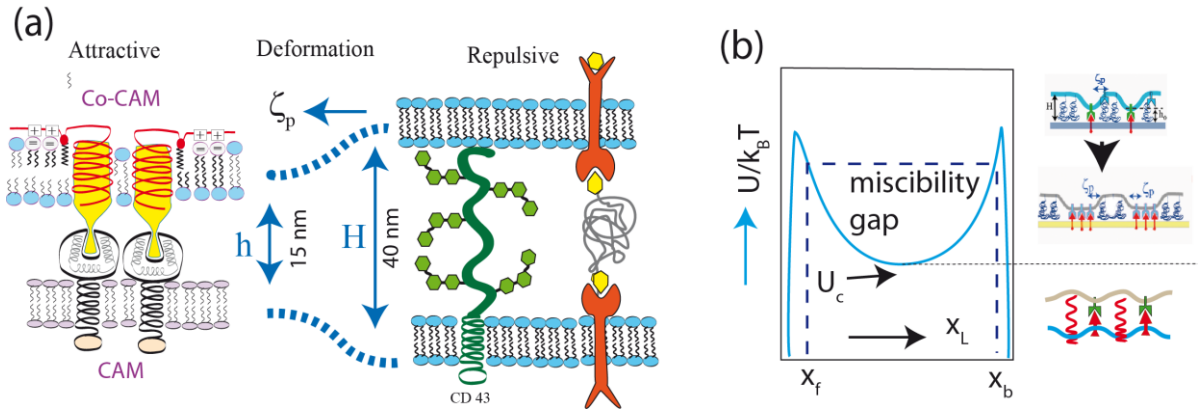

Figure 5 (a) Top: *Schematic view of three major forces controlling the primary phase of cell adhesion. Left: the short range attractive lock-and-key force (typical ranges of h ~ 20 nm). Right: the repulsive force mediated by membrane proteins with large extracellular domains (here CD 45, CD 43 and ICAM) or hyaluronic acid (HA) molecules anchored to membrane receptor of the CD 44 family. Middle: elastic stress caused by length mismatch (H≠h. The range of the deformation is determined by the persistence length* ζ_p *[Eq. 3].*

(b)Phase diagram of adhesion states. The ordinate shows the normalized bending energy and the abscissa the volume fraction of ligand. U_c *marks the lower critical point of the miscibility gap. The right side at the top shows the long range attraction of the isolated CAM-CAM pairs and microdomain formation. The bottom shows a homogeneous state which is realized at very low CAM concentrations and small distance mismatches (H-h).*

The decay of the adhesion zone into regions of tight and very weak binding is reminiscent of the phase separation in lipid-protein bilayers [Sackmann 1996] and the Cahn model of first order wetting [Cahn 1977]. However, while the driving force for these classical phase separation processes is the effective lateral attraction between molecules (characterized by the Flory Chi-parameter), the adhesion-induced domain formation is driven by the local deformation energy (U). The attraction between two linkers results in the reduction of the internal energy cost for H<h by

$$U = 8V''(H - h_0)^2 \zeta_p^2 \qquad (8)$$

Note U is a measure for the energy costs which has to be paid to compress the glycocalix by (H-h_0) over a disk of radius ζ_p (see [Bruinsma et al.2000]). The clustering of the CAM-CAM pairs is counteracted by the associated reduction of the mixing entropy which has been estimated by Bruisnma et al. [Brunisma et al 1994]. Based on this work the Helmholtz free

energy change associated with the lateral phase separation can be expressed in the form [Bruinsma et al 2000]:

$$\Delta F / k_B T \approx \alpha\, x \ln x + (1-x)\ln(1-x) + \frac{1}{2} zU\, x(1-x) \qquad (9)$$

with $\alpha = (1-\Gamma/2) \approx 0.44$. x is the molar fraction of bound CAMs in the adhesion disc, z is the coordination number and is $\alpha \approx 0.44$. This free energy expression closely resembles the Flory free energy of polymers solutions, with the elastic energy zU playing the role of the Flory χ-Parameter. The reduction of the entropy of mixing by the factor α corresponds to the reduced translational entropy of the macromolecules in the Flory Huggins lattice model. It is a consequence of the change of the conformation of the boundary lipid. Thus, if a CAM-CAM pair is moved to a different site in the lattice it has to carry the lipid in the halo with it.

Figure 5 shows the U-x phase diagram predicted by Equation 9. It exhibits a lower critical point. At $U << k_B T$ (or small height differences $H-h_0$) the links are randomly distributed within the adhesion disc (see bottom of Figure 5c, while at $U >> k_B T$ it decays in zones with high and low densities of CAM. Clearly, the former correspond to regions of tight adhesion and the latter to unbound zones. The critical point can be calculated by standard procedures yielding

$$\frac{zU}{k_B T} = 11/4$$

The following consideration shows that the critical point is below physiological temperatures. For a height difference $(H-h_0) \approx 20$ nm, $V'' \approx 10^{12}$ Jm^{-4} and $\zeta_p = 25nm$ one obtains for z=6: $zU = 48V''(H-h_0)^2 \zeta_p^2 \approx 1200 k_B T$. Clustering of receptors at physiological temperatures is thus expected even for small height differences: $H-h_0 \sim 2$ nm.

Concluding remarks: The wetting model is helpful to explore the conditions under which adhesion is possible and relates the state of adhesion to the membrane bending elasticity and the height difference $(H-h_0)$, which can be controlled by the repellers. The analogies to the Cahn model of first order wetting and the Flory model of polymer solutions allows us to understand cell adhesion within the framework of classical thermodynamics and continuum mechanics.

The state of adhesion is also controlled by the competition between Van der Waals attraction and electrostatic repulsion mediated by the charged glycolipids exposing sialic acid residues (such as GM1 to GM3) and sialyl Lewis X oligosaccharides [Smith et al 2006].Interestingly, the concentration of some charged gangliosides is elevated in cancer cells. The highly charged glycoproteins exposing several 10 nm long chains into the extracellular space exert both electrostatic and steric repulsion forces. We will present simple models of the electrostatic repulsion forces exerted by glycolipids end polyelectrolytes in the Appendix A. In Chapter VIII we show that the generation of myelin sheath around axons of the central nerve system requires the abolishment of electrostatic repulsion

A different method of the calculation of phase diagrams has been developed by Boulbitch et al. [Guttenberg et al 2001]. It is, based on the analysis of the membrane bending deformation along the contact line of adhesion. This so called "boundary stress analysis" model is presented in Appendix C**.**

V.2. On the Kinetics of Adhesion and Organization of Adhesion Zone

The distribution of adhesion domains and unbound regions within the adhesion zone between vesicles and supported membranes is determined by many factors: the binding energy w per CAM-CAM pair, the CAM and repeller concentrations (c_L and c_R) and the balance of tensions at the contact line (see Figure 6 below). The initial state is also determined by the kinetics of adhesion which is considered in the following.

Biomimetic model membrane studies and computer simulation studies show two scenarios of the adhesion kinetics, for the case of medium linker binding energies ($w \approx 10$ k_BT) such as integrin-RGD linkers shown in Figure 1 [Boulbitch 2001].

- At small RGD ligand concentrations, the growth rate is determined by the rapid RGD ligand diffusion ($D_L \approx 1 \mu m^2$/sec). The radius of the adhesion domain growth with a square root law: $R(t) \approx At^{1/2}$. The growth coefficient A increases nearly linearly with the linker concentration c_L.
- At high concentrations the growth kinetics is controlled by the CAM-CAM association dissociation-equilibrium resulting in a linear growth law: $R(t) \approx const$. The growth rate dR/dt decreases exponentially with the repeller concentration and domain formation is eventually abolished by the repulsion force of the repellers.

The metastable organization of the adhesion zone depends in a subtle way both on the linker binding energy w and concentration c_L. If the binding energy is of the order of k_BT, randomly formed adhesion domains bind and decay continuously resulting in the random formation of small adhesion domains within the adhesion zone (see Figure 6 and [Reister Gottfried 2008). If the adhesion strength is high, two scenarios are observed. At high linker density an initially formed domain growths rapidly until the whole adhesion zone adheres strongly. The vesicles can assume spherical cap shapes and even explode. If the linker density is decreased a ring like tight adhesion domain is formed with the central part of the adhesion zone bulging upwards (see Figure 6b). The formation of such a sombrero-like shape is necessary to establish mechanical equilibrium of the adhering shell. The stability is determined by the balance of lateral tensions σ both at the outer L_{ca} and the inner L_{ci} contact line as illustrated in Figure 6b. Below we will see that such sombrero shapes of the adhesion zone can play an important role as global reaction spaces (see Figure 12b).

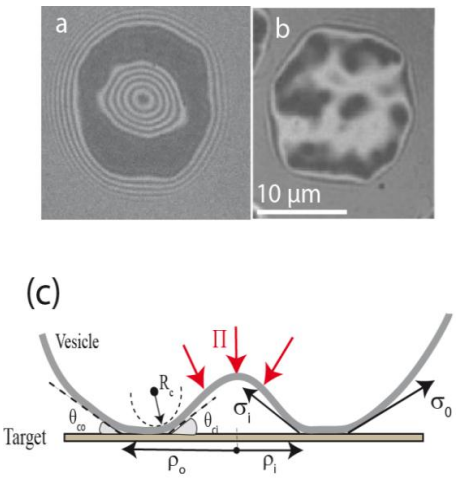

Figure 6 *Top: Control of the shape of zones of tight adhesion by variation of chemical potential of receptor. The adhesion mimicking system consists of giant vesicles doped with gangliosides exposing the blood group determinant sialyl LewisX, while polyethylene oxide head groups serve as spacer. The target cell consisted of selectin-E receptors adsorbed on solid surface. The chemical potential of the CAM (E-Selectin) was controlled by the addition of monoclonal antibodies against selectin . Left: formation of ring like adhesion domains associated with formation of central dome. Right: formation of random distribution of adhesion domains after reduction the concentration of high affinity receptors through monoclonal antibodies of selectin (see Chapter VI.2). Images taken from PHD work of Barbara Feneberg, Technical University Munich 2003).*
Bottom: Mechanical stabilization of the Mexican hat-like shape of giant vesicle adhering on supported membrane for the situation of ring-like adhesion domain formation. The total spreading pressure of the outer contact line (radius ρ_0) is balanced by that of the inner contact line (radius ρ_i): $\rho_0\sigma_0 = \rho_i\sigma_i$.

V.3. Down-Regulation of the Adhesion Energy by the Lateral Osmotic Pressure Effects

A frequently underestimated effect in biological literature is the weakening of the adhesion strength by the osmotic pressure exerted by the repellers and CAMs expelled from the zones of tight adhesion. In cells this effect can be particularly large since the area density of the repellers, forming the glycocalix, can often be larger than the CAM. The weakening of the binding energy can be estimated on the basis of the following simple argument. We consider the situation a vesicle doped with mobile ligands adhering on a target membrane with immobile CAMs. Let the energy per CAM-ligand pair be w, the total linker density ρ_L and the repeller density ρ_R (measured in molecules m^{-2}). By ignoring the adhesion induced elastic deformation, the free energy density of adhesion can be approximately expressed in terms of the chemical potentials of the repellers and CAMs as

$$\Delta g_{ad} = W_{ad} - \pi_R - \pi_L \approx w\rho_L^b - k_B T\left\{\rho_L^f + \rho_R\right\} \qquad (10)$$

where ρ_L^b and $\rho_L^f \approx \rho_L$ are the densities of the bound and free linkers densities in the adhesion domain.

We consider the example of Figure 2 [Gönnenwein et al.2003]: w ≈ 10 k_BT: $\rho_L^b \approx 0.25\text{x}10^{16}\,\text{m}^{-2}$ (corresponding to a minimum lateral distance between integrins of 20 nm); $\rho_R \approx 2mole\% \approx 2x10^{16}m^{-2}$. The binding energy per unit area within the tight adhesion zone is $W_{ad} \approx 1\text{x } 10^{-4}\ \text{Jm}^{-2}$. The osmotic pressure is of the order $\pi_R \approx 8\text{x}10^{-5}$, showing that the gain in adhesion energy is nearly compensated by the osmotic pressure. The direct measurement of the work of adhesion is even lower: $W = 3x10^{-6}$ which is a consequence of neglecting the elastic energy cost. In cells the osmotic effects may be overcompensated by coupling of the CAMs to the actin cortex.

The above approximation assumes that the reservoir of receptors and CAMs is unlimited. A rigorous analysis has to consider the finite receptor and repeller concentrations in the adhering shells. This problem is considered in the thermomechanical model [Smith and Seifert 2005]. Similar to Eq. (1), the energy functional (ΔG_{adh}) has to consider several contributions: first, the balance of the energy gain (- ΔE_{bond}) associated with the bond formation; second, the energy cost of the adhering shell deformation (ΔF_{bend}); third the gain in adhesion energy, expressed in terms of the spreading pressure W, and fourth, the translational entropy ($\sum_i \Delta S_i$) associated with the redistribution of attractive and repellant CAMs.

$$\Delta G_{adh} = \Delta F_{bend} - W - \Delta E_{bond} + \Delta S \qquad (11a)$$

The spreading pressure is determined by the change of the Gibbs free energy ΔG_{adh} associated with the gain (ΔA_c) in contact area A_c:

$$W = -\frac{\partial \Delta G_{adh}}{\partial A_c}\ \Delta A_c \qquad (11b)$$

To account for the spreading pressure the two equations (5a and 5b) have to be solved self consistently by considering the constraints of constant area and volume of the shell.

The translational entropy is expressed in terms of the logarithm of all possible positional configurations of the CAMs, including ligands residing in the bulk solution [Smith et al 2008]

$$\Delta S = k_B T \sum_i \ln \Omega_i \qquad (12c)$$

An example of the detailed calculation of ΔS can be found in [Smith et al. 2006].

VI. Basic Physical Concepts of Cell-Cell Adhesion Learned From Model Membrane Studies.

VI.1. Control of Cell Adhesion Strength by Interactive Actin-Receptor Crosstalk

Cell adhesion starts with the rapid formation of micro-domains of tight contact formed by diffusive segregation of bound pairs of cell adhesion molecules (exhibiting diffusivities $D \approx 0.1\ \mu m^2\ s^{-1}$). Since resting cells expose typically about 10^4 receptors of a certain type, clusters of linkers could form in the time scale of seconds. The nucleation of CAM clusters is further accelerated by pushing forces generated by membrane bending excitations [Bruinsma et al 2000]. In a secondary step the intracellular domains of the CAMs bind to the actin cortex, resulting in the stabilization of the adhesion domains by two mechanisms:

- A primary mechanism consists in the increase of the binding affinity

of receptors (such as integrins) expressed in terms of the binding energy w (see Appendix B), which is often accompanied (or even triggered) by the binding of the CAMs to F-actin (see Figure 7 below and Glossary "Integrin activation")

- A second (generic) mechanism consists in the increase of the adhesion

strength (measured in terms of the spreading pressure W) by coupling of the receptor clusters to the actin cortex, which is a consequence of the increased bending stiffness of the cell envelope (Simson et al. 1998).

Figure 7 shows the molecular mechanism mediating the activation of the integrin affinity by binding of the intracellular domain of the beta-chain to the major actin-membrane coupling protein talin. Talin belongs to the class of FERM-proteins (together with ezrin, moesin and band IV.1) which exhibit a specific domain (FERM) that binds specifically to the beta-chains of integrins [Wegener et al 2007].

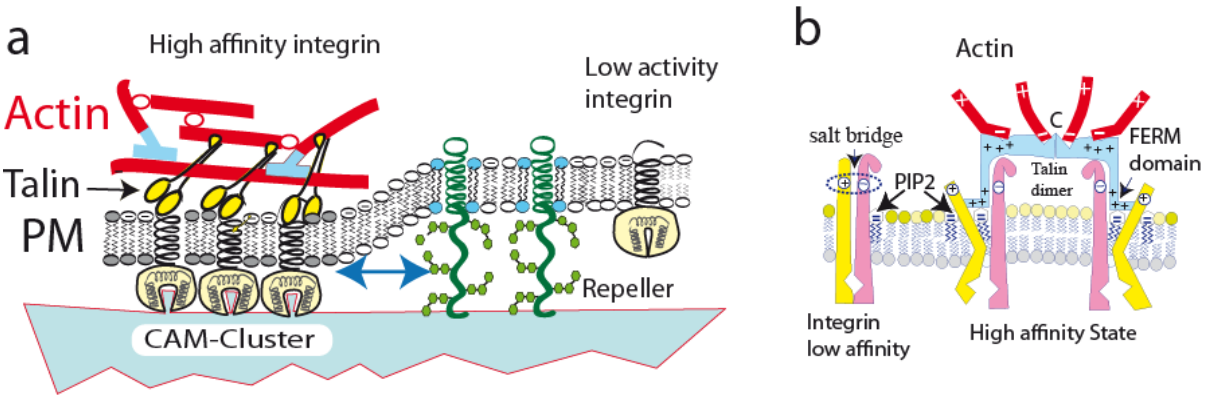

Figure 7 *(a) Coupling of actin gel patches to cluster of CAM of integrin family via talin, which is accompanied by a drastic increase of the integrin binding affinity (Simson et al 1998).*

(b) Molecular model of integrin activation by binding of the talin FERM domain to its beta chain, resulting in the opening of the binding pocket of integrins. The increase in affinity is mediated by uncoupling of salt bridges, formed between the intracellular domains of the integrin dimer, which is mediated by binding of the FERM domain of talin to the beta chain [Wegener et al 2007]. Moreover, the FERM domain of talin is also directly coupled to the

membrane by electrostatic forces and phosphoinositides (PIP2/PIP3. Note first, that talin forms dimers linking two integrins and second, that it has several binding sites for F-actin. Thus actin gel patches can form without contribution of other actin cross-linkers.

In the resting state of cells talin resides in the plasma membrane in a sleeping conformation. Activation by phosphorylation [Wegener et al 2007] exposes the FERM domain and talin is recruited to the membrane by binding to PIP2/PIP3 via a pleckstrin homology domains and electrostatic-hydrophobic forces [2]. Talin tends to form dimers and exhibits several actin binding sites, both at the FERM domains and the C-end. It can thus form gel patches and stabilize the adhesion domains. A second effect of talin is the increase of the affinity of integrins by opening their binding pocket by a mechanism shown in Figure 7. In summary, talin is a major driving force of receptor clustering and adhesion domain formation of cells (see also Glossary " integrin activation).

VI.2. Cell Unbinding by Extracellular Antagonists of CAMs.

A biologically important control mechanism of the cell tissue adhesion consists in the blocking of the binding sites for CAMs on the tissue surface. This mechanism is often utilized by metastatic cancer to facilitate their invasion of tissue . The physical basis and consequences of this mechanism has been studied by biomimetic systems Smith et al.2006]. Giant vesicles composed of 1:1 lipid/cholesterol mixture were doped with 1% lipids exposing PEG macromolecular head groups and 8 mole% of sialyl-LewisX- exposing glyco-sphingolipids which bind selectively to E-selectins. The target tissue consisted of glass substrates covered with E-selectin (about 3000 molecules/μm^2). The CAM binding pocket for the ligand is blocked by antibodies.

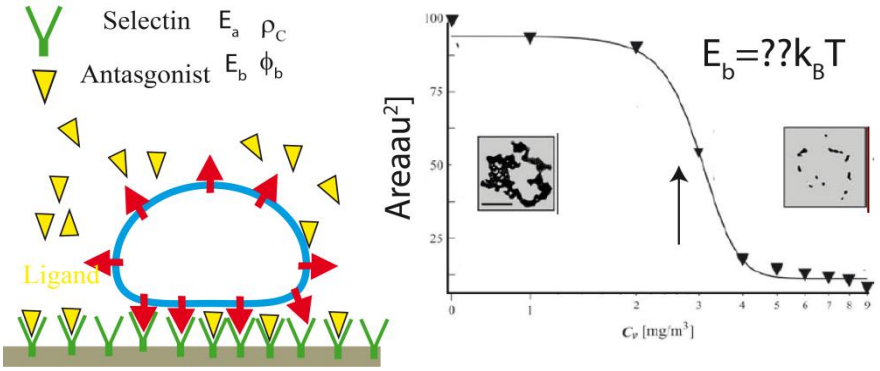

[2] For a detailed description of the electrostatic-hydrophobic binding of proteins and the associated activation of the proteins see Sackmann Lecture Note "Electrohydrophobic membrane coupling of proteins" www. biophy.de.

Figure 8*Model system used to study the uncoupling of adhesion domains by blockade of CAM binding sites on the artificial tissue. Left: Cartoon showing the major players involved. E_a and E_b are the binding energies of the ligand and selectin antibodies. Right: Total area of occupied by tight adhesion domains within adhesion disc, plotted as a function of antibody concentration in bulk solution.*

The most intriguing result of this experiment is the threshold behavior of the antagonist-mediated abolishment of the adhesion. The total area of tight contact A_c decreases first weakly with increasing concentration of the antagonist but drops abruptly by about a factor of 100 within a narrow concentration regime at the threshold value C_V*. C_V* depends sensitively on the ratio E_b/E_a of the binding energy of the antibody (E_b) and the ligand (E_a). The threshold behavior of the experimental A-versus-C_{AB} curves can be explained quantitatively by the thermomechanical adhesion model [Smith et al 2006].

VI. 3. A Fundamental Difference between Cell-Cell and Cell-Tissue Adhesion

Comparative studies of giant vesicles adhering on target membranes doped with mobile and immobilizes CAMs (integrins) revealed fundamental differences between cell-cell adhesion, where both linkers are mobile, and cell-tissue linkage were the tissue located co-receptors are immobile [Smith et al 2008]. First, the total area of tight adhesion and the work of adhesion W of each domain are much higher for mobile CAMs, suggesting a higher packing density of CAM-CAM pairs. Second and most importantly, the two systems respond very differently to external forces (see Figure 9)

- If an external lift force is applied to vesicles adhering on target with fixed CAMs, the bonds located at the edge of the contact zone are stretched and eventually break, reducing the contact area (see transition from t_1 to t_2 in Figure 9a right side). Under constant force the vesicle eventually unbind which enables measurements of unbinding forces of single bonds [Guttenberg 2000]. To re-establish thermo-mechanical equilibrium after switching of the force, new bonds are formed within the reduced contact area (see transition t3 to t4 in Figure9, right). For that reason, the total adhesion area remains constant if the force is switched on and off repeatedly (see Figure 9a middle and left).
- In striking contrast, the adhesion between membranes with mobile CAMs is strengthened under external forces. Within seconds after switching on the force, the bonds close to the contact line move laterally. New CAMs join and enforce the adhesion strength of domains under stress (Figure 7b, right side). The vesicle cannot be lifted off the target. The force-induced condensation of CAM-CAM pairs results in the monotonous growth of the contact zone if external force pulses are applied repeatedly (Figure 7b right).

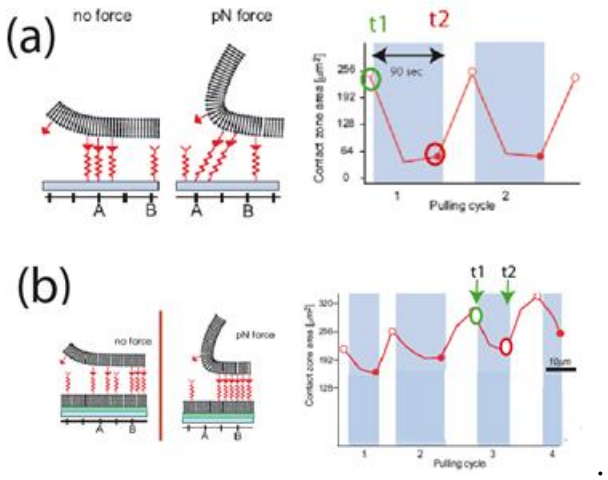

Figure 9 *Experiments exploring the response of adhering shells to external lift forces mimicking the case of cell-cell (all CAMs mobile) and cell-tissue adhesion (one CAM type fixed). Vesicles are doped with 1% RGD and 1% PEG lipid. The supported target membrane is functionalized with mobile and immobile integrins (100 CAMs/µm^2), respectively. (a) Situation of fixed integrins. Left side: lift force induced breakage of bonds. Right side: change of tight contact area by cyclic application of lift forces, indicated by blue bars (f=4pN). Note that new bonds are reformed after relaxation of the force. Therefore the total contact area remains constant during the repeated application of force pulses. (b) Situation of mobile integrin in target membrane Left side: Schematic view of condensation of CAM-CAM pairs close to the contact line after force application. Right: change of contact area by cyclic application of lift forces (f=4pN). Note that the contact area increases monotonically with the number of pulses, despite of the transient decrease of A_c at the end of the force pulses (see transition t1 to t2).*

The force induced strengthening of mobile linkers is very fast (<1sec). This can play an important role for the sub-second adaption of cells to changing elastic stresses ~~in~~ before the cell can respond by reorganization of the actin cortex. Under physiological conditions, this adaption is mediated by the reorganization of the actin cortex and microtubule actin crosstalk and can take several minutes (see ChapterVII.3 below and [Sackmann and Merkel], Kapitel 28.4]).

VII: Biological Paradigms of Cell Adhesion

VII.1. Biological Paradigm of Cell-Cell Adhesion: Immunological Synapses

A vital biological process is the stimulation of freshly born (=naïve) lymphocytes (T-cells) by encounters with antigen presenting cells (APC, see Figure 10a and b), such as dendritic cells (DC)**.** The naïve T-cells move from the bone marrow to the lymph node were they encounter specific antigen exposing cells, called dendritic cells. Sequential or continuous adhesion of the T-cells on the APC stimulates the production of cytokines, such as interleukin II (IL-2), which eventually leads to the division of the generating cell and other T-cells called clones [von Andrian 2003/2008]. The stimulation can also be mimicked under *in vitro* conditions. First, by embedding the DC in collagen networks where they are encountered transiently by the naïve T-cells [Gunzer et al. 2000] and second , by mimicking DC by supported membranes doped with antigen-MHC complexes [Varna et al. 2005], [Freiberg et al. 2002] (see Figure 10a, right). In both cases the T-cells are stimulated after about >12h. The physical basis of the process has been described in great detail previously (see [Sackmann 2010] and footnote [3] on next page. We therefore summarize here only results to demonstrate that adhesion domains play a key role as local reaction platforms that promote the expression of cytokines by the coordinated activation of two transcriptional pathways.

The electron micrograph of a T-cell adhering to a virus infected cell shows that the adhesion zone is not homogeneous but decays into patches of tight adhesion (see Figure 10a). The adhesion domains are formed by lateral aggregation of antigen-MHC-II complexes (AG-MHC) linked to T-cell receptors (TCR). Electron microscopy studies based on immune labeling with antibodies to talin [Freiberg et al 2002] show that adhesion is also driven by formation of integrin-ICAM-1 links (see Figure 10a right). The binding constant of ICAM-1-Integrin pairs is of the order $K_d \sim 100$ nM (corresponding to a binding energy of $w \approx 7k_BT$;see Supplement S3) , while that of TCR-MHC-AG complexes is much weaker and lies around 10 μM ($w \approx 4k_BT$) [Stone et al 2009]. It is therefore assumed that the ICAM-integrin pairs drive the adhesion and may even aggregate together with the TCR-AG-MHC pairs.

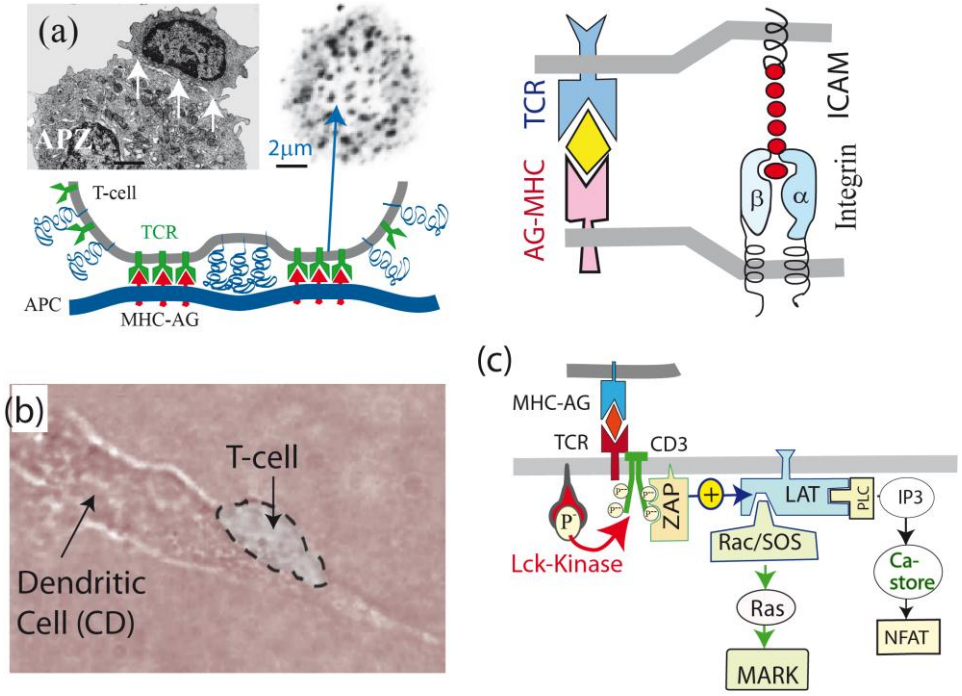

Figure 10*Top left: Electron micrograph showing T-cell adhering on antigen presenting cell (APC) by generating domains of tight adhesion separated by unbound zones (image reproduced from [Sackmann 2011]).Top right: direct visualization of adhesion domain by fluorescence labeling of T-cell receptors (after [Varna 2005]). Bottom: Schematic view of adhesion-induced domain formation. Top right: the adhesion domains are possibly formed by co-aggregation of TCR-AG-MHC and integrin-ICAM-1 linker pairs, as discussed in the main text.*

(b) Phase contrast micrograph of T-cell adhering on antigen presenting dendritic cell. Image reproduced from [Gunzer et al 2000] with permission of the authors.

(c)Simplified scheme of genetic expression of the cytokines Interleucine II (IL-2) by binding of the MHC-AG complex to the T-cell receptor (TCR) which is tightly associated with the co-receptor CD3. The CD3 phosphorylation activates the membrane bound adaptor protein LAT, which in turn stimulates two pathways of genetic expression. One is mediated via the transcription factor NFAT and the other via the MAPK signal cascade. Please note here that Lck is called a non-receptor tyrosine kinase since very similar reaction pathways are opened by classical membrane bound receptor tyrosine kinases (for an example see Figure 18 below)

The adhesion domains formed by T-cell-APC adhesion are a condition *sine qua none* for the T-cell activation. The key step of the signal transduction consist in the phosphorylation of the tyrosine groups at the tail of the integral protein CD3 through the membrane bound kinase Lck (see Figure 10) which induces the binding and activation of the membrane bound adaptor protein LAT. The activated binding pockets of LAT recruit, and thereby activate, the key activators (the phospholipase C□ (PLC-□) and the GTPase Ras) to the membrane. They trigger the two parallel pathways required for the effective genetic expression of the cytokine IL-2 [3]. The T-cell activation is a paradigm of genetic expression by cytokines. It has been extensively studied and is rather well understood.

As is well known, the function of each kinase is counteracted by a conjugate phosphatase. In the case of the Lck kinase this role is played by the phosphatase CD45. Owing to its large extracellular domain, extending by about 40 nm into the extracellular space, it can only abolish the CD3 phosphorylation if the lymphocyte is free. Its function is inhibited after formation of adhesion domains since it is expelled from these reaction platforms. This shows that adhesion domain formation is a are a condition sine qua non for the T-cell activation (see figure 11).

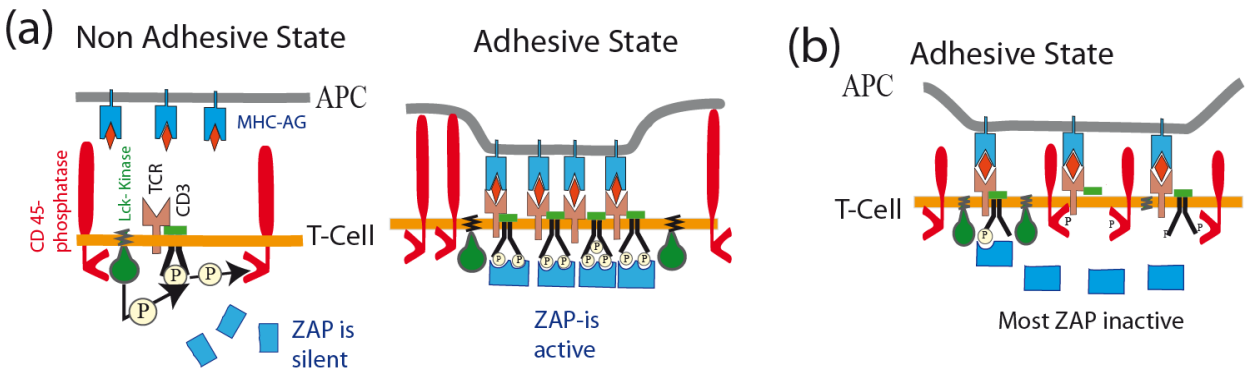

Figure 11 *(a) Model of activation of T-cells by microcluster formed during the initial phase of T-cell-APC encounters (that is before the formation of large central SMACs shown in Figure 12). The 70 kDa kinase ZAP-70 is activated by binding to the phosphorylated tyrosine groups of the [4]cytoplasmic chain of the co-receptor CD3. Left side: Situation before T-cell adhesion. The ZAP activation is constantly abolished by CD45-mediated dephosphorylation of CD3. Right side: formation of immune synapse (IS) by lateral clustering of bound TCR-MHC-AG pairs resulting in the expulsion of the inhibitor CD45 by steric forces.*
(b) Demonstration of CD45 self-inhibition model by [Choudhuri 2005]. By reducing the length of the extracellular domain of CD45 it can diffuse into the tight adhesion domain and prevent the activation of ZAP as in the case of the non-adhering state. The same abolishing effect was observed by prolongation of the extracellular domains of the MHC-receptor.

[3] A detailed description of the T-cell activation and models of the function of immunological synapses is presented in: Lecture notes on biological physics" Physics of Immunology" freely accessible via www.biophy.de

In summary, the phosphatase CD45 plays a twofold role: it inhibits the CD3-phosphorylation and acts as buffer molecule counteracting adhesion (together with other glycoproteins of the glycocalix, such as CD 43). Convincing experimental evidence for this model is provided in beautiful experiments by Choudhuri *et al [Choudhuri 2005]*. The authors changed the lengths of the extracellular domains of both the CD44 and the MHC receptor and showed clearly that the immune response is suppressed if the length of the extracellular part of CD45 is considerably longer than that of the TCR-AG complex. Below we will present other examples of cell proliferations triggered by formation of adhesion-induced microdomains. In this case other proteases with long extracellular chains could act as inhibitors, such as CD 148, which exposes five fibronectin type III repeats each about 4-5 nm long. Further evidence for the above model was recently provided by biomimetic experiments [James and Vale 2012].

VII.2. Global Reaction Space Generation by Cell Polarisation and Actin-MT Crosstalk.

The activation of naïve T-cell consists of a primary and a secondary process. About 10 minutes after the T-cell-APC encounters the adhesion zone between the cells undergoes a dramatic reorganization. The two types of domains segregate. The integrin-ICAM-1 clusters move towards the contact line forming a ring-like zone of tight adhesion. The T-cell becomes polarized assuming a pear-like shape, which is attributed to two processes: first, the increase of the integrin binding affinity by talin (see Figure 7) and second, by the transfer of the co-receptor ICAM from the body of the T-cell to the nascent adhesion ring by active transport [Wülfling et al 1998]. The polarized shape is stabilized by coupling of the microtubule plus ends to the actin cortex (see Figure 14 and Figure 15, further below). The TCR-AG-MHC domains are actively transported towards the center of the adhesion disc where they accumulate and form large complexes. These “supra-molecular activation cluster” (SMAC) are assumed to serve the recycling of the immune synapses.

From the point of view of the physics of cell adhesion, the most intriguing aspect of the secondary process is the polarization of the T-cell during the formation of the ring like adhesion zone. It forms a gasket separating the outside space from a spacious inner dome like pocket. The latter forms a closed reaction space which plays an important role for the destruction of infected cells by killer cells (see Figure 12b).

The central question is how the polarized state of the cell is mechanically stabilized. In Figure 6 we showed that domelike spaces can be stabilized by the balance of the membrane tension generated at the inner and outer contact line of the adhesion ring. This mechanism is also effective in the present case. However, the dome shape is mainly stabilized by coupling

of the microtubule plus ends to the actin cortex. The MT-actin coupling can be mediated by specific binding proteins (so called plus-end proteins see Figure 15 below) or by dynein motors coupled to actin as shown in Figure 12b right side (see also [Combs et al 2006] and [Sackmann 2010]). In the former case a one dimensional spreading pressure Σ pushes the MT towards the rim of the dome. In analogy to the spreading pressure of membranes, the tensile force Σ can be expressed as

$$w = \Sigma(1 - \cos\Theta_c) \qquad (13)$$

where w is the binding energy per unit length of MT and Θ_c is the contact angle defined in Figure 12. In the second case the pushing force F_R of the MT towards the contact line is generated by the attempt of the dynein motors to walk on the MT towards the centrosome. Besides the actin bound fraction, numerous MT exhibit dangling plus ends. They have been shown to act as tracks for the rapid transport of vesicles between the Golgi and the SMAC [Stinchcombe 2006]

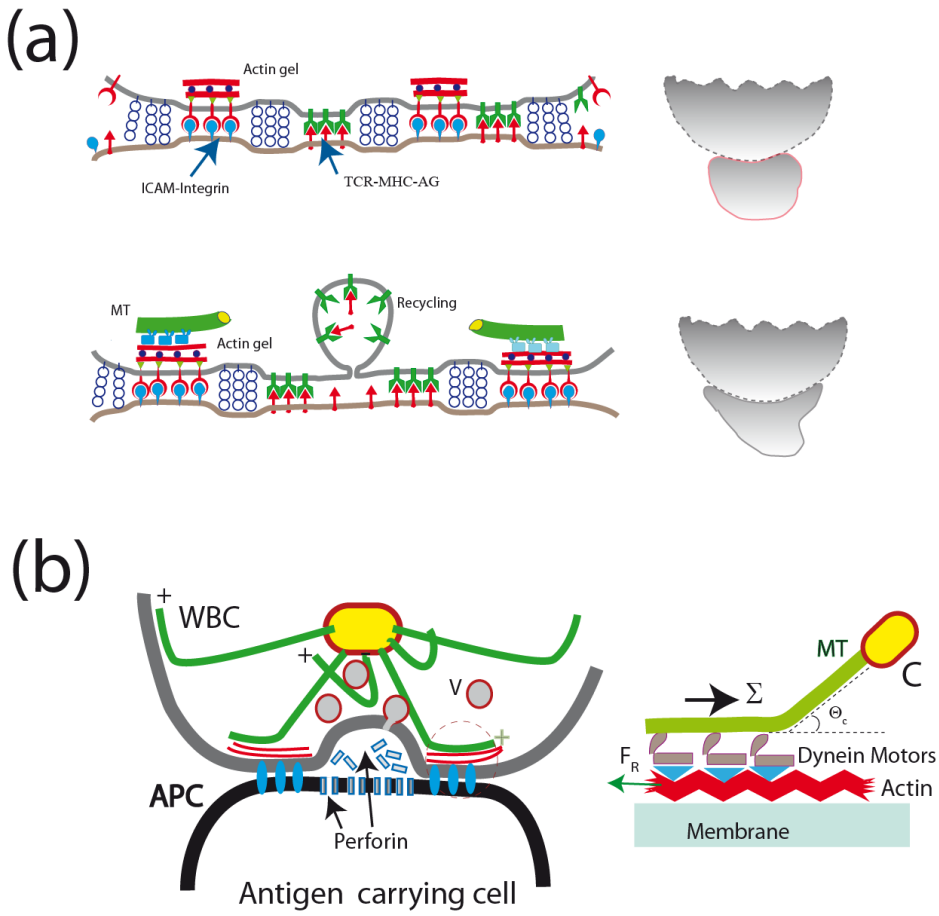

Figure 12*Left side: Two-stage model of reorganisation of T-cell-APC adhesion zone as suggested by visualisation of talin and Lck distribution [Varna et al. 2005]. The top image shows the situation 3 min. and the bottom 25 min. after contact formation. Right contours of the cells redrawn from phase contrast micrographs [Freiberg et al. 2002]. The left side shows that the initially statistically distributed clusters of talin move towards the rim of the contact zone and stabilize the ring-like adhesion domain. Moreover, the contact area between the*

cells shown on the right side growths by about 20 %, whereby the originally nearly spherical cell assumes a polarized pear-like shape.

(a) *Left side: Mexican hat like reaction space as formed by cytostoxic cells adhering on infected target cells. The reaction space is isolated from the extracellular space by a ring-like zone of tight adhesion acting as gasket. The global shape is stabilized by microtubules which link the actin cortex to the centrosome. A second fraction of MT exhibits dangling plus ends which can dynamically shrink and grow. They serve as tracks for the rapid transport of secretory vesicles and endosomes by dynein and kinesin motors [Stinchombe et al.2006]. Right side: model of mechanical stabilisation of cell shape by tangential coupling of MT to the actin cortex by dynein motors as demonstrated by Combs et al. [Combs et al.2006]. The tensile stress Σ in the microtubule is generated by the dynein motors which tend to walk towards the minus-end of the MT. Σ is balanced by the reaction tension generated in the actin cortex.*

VII.3. Endothelial Cell Layer: a Paradigm of Cell- Cell and Cell-tissue Adhesion

The barrier between blood and tissue is formed by confluent monolayers of endothelial cells (ENC) lining the inner wall of blood vessels. The endothelium is stabilized (i) by cell tissue adhesion through binding of integrins to proteins of the basal membrane (collagen IV, and (ii) by cell-cell adhesion mediated by the self-recognizing (homophilic) CAMs cadherin and PECAM (Figure13). The co-cluster of cadherin and PECAM [Newman 1997], together with the membrane bound receptor of the growth factor VEGF, form a stress sensor that plays a key role for the adaption of the cell tissue adhesion strength to the varying hydrodynamic shear forces in blood vessels [Tzima et al 2005].

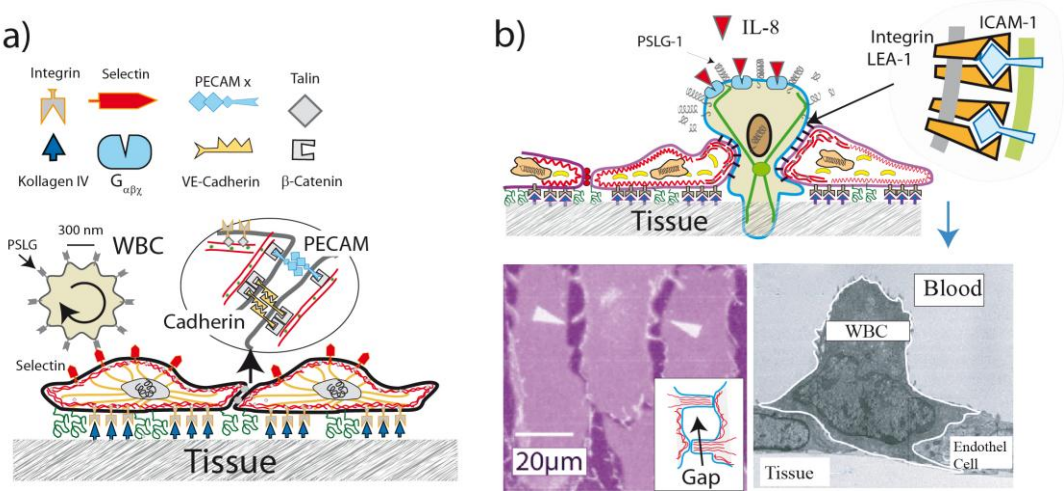

Figure 13 *Schematic view of endothelia cell monolayers with ahering WBC in the resting state.The leucocyte (WBC; shown on the left side) exposes ~5000 microvili (length 0.3-0.5 µm; width 150 nm, [Hammer and Apt 1992]). The number of PSLG-1 receptors (5x105) is 100 times larger than that of microvilli, suggesting that the tip is coupled to several PSLG-1-*

selectins bonds. The WBCs expose receptors for cytokines (abbreviated as $G_{\alpha\beta\gamma}$) which activate the cell through the heterogenous membrane bound GTPase $G_{\alpha\beta\gamma}$.

(a) Pentration of excited lymphocyte through the ENC-layer triggered by cytokines (such as interleukin-8). They bind to specific receptors on the blood cells which increases the density of high affinity integrins LFA-1 on the WBCs while the repellant glycoproteins .are removed from the front. Bottom right: electron micrograph showing activated cell (granulocyte) penetrating through endothelial cell monolayer (reproduced from [Cinamon et al 2001]) The driving force is provided by the he gain in binding energy between integrin (LFA-1) and ICAM.. Bottom left: opening of gap between ENC monolayers by the hormon histamin and thrombin after[Feneberg et al 2004].

A key adhesion controlled process considered here is the enforced permeation of leucocytes through the walls of the vessels at sites of inflammation. Most of the time the WBC patrol the body by rolling along the surface of the endothelium. The velocity depends on blood flow velocity V_B , varying from v = 6± μmsec-1 for $V_B \approx$ 400 μmsec-1 to v=70 ± μmsec-1 for 1400 μm sec^{-1}. This V_B dependence is expected since the shear force in blood capillaries (radius r) is proportional to V_B. The radius of granulocytes is $R_{WBC} \approx 5\mu m$ $R_{WBC} \approx 5\mu m$, the blood viscosity and the total force on the cell is about 10^{-9} N [Atherton and Born 1973].

To maintain the WBC on the surface of the endothelium during their rolling motion they are locally coupled to the endothelial cells (EC) by specific binding between CAMs of the selectin family on the ENC surface and the (about 10^5) glycoprotein PSLG-1 on the blood cells. The PLSG-1 linkers are accumulated on the tips of the ~ 0.5 μm long microvilli extending from the cell surface. The number of microvilli varies from 1000 to 1000 (for numbers see [Hammer and Apt 1992]). PSLG-1 exhibits a FERM binding domain and can thus couple to the actin filaments penetrating into the villi, via moesin or ezrin (see [Majstoravich 2004] and [Sundd 2012]). In this way the WBC-ENC bond strength can be rapidly adapt to shear stress (Σ) fluctuations by changing the area of contact between microvilli and ENC [Majstoravich 2004]. This adaption can be explained now in terms of the force induced increase of the linker density as demonstrated by biomimetic model studies (see Figure 9 Chapter VI.3).

A dramatic change of behavior of the WBC occurs at sites of inflammation by binding of cytokines to $G_{\alpha\beta\gamma}$ linked receptors, triggering the increase of the integrin (LFA-1) affinity (see Glossary " Integrin activation" and [Lun et al 2002]). The cell becomes polarized with the front adhering strongly on the surfaces of adjacent ENC by binding of the high affinity integrin LFA-1 to ICAM-1, while the repellant selectins are cleaved at the front by proteases or move to the trailing end.

Interestingly, the density of high affinity LFA-1 linkers is drastically increased by exocytosis of vesicles loaded with LFA and proteases [von Andrian et al 1991]. The polarized state of the cell is stabilized by microtubule actin cross-talk as described below (Figure 14).

VII.4. Adhering Cell polarization by Actin-MT Crosstalk.

The biological examples shown above confirmed and underlined the important function played by repellant CAMs for the control of cell adhesion as suggested by biomimetic model studies. The repellers are linked through FERM binding proteins (say ezrin) to the actin cortex and can actively control the shape of adhering cells, such as the polarization of T-cells in lymph tissue [Nigel et al. 2002], [Walker and Green]. The front adheres tightly to APC through integrin-ICAM-1 links (forming immunological synapses or SMACs), while the repellant selectins and CD43 move to the trailing end (often called uropod), where they can adhere weakly on endothelial cells or tissue through the repellant CAMs.

MT as scaffolding complex and cell polarizer: The MT plus-ends associate with F-actin via plus-tip proteins (such as Clip 170). They simultaneously act as scaffolding complexes which recruit several effector complexes involved in the structuring of the actin network. First, it can recruit Rac-1 and WASP and trigger the local growth of branched Arp2/3 linked actin as shown in Figure 14d and demonstrated by Dovas and Cox [Dovas and Cox 2010]. Second, it can associate with ezrin and the activated Rho-A GTPases (RhoA*). RhoA* activates the kinase ROCK (=Rho-associated protein kinase) which in turn triggers the formation of active micro-muscles couple to adhesion domains serving the retraction of uropods during cell migration (see Figure 14c).

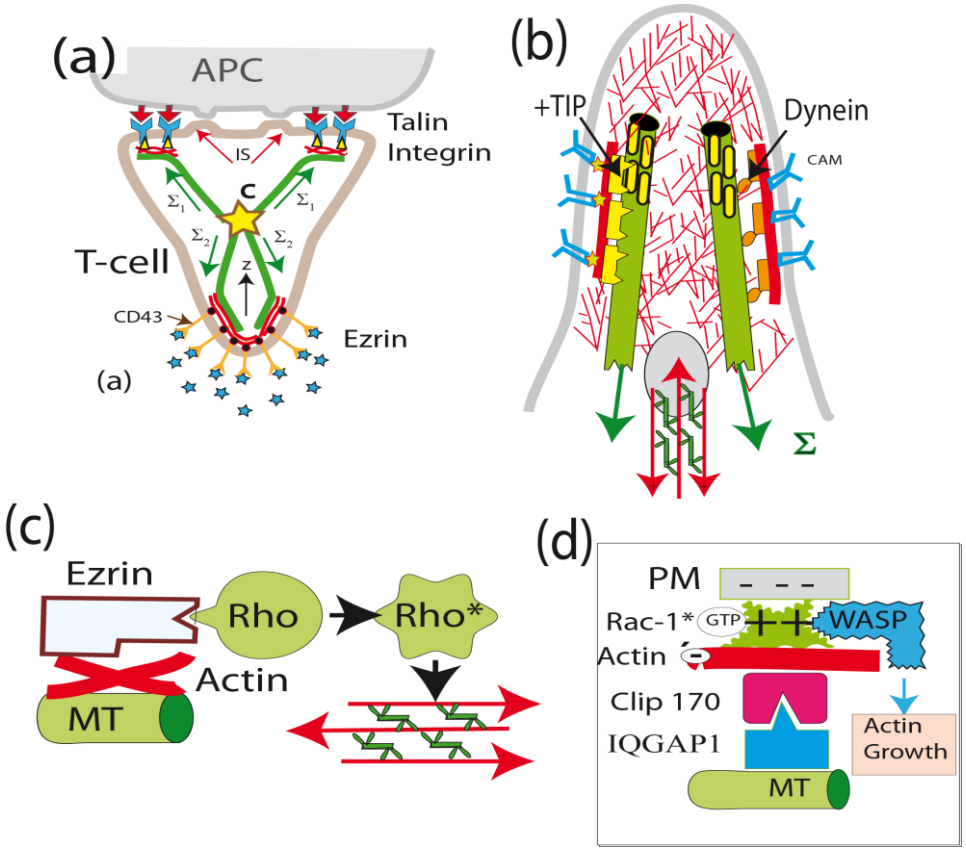

Figure 14 *(a) Model of bipolar polarization of T-cells moving in lymph tissues and encountering an antigen exposing dendritic cell (see BOX Figure 1a). Note that the mechanical cell stability is determined by the balance of the traction forces in the MT which can be generated by passive MT-actin coupling or dynein motors (as shown in Figure 9b). (b) Detailed view of rear of polarized cell showing the MT-actin coupling by passive linkers (left) and dynein motors (right). The yellow bars on the MT plus ends stand for regulators of the actin polymerization such as the IQGAP/Clip 170 complex which activates the actin gelation (see (c)).*
(c) Mechanism of F-actin-MT coupling via the complex Clip170/IQGAP1, which can recruit and activate Rac-1 which in turn activates the actin polymerization promotor WASP.[Dovas and Cox 2010]. (d) Activation of Rho-A GTPase coupled to ezrin -MT complex. GTP-Rho-A triggers the activation of the myosin-light chain kinase (MLCK), resulting in the self-assembly of stress fibers (micro-muscles) which are coupled to adhesion domains.

The global cell shape is stabilized by passive and active coupling of the microtubules to the actin cortex. Active coupling is mediated by the ADAP-dynein complexes-as shown in Figure12, and passive coupling mediated by plus end binding proteins (+TIPs) such as the IQGAP-1/CLIP 170 complex (Figure 14d). The traction force in the first case is determined by the number (n) and activity (force f) of dynein motors: $\vec{\Sigma}_{act} = n\vec{f}$ and in the second by one dimensional analogon of Equation 4a. In equilibrium the sum of all traction forces must be zero:

$$\sum_1 \vec{\Sigma}_i = \sum_i \vec{\Sigma}_{i,act} + \sum_i \vec{l}_i \, w(1-\cos\theta_{ci})^{-1} . \qquad (13)$$

$\vec{l}_i$ is a unit vector in the direction of the microtubule, w is the energy per unit length gained by the binding of actin to microtubuli through the plus end proteins (see Figure 6). Any shape change triggered by external forces can be balanced by changes in the traction forces. The adaption of the actin-MT coupling to external forces is very rapid (~0.1 sec) as demonstrated by magnetic tweezers experiments [Heinrich and Sackmann 2006].

The complex between MT tips and ezrin triggers the activation of the Rho-A GTPase. This results in the self-assembly of micromuscles [Majstoravich et al. 2004] serving the retraction of the uropod during cell migration.

VII.5. Adhesion controlled pathfinding of axons by filopodia

The growth of axons in tissue is guided by interplay of cell-cell and cell-tissue adhesion. Axon growth cones penetrate in a quasi-random fashion through the tissue (Figure 13). From the tip of the growth cone and the shaft, finger-like extensions (filopodia) protrude randomly, searching for signals from other cells or for adhesion sites. Two major regulators of axon pathfinding are integrin-laminin adhesion domains and signal molecules of the ephrine family recognized by specific cell surface receptors. The growth direction is controlled by two adhesion mediated signaling pathways:.

The laminin mediated pathway: filopodia are pushed forward by prolongation of actin bundles, triggered by stimulation of the growth promotor formin (Dial-1) activated by the GTPase Cdc42 [Faix and Rottner 2006], [Lan and Papoian 2008], Zidovska and Sackmann 2001]. The protrusions encountering clusters of laminin in the tissue are stabilized by recruitment of high affinity integrins ($\alpha_6\beta_1$) and by binding of FERM proteins, (such as ezrin), to the integrin beta-chains (see Figure 12). This requires the assembly of a minimum number of integrins and PIP2/PIP3 at the tip of the long protrusions which may be several µm long. The PIP2/3 serves the activation of Cdc42 recruitment to the plasma membrane through electrohydrophobic forces [5]. Integrins and PIP2 (or PIP3) can be enriched at the tip by rapid transport through the motor protein myosin X which exposes both FERM domains and PIP2/3-binding pleckstrin homology domains (see [Watanabe et al 2010] and [Zidovska and Sackmann 2011]). The tips of the stablilized filopodia act as loci for the growth of branched Arp2/3-linked actin network. The growth of branched actin gels is assumed to occur through the activation WASP through MT-coupled activated GTP-Rac-1 (see Figure 12b). Moreover, Rac-1 serves the stabilization of the MT by de-activation of the microtubules destabilizing factor stathmin.

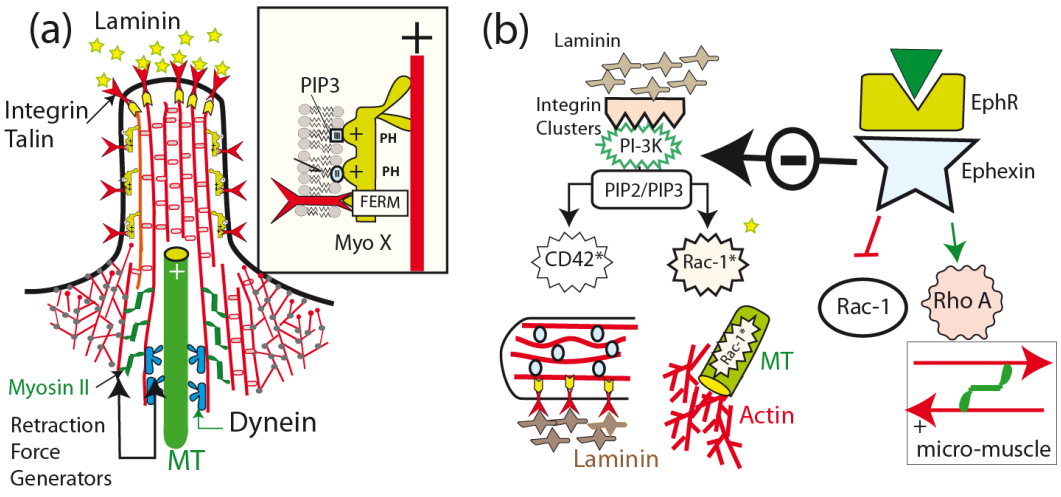

Figure 15 *Protrusion and retraction of filopodia. (a) Filopodium with partially penetrating microtubules and assemblies of actin-myosin II micro-muscles at base of actin bundles. The MT tip can recruit Rac triggering the branched actin gel growth as shown in (b). At the base actin-myosin stress fibers can be formed by activated Rho-A GTPase which serve the retraction of the filopodia. The tip can form adhesion domains by binding of integrin to laminin clusters (see text).*
(b) Left side: Activation of GTPase (Rac-1, Cdc42) through PI-3K, stimulated by integrin-laminin clustering (see Figure 24). The activated GTPases are bound to stable MT and to*

[5] A detailed summary of the membrane binding and activation of enzymes by electrostatic and hydrophobic forces can be found in "Hydrophobic-Electrostatic Membrane Coupling of Proteins "Lectures in Biological Physics www.biophy.de

actin bundles via IQGAP/Clip 170 complexes (see Glossary). Thus both branched and bundled actin gels can form. Right: activation of Rho-A by the ephrin mediated pathway which activates Rho A through the specific guanine exchange factor (GEF) ephhexin. Note that Rho-A inhibits the PI-3K mediated pathway and thus the actin polymerization . This facilitates the retraction of the filopodia as shown in Figure 15.*

*The ephrin-mediated pathway (Figure 16)**:*** The long range pathfinding of axons is controlled by signaling molecules of the ephrin (eph) family and the conjugate receptors (ephR). Ephrins are membrane bound signaling molecules and thus require cell-cell contact to become active. Figure 16 shows the repulsion of axon cones by neurons exposing ephrine B2 binding to Ephr-B. This triggers the activation of Rho-A via the specific guanine exchange factor (GEF) ephexin which is activated by membrane anchoring through binding to PIP2/PIP3 via pleckstrin domains (see Glossar "GTPase activation").

Excited GTP-Rho-A activates the kinase ROCK which switches on the myosin light chain kinase (MLCK) and triggers the activation of actin-myosin micro-muscles in the growth cone (see Figure 15b). They can pulled back the filopodia, provided they are not bound strongly to the substrate via laminin-integrin clusters. In fact, the adhesion strength of these adhesion domains can be reduced by two universal mechanisms:
First, by inhibiting the actin polymerization through activated GTPases (Cdc42 and Rac-1). As shown in Figure 15b this occurs simultaneously with the activation of Rho-A by ephexin which inhibits the PI-3K mediated pathway.
Second, by decomposing the actin membrane linker talin (or ezrin) through the protease calpain, which is activated by binding of R-Ras to the transmembrane protein Fram 38 (which is located in the ER-membrane). This protein triggers the release of Ca from Ca-storing vesicles which activates the Ca dependent protease [McHugh et al. 2000] (see also Glossary integrin affinity).

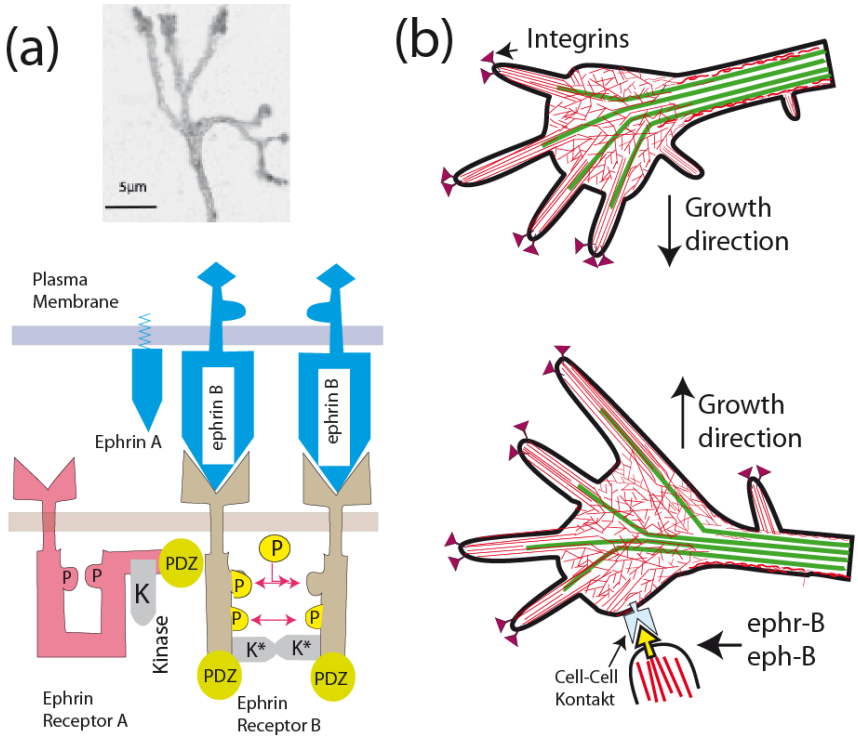

Figure 16 *Ephrine mediated retraction of filopodia and redirection of axon growth. (a) Top: typical view of tip of axon growing on laminin covered surfaces (modified after [Grabham2003]). Bottom: schematic view of membrane bound signal molecules ephrins (A and B) and receptors Ephr-B (of RTK type) embedded in top and bottom membrane, respectively. The left side* number of CAMs needed to activate actin gel formation by binding of integrin □-chains to FERM proteins. *shows a single receptor in the sleeping and the right a dimer in the active conformation, in which the tails are mutually phosphorylated and the kinase K is activated. Note that the stimulation of the ephr-B occurs by mutual phosphorylation of the cytoplasmic domains of two receptors. Activation is therefore only triggered by clusters of eph-R*
(b) Retraction of filopodia at bottom by activation of Rho-A GTPase through interaction of the Ligand eph-B, exposed by target neuron, with receptor ephr-B on growing axon. The axon grows in a new direction.

The above examples show: by studying the guidance of axon growth we can learn much about the interactive control of adhesion by interfacial forces and cell signaling. To act as feelers of the environment, the several µm long filopodia-like protrusions must expose actin coupled CAMs at the tip and also PIP2/PIP3 to promote actin bundle growth by GTPase switches (such as Cdc42). These activators can be transported to the tip by myosin X walking on actin filaments with speeds of 500 nm sec^{-1} [Watanabe 2010]. The adhesion domain formation mediated by the EM proteins enables cells to adhere strongly and resist the retraction forces until branched actin gels are formed. Further studies are required to find out whether the weakening of the links by Rho GTPases (shown in Figure 15b) is universal mechanism of dynamic adhesion strength control.

VIII. Myelin Sheet formation Requires the Suppression of Electrostatic Forces.

Introductory remarks: An enigmatic adhesion process is the formation of lipid/protein multilayers (myelin sheaths) around axons of vertebrates. The introduction of the myelin was an essential step towards the evolution of vertebrates. It allowed nature to overcome the problem that the propagation velocity of nerve signals in axons decreases with the square root of the inner axon diameter. It accelerated the propagation speed of action potentials from 1 m sec^{-1} of Squid axons to 100 $msec^{-1}$ of human beings . Imagine how big human beings would have to be to achieve the same speed by using the classical squid axons? For more details on the nerve conduction and references see [Sackmann and Merkel 2010] Chapter 16)

In the CNS the myelin is formed by oligodentrocytes wrapping collapsed lobes of their envelope several times around the axon tube. In the peripheral nerve system myelin is formed by Schwann cells. The major difference between the two cells is that Schwann cells form only one myelin wrapping around the axon and remain bound to it, while oligodentrocytes can form several myelins at different axon cables, enabling a much higher packing density of myelinated axons (see Figure 1).

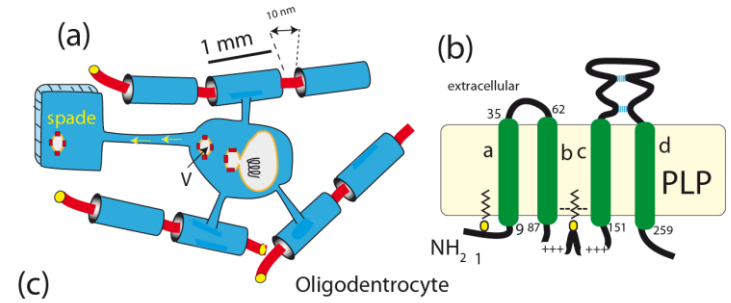

Cholesterol	Sphingomyelin	Phosphatodylserine	galactolipid	Cerebroside	Cerbroside Sulfonated
50 mole %	8 mol%	5% mole%	27 mole%	23mole%	4mole%

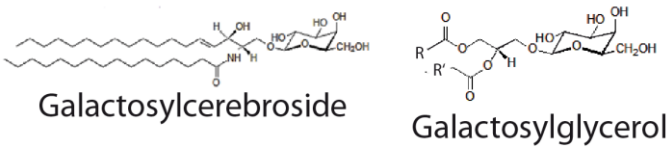

Figure 17 *Oligodentrocytes generating axon sheath around several axons in the central nervous system. The cells extends filopodia-like protrusions. If the tip encounters naked axons they form flat plate like plates by tight adhesion of the two juxtaposed plasma membranes (see Figure 2b). As indicated in Figure 1a by the arrow, the flat plate is generated by constant transport of vesicles (split form the endoplasmatic reticulum) which carry the membrane proteo-lipd proteins PLP (PLP and DM 20). (b) Molecular structure of integral membrane bound proteo-lipid protein PLP and DM-20. Both isoforms span the membrane with four alpha helices, but DM-20 differs from PLP by the lack of the segment between helix b and c*

which exhibits 6 basic residues, Moreover, bothe proteins are anchored in the intracellular leaflets by several fatty acid chains (see [Weimbs and Stoffel 1991]).

(c) Lipid composition of axon in mole % (assuming that the molecular weight of cholesterol is half that of phospholipids. 20 % of the cerebrosides are sulfonated by replacement of CH_2OH by a negative SO_3^- group. The bottom shows the molecular structure of the galactosylceramide (also called galactocerebroside) and galactolipid . The latter has the same structure as phospholipids with the phosphate negative phosphate groups replaced by polar galactose. Note that sphingomyelin has the same structure as cerebrosides and column 4 comprises also this lipid..

Composition of myelins: The lipid composition of cells of the CNS differs remarkably from that of body cells (see [Sackmann and Merkel 2009], Chapter 9]), while that of oligodendrocytes and other cells of grey matter is quite similar (see Figure 17c). The cholesterol content of the plasma membrane of oligodentrocytes (50 mole%) is somewhat higher than that of erythrocytes (~45 mole%). The sphingomyelin content of the brain cells is by a factor of 2 lower. But this reduction is compensated by a rather high content of cerebrosides which exhibit the same sphingosine backbone. Another remarkable feature is the high content of glycerophospholipids (galactolipid). This component exhibits the same backbone as phospholipids while the head group is polar instead of zwitterionic or charged. Two major acidic lipids are phosphatidylserine (5%) and cerebrosides with acidic sulfate groups (4.8 mole%). The former is located in the cytoplasmic leaflet and plays a key role for the collapse of the juxtaposed plasma membrane by the myelin basic protein (MBP, see Figure 18). The latter resides in the extracellular leaflet.

Most remarkable is the change in the fatty acid chain composition during the development. During the first 20 days after birth the palmitic acid (C16) chains are replaced by stearic acid (C18) which eventually amounts to 80 %. Simultaneously the cholesterol content increases. In summary, in adult brains myelin preparations contain cholesterol: phospholipid: galactolipid in a molar ration 4:3:2

The protein composition of myelin is unique. Myelin formation is mediated primarily by two protein families: the positively charged myelin basic protein (MBP) and the proteolipd protein[6] (PLP) and its isoform DM-20:

- MBP induces the tight coupling of the two juxtaposed plasma membranes

of the spate like lobe. The collapse of the plasma membrane lobe is mediated by electrostatic interaction between basic residues of the MBP and the acidic lipid of the intracellular leaflet, which contains about 5% acidic phosphatidylserine. Measurements of the interfacial forces

[66] Proteolipids are specific type of protein with attached fatty acitds including myristic acid and palmitic acid.

with the surface force apparatus suggest that the collapsed plasma membrane lobe is about 5nm thick [Hu et al 2004], in good agreement with the electron microscopic measurement of the electron density map (see [Quarles et al. 2006]) and figure 18.

- The PLP family comprises two members: PLP and DM-20. They form four membrane penetrating alpha helices (a-d in Figure 17). Elegant biochemical analyses show first, that the N-and C-terminal penetrate into the cytoplasmic side, together with a loop of 34 amino acids, and second, that the extracellular side forms a short loop (~25 residues) and a long loop (~56 residues) folded by two S-S bonds on the extracellular side (see dashed bars in Figure 1b and [Gow et al 2004]). The intracellular loops between the helices b and c harbors 6 basic residues which bind to charged lipids. The loops are the further anchored in the membrane by four fatty acids [Schliess and Stoffel 1991]. PLP binds strongly to microdomains rich in cholesterol (rafts) [Simons et al 2000], which in turn are expected to assemble with long chain saturated lipids (C18), such as the galacto-cerebrosides and glacto-glycerolipids. This conclusion is suggested by the phase diagram of phospholipid-sphingomyelin- cholesterol mixed membranes [Sackmann 1996 and (Merkel and Sackmann 2010], Chapter 9]. Further evidence for this pretention is provided by the finding that the long chain saturated lipids become enriched during the myelin formation as mentioned above.

The high content of saturated lipids and cholesterol plays an essential role for the function of myelin sheath as electrical insulators. Mixtures of cholesterol and saturated lipids are fluid and are distinguished by high lateral packing densities and, as a consequence, by high lateral compression moduli K. Thus K is 3 to 4 times higher for 1:1 mixtures of cholesterol with myelin sphingolipids than with phospholipids (see [Sackmann 1995] table I). Since the passive ion permeability of lipid bilayers is inversely proportional to the compression modulus, the insulating properties of myelin are much better than those of normal cell envelopes (see conclusions).

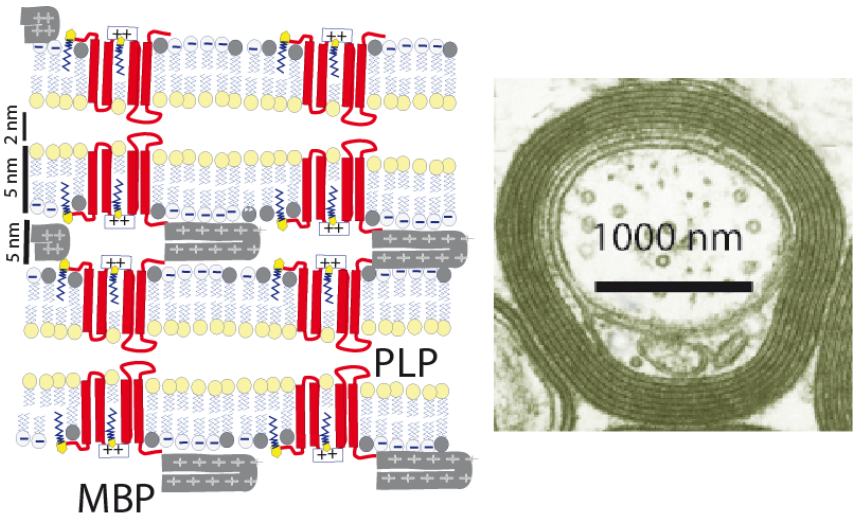

Figure 18*Model of myelin sheath as suggested by electron microscopy and biochemical analysis of the PLP proteins. The juxtaposed plasma membranes of the spate like protrusions*

(see Figure 17) are attracted by the myelin basic protein (MBP). The distance between the surfaces is ~5 nm as suggested by surface forces studies [Hu et al 2004]. The distance between the surfaces of the extracellular membrane leaflets is about 2.0 nm. The right side shows a myelin wrapping from the CNS (Figure reproduced and modified from [Quarles et al. 2006].

Physical basis of myelin membrane collaps.

From the point of view of the physics of cell adhesion myelin formation by condensation of opposing plasma membranes lobes (coupled by MBP) is amazing, considering the repulsive interfacial forces mediated by membrane bending excitations and the glycocalix constituents . In the discussion of electrostatic interfacial forces in Appendix C we saw that the glycoproteins would certainly prevent myelin formation. Even after removal of these repellers, van der Waals (vdW) attraction is overcompensated by the electrostatic disjoining pressure generated by 5 mole % glycolipids at interfacial distances larger than h=1.5 nm.

This enigma was solved in recent elegant studies of myelin formation by Bakhti et al [Bakhti et al 2012]. These authors showed by various biochemical and biophysical techniques that a prerequisite of myelin formation is the down-regulation of the acidic glycolipid synthesis and the glycoproteins. The adhesion between the collapsed cell lobes forming the spate like myelin sheets is then expected to be determined by the balance of VdW attraction and steric repulsions. The vdW attractive potential at h=2 nm is of the order of $V \approx -k_B T / 12\pi h^2 \approx 3x10^{-4}\, Jm^{-2}$ (corresponding to an attractive pressure of 10^5 Pa ,see Appendix A).

The inter membrane distance of h≈2nm could be determined by the repulive force mediated by the external loop of the LPL and the head groups of the galactolipids which are about 0.6 nm long. The average lateral distance between these lipids (comprising 30 % of total lipid) is about 1.5 nm and the galactose head group could thus well maintain a distance of h~1.2 nm

The short extracellular distance of ~ 2 nm and the presence of the high content of the polar galactolipids (instead of zwitterionic and acidic lipids) at the outer leaflet of the plasma membrane improves the electrical insulating properties of the myelin. Due to the low content or even absence of zwitterionic lipids the ion concentration is very low. Consequently, the ohmic resistance and therefore the energy dissipation during the actin potential propagation is very small. In other words the myelin sheath comes close to an ideal capacitance with zero energy loss.

In summary, the formation of myelin shows most impressively how nature optimizes many physical properties of bio-membranes by adjusting the lipid composition. The myelin formation requires the rapid transport of vesicles carrying the PLP to the tip of the filopodia-like protrusions. An interesting question is whether the vesicle transport is accelerated by the formation of networks of tube like protrusions penetrating from the endoplasmatic reticulum to the tip of the protrusions. As shown by the group of Rapperport such reticular networks are formed by a family of proteins called reticulons. As shown by Gow et al [Gow et al 1997]

such reticular networks of ER tubes form indeed during overexpression of PLP. In this way the newly synthesized PLP could be transported to the tip of the protrusions by lateral diffusion. The physical basis of the formation of reticular networks of ER tubes has been proposed in E. Sackmann “Lecture Notes on Biological Physics” “Endoplasmatic Reticulum Shaping by Generic Mechanisms and Proteins” , freely accessible via www.biophy.de.

Physics of cell adhesion Part II:

The role of the glycocalix.

Abstract:

In this part we discuss several biological examples showing the important role of the glycocalix. Mixed microdomains of integrin and glycoproteins can form by actin mediated co-clustering and act as reaction centers triggering cell proliferation. A phosphorylation switch (based on the actin-membrane coupler merlin) enables the on-off switching of cell proliferation. A unique role is played by the multifunctional glycoprotein CD44 which can act as activator and inhibitor of cell adhesion and trigger cell division by lateral coupling with growth factor receptors. A model of lateral inhibition of cell proliferation by the growth factor blockade through CD 44 grafted hyaluronic acid films is described. Finally, some ideas on the dysfunction of the adhesion by transformed cells are discussed,

IX.1 General Structure of Glycocalix.

Introductory remarks: Most work on cell-tissue adhesion concentrates on the role played by integrin and adhesion-mediated integrin clustering for the regulation of cell proliferation and migration. From model membrane studies we learned that integrin clusters formation requires that the CAMs are mobile in both surfaces or the ligands of tissue must by clustered as well (see [Ana Smith 2008]). Under physiological conditions the density of ligands exposed by the tissue surfaces is low and the ligands recognized by CAMs such as fibronectin or collagen IV are immobile. This is where the glycosilated membrane proteins forming the glycocalix come in. Major representatives include: membrane bound syndecans**,** the hyaluronic acid receptor CD44, the glycoproteins exposing large head groups, such as CD43. These proteins expose 40 to 50 nm long and semiflexible oligo-sacharides which bind and penetrate into the tissue. The role of the glycocalix has moved in the center of interest since the discoveries that the transformation of cells is often accompanied by modifications of the glycocalix. In the following we discuss the control of cell adhesion and cell locomotion by the glycocalix on the basis of the general physical concepts suggested by the model membrane studies and theoretical models.

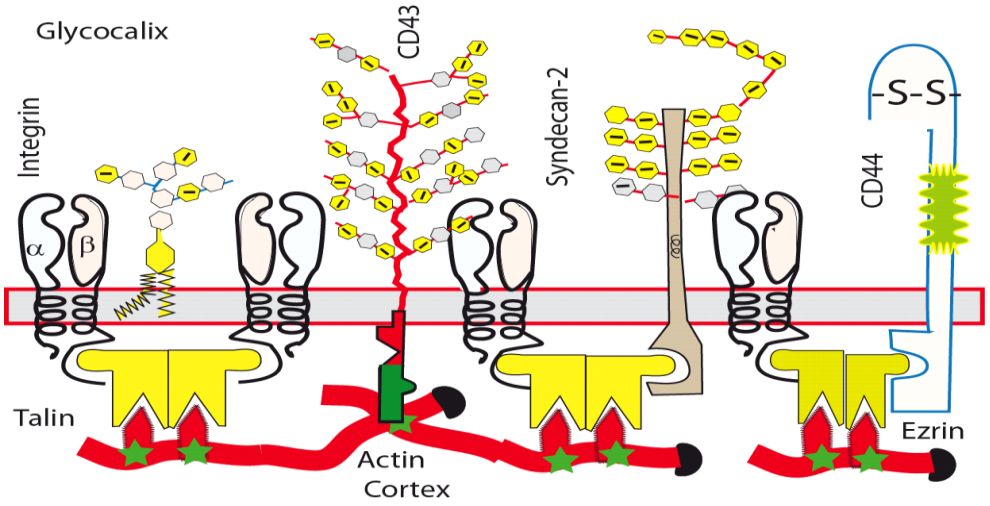

Figure 19 *Schematic view of composite cell envelope, stressing the intimate coupling between the membrane proteins involved in adhesion and the actin cortex. Many major proteins forming the glycocalix expose specific peptide domains which bind FERM homology domains of actin-membrane coupling proteins band IV, ezrin, radixin, moesin (FERM) family. Many of these proteins form dimers and can connect pairs of membrane proteins, such as two integrins or integrin with syndecan. In this way adhesion domains may be formed in which different CAMs are assembled.*

The glycocalix controls cell adhesion, proliferation and migration in various ways:

1. It is highly negatively charged and can therefore control the access of growth factors and cytokines to the receptor binding sites or store and enrich small signal molecules or anticoagulant factors impeding thromboses.

2. The reorganization of the constituents of the glycocalix plays a key role for the polarization of cells during locomotion (see Figure 14a).

3. The extracellular domain of glycoproteins such as syndecans and Cd44 can be cleaved by proteases close to the cell surface and switch cells from adhesive to non-adherent states.

Below we summarize some examples of fundamental importance.

IX.2: Integrin Clusters act as Reaction Centers Mediating Cell Proliferation

Introductory remark: In the adult body cell proliferation is frequently mediated by adhesion-induced clustering of integrin together with the recruitment of receptor tyrosin kinases (RTK). Activation of RTK triggers the binding of activated FAK to integrin β-chains. FAK is activated whenever tyrosine kinase receptors are recruited to the integrin clusters and receive a signal molecule. In resting cells FAK resides in the cytoplasm in a sleeping configuration by self-binding of the C- and N-ends (see Figure 16; [Parson 2003] and Glossary “FAK”). After activation it exposes a FERM domain and can constitutively

associate with the β subunit of integrin receptors. Activated FAK stimulates the PI-3K kinase by phosphorylation, which in turn switches on the protein kinase B (PKB ≡ Akt). FAK can switch on PKB also via other pathways such as by the excited fragments of the heterogeneous GTPase $G_{\alpha\beta\gamma}$. (For other functions of FAK visit Glossary "FAK"). The activated PKB controls cell proliferation by a rather involved mechanism, shown in Figure 20, below.

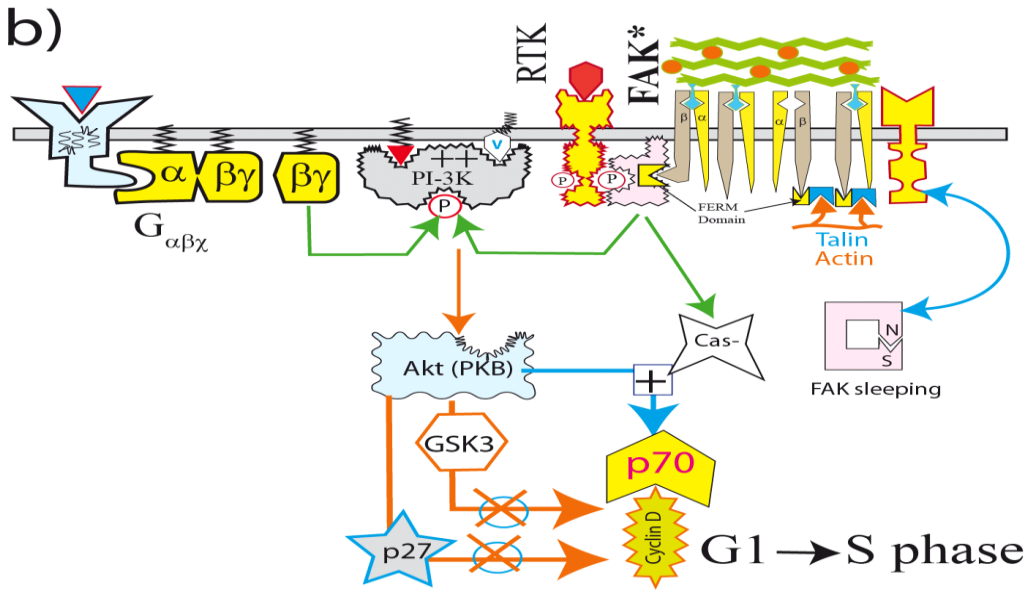

Figure 20 *Simplified view of general mechanism of cell proliferation via signal pathways triggered by the PIP3-generator PI-3K (see Glossary) which is mediated by the protein kinase B (Akt). Two mechanisms of PI-3K activation are shown: Left: Activation by the heterogeneous GTPase $G_{\alpha\beta\gamma}$ and right: by RTK hormone receptors. In the resting state FAK resides in a sleeping conformation in the cytoplasm by complex formation of the N-and C-ends. The activated FAK can constituently interact with integrin through binding of its FERM domain to the beta chains. At the bottom, the regulation of cell growth and survival by activation of the PI3K/PKB (Akt) pathway is shown which is described in the text below. Please note that in reality PKB is activated by membrane linkage to specific lipid anchors such as diacylglycerol (DAG) which is generated by phospholipase C_γ (for details see Lecture Note Electrohydrodynamic switching of proteins www.biophy.de). Note that FAK* can also activate the scaffolding protein Cas (see Glossar Src/Cas).*

The transition of the cell cycle from the resting state G1 to the phase S is mainly controlled by cyclin D and associated, cyclin dependent, kinases. The serine /threonine kinases GSK-3-beta (glycogen synthase kinase 3-beta) mediates the decomposition of cyclin D and the protein p27: an inhibitor of the cell cycle. However, the effect of the two inhibitors is overcompensated by the kinase p70 which is also activated by Akt and which which directly accelerates the biosynthesis mediated by ribosomes.

Now, the old question arises why integrin clustering is essential for cell proliferation. Similar to the situation of the activation of immunological synapses, the phosphorylation of

the cytoplasmic tails of the RTK is counteracted by the membrane bound phosphatases CD 45, unless its access is prevented by domain formation (as shown in Chapter VII.1, Figure 11). Another membrane bound phosphatase with long extracellular domain is CD143 which is found in hematopoetic cells such as T-cells. It exhibits eight to ten fibronectin type III motifs in its extracellular domain corresponding to a length of 35-40 nm nm. Similar to CD45 it is expected to be expelled from tight adhesion domains. Another question concerns the down regulation of the activity to the reaction centers. As in the case of the IS occurs through endocytosis via the clathrin-mediated pathway and degradation of the RTK by lysosomes. Evidence for this model is provided by the observation that dysfunctions of this pathway of signal termination can cause cancer [Bache2004].

IX.3. Membrane bound proteoglycans of syndecan family as CAMs and co-CAMs:

The family of syndecans comprises four members and are expressed in most mammalian cells. Syndecans are membrane bound proteoglycanes consisting of a protein chain (called core protein) to which negatively charged oligosaccharides side chains composed of 10 to 50 disaccharides are coupled. In general, the sugar side chains consist of negatively charged chondroitin sulfate (a disaccharide with two negative side chains: $-SO_3^-$ and $COO^{-\cdot}$) and heparan sulfate (HS) a disaccharide with two negative $-SO_3^-$side groups. The heparan sulfate (HS) chains attach to specific binding sites of extracellular matrix proteins, including fibronectin, vitronectin, laminins and the fibrillar collagens (see [Lodish 1996] Ch. 19; [Albrecht 1996] Ch.19).

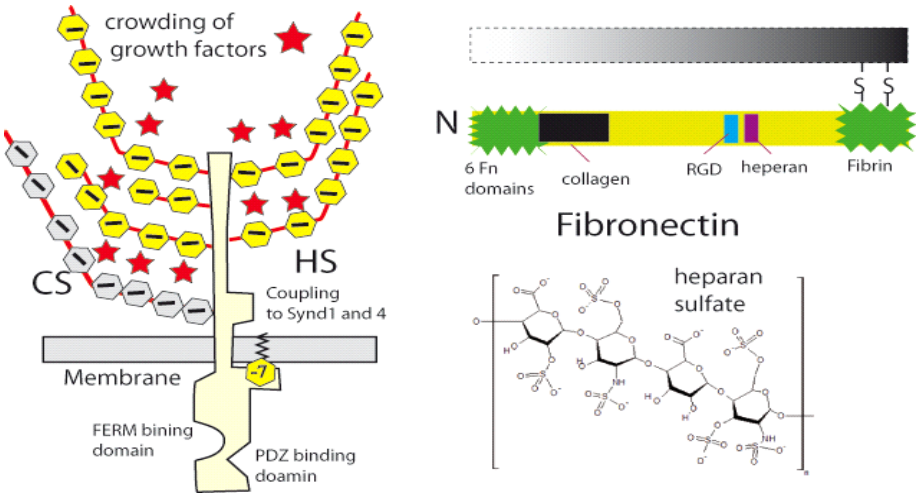

Figure 21 *The left side shows a schematic view of syndecans. The sugar dimers CS and HS can weakly bind growth factors (GF, red stars) and can thus accumulate these signal molecules at the cell surface. The outer domain (the N-terminal) exposes negatively charged oligosaccharides composed of heparin sulfate and chondroitin sulfate. They may comprise 10*

to 50 di-saccharides, each with a length of about 1nm.For that reason the extracellular domains of the syndecans are expected to be straight even at high ionic strengths. Segments of the core protein can mediate the syndecan complex formation. The right side shows at the top the domain structure of fibronectin. It exhibits several binding domains for CAMs. Two monomers are linked by S-S-bonds. Most interesting is the close proximity of the RGD binding sites for integrins and syndecans enabling the binding of syndecan-integrin complexes to the EM. The image at the bottom right shows the structure of the heparan sulfate which binds to many extracellular matrix molecules

The four syndecan family members share some common structural elements (see also Glossary "Syndecan") and can control cell adhesion in various ways. First, they can act as CAMs and mediate the adhesion of cells to the EM**.** Second, the extracellular core protein bearing the glycosaminoglycan chains can be cleaved by metal proteases. The liberated proteoglycan fragments can impede syndecan mediated cell adhesion by binding to the conjugate ligands of the EM. Third, binding of the HS side chains of syndecans to the EM can induce clustering of the glycoproteins at the cell surface. Since some syndecans expose FERM binding domains, actin gel patches can bind to and stabilize the syndecan domains, very similar to the adhesion complex formation by integrin-actin crosstalk.
Often syndecans form lateral domains together with integrins and receptor tyrosine kinases (RTK) to elicit cell proliferation. This mechanism can be well explained on the basis of adhesion induced domain formation (see Figure 20). The long oligosaccharide chains (comprising up to 50 di-saccharides) are much longer than those of integrins. They can extend at least as far out into the extracellular space as the head groups of the glycoproteins CD 43 or the phosphatase CD 45 extending 40 nm), that is the two-dimensional integrin/syndecan clusters can bind to the EM, despite of the presence of CD43-glycoproteins. Most importantly, the syndecans can bind directly to the integrins by lateral attraction or indirectly by coupling to the actin cortex through linker proteins exposing FERM domains.

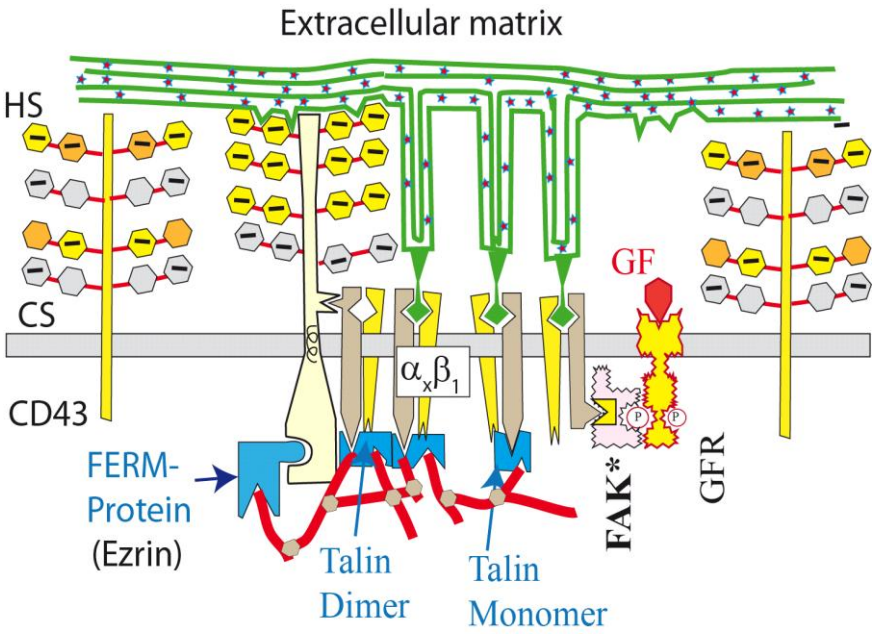

Figure 22 *Formation of two-dimensional integrin adhesion domains in the presence of glycocalix component exposing large extracellular domains, such as CD 43, CD 44 or CD 45. The integrins can form mixed complexes with syndecans or they could be recruited to actin patches assembled by the syndecans. On the right side the direct recruitment of an excited growth factor receptor(GFR) to the integrin cluster is shown. The coupling is mediated by binding of the focal adhesion kinase (FAK) to integrin via its FERM domain.*

In summary, by forming mixed complexes with syndecans, integrins can form adhesion induced micro-domains in the presence of long range repellers. These microdomains could stimulate cell growth by recruitment of growth factor receptors acting as receptor tyrosin kinases as described already in Figure 22. This has been verified for the growth factor insulin which forms complexes with syndecan-1 coupled to integrin $\alpha 5\beta 3$ [Beauvais 2004]. The growth factor receptors cannot bind directly to actin. However, as shown in Figure 22 this is achieved indirectly by recruitment of the GFR to the syndecan-integrin domains. Some cancer mediated modifications of the syndecan pattern on the cell surface and possible dysfunctions of cell signaling will be discussed below.

IX.4. Cd 44 a Key Regulator of Cell Adhesion and Contact Inhibition-Cancer Induced Modifications.

Introductory remark: The hyaluronic acid (HA) receptor CD 44 has become a major target of cancer research since the discovery that many transformed cells overexpress CD 44, for instance by 30% in breast cancer cells. The increased CD 44 expression is expected to play a key role for the invasion of tissue by metastatic cells [Thorne 2004]. CD44 can form several hundred isoforms and small structural changes by mutations can alter their behavior

drastically. Most importantly, CD44 can form cooperative complexes with receptors of growth factors (GFR) and are therefore involved in cell proliferation.

CD 44 can modulate its own expression and control cell migration through its intracellular and extracellular peptide fragments. Extracellular fragments are cleaved by specific metal proteases called sheddases. These fragments can impede adhesion by blocking binding sites on the tissue (as described in Chapter VI.2). The intracellular fragments can control the expression of CD 44 (see Glossar "CD44"). In this sub-chapter some important consequences of these unique features of CD44 for the control of cell adhesion and the dysfunctions of cancer cells will be described.

A major cause of cancer is the loss of the cells capacity to stop cell growth above an upper threshold of the cell density. Cells loose the capacity of sensing the cell density and arrest cell growth by lateral inhibition. Since cells feel each other first through the gycocalix, components of this soft extracellular film are expected to be involved in contact sensing and lateral inhibition. One possible candidate is the HA-receptor CD44, as suggested by the observation that the expression of the glycoprotein CD44 and its variants are drastically changed in transformed cells [Morrison 2004], [Sackstein 2008].

CD44 structure and functions: CD44 is a multi-purpose membrane protein which is involved in several processes controlling the reorganization of the actin cortex during cell adhesion and migration. The CAM consists of three domains: the extracellular domain (363 AAs, segment 1-269), the trans-membrane domain (21 AA) and the C-terminal cytoplasmic domain (72 AAs, segment 290-360). The latter exhibits several specific binding sites for intracellular proteins, in particular, FERM domain or PDZ domain carrying proteins (see [Thorne 2004).

CD 44 exists in a standard form (CD44s) and 10 different splice variants CD44v, which is indicated in Figure 23 by the green corrugated mantle). Due to the glycosylation of the variable domains of CD44v, the molecular weight can increase dramatically from 37 to 180 kDa.

The CD44s is mainly expressed by hematopoietic stem cells residing in the bone marrow. In contrast, the CD44v variants are predominantly expressed in epithelial cells and non-hematopoietic cancer cells. A most important variant discussed further below is the HCELL-receptor which is the major cell surface receptor for hyaluronan (HA).

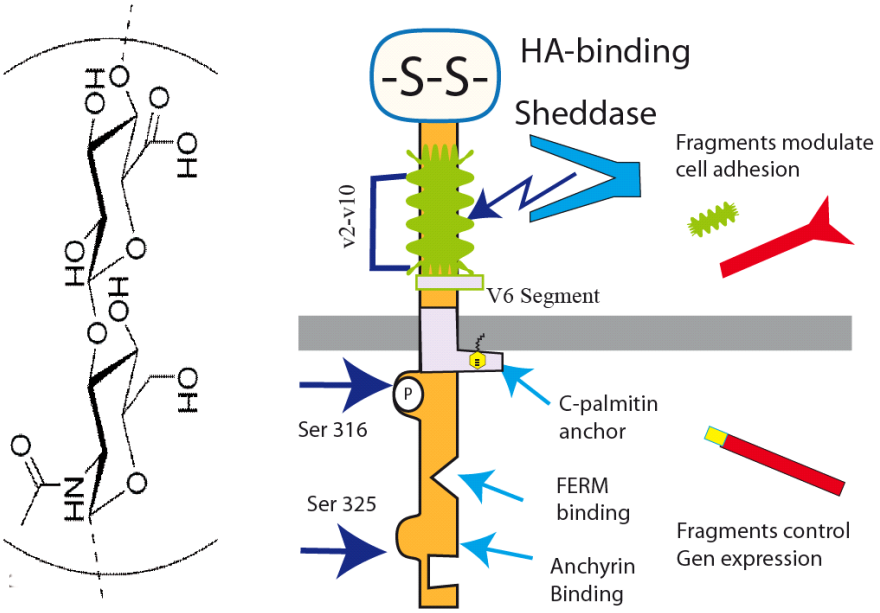

Figure 23 *Domains structure of CD 44. Left: Molecular structure of disaccharide forming HA-polymers. The contour length is about 1nm.*
Right: Domain structure of CD44 receptor. The extracellular domain comprises the HA binding head group (stabilized by S-S-bonds) and the variable domain v2-v10 indicated by the green corrugated mantle. The segment v6 mediates the formation of CD44/RTK complexes. The cytoplasmic domain exposes a PIP2 binding domain which is assumed to stabilize the membrane binding by electro-hydrophobic forces and a binding pocket for FERM domains. The extracellular domain can be cleaved by metal proteases (sheddases) and the fragments can affect the cell adhesion (see text and Chapter VII.4). The intracellular segment can be cleaved by specific proteases and the debris can modulate the expression of various proteins including CD44 itself.

The CD44 variants are modified in many ways by coupling of numerous Glycosamino-glycans (GAG, see Glossary), such as chondroitin sulfate (CS) and heparan sulfate (HS). One major member of this family exhibits a lectin-like domain at the N-terminus pointing into the extracellular space (residues 21-178) which recognizes hyaluronic acid (HA). Another very important CD44 family member, generated by posttranslational modifications, is the HCELL-receptors (where HCELL stands for Hematopoietic Cell E-selectin/L-selectin Ligand). This glycosylated form binds to E- and L-selectins and mediates the transport of human hematopoietic stem cells and mesenchyme cells to the bone marrow. In fact, HCELL is the most strongly binding CAM for E- and L-selectin on human cells. Finally, CD 44 can bind to many other proteins. Examples are: fibrin and fibrinogen but also osteopontin, collagens, metal proteases and the integrin variant VLA-4 (≡ integrin $\alpha_4\beta_1$) which is expressed on the surface of activated leucocytes. CD44 is considered as a receptor of HA (which is a non-

sulfonated GAG). The binding of HA by CD44 is mediated by the lectin like head group. Despite of this structural feature it has been found that cells that display a high density of CD44 do not constituently bind HA. The capacity for HA binding is controlled by the posttranslational modification of the GAGs, such as coupling of SO_3^- carrying sugar molecules.

***CD44 is a growth factor regulator*:** A unique feature of the variable isoforms CD44v is their complex formation with many growth factor receptors (GFR) acting as tyrosine kinase receptors (TRK). These include (i) the receptor c-METR of the hepatocyte growth factor c-MET (considered more closely below), (2) the receptor HER-2 of the epidermal growth factor receptor family and (iii) the receptor TGFR-beta of the transforming growth factor TGF-β, which controls the apotosis, proliferation and differentiation of cells. A well-studied example is the crosstalk of CD 44 with MET-c. MET-c triggers the formation of new blood vessels during embryogenesis. It plays a key role for cancer generation since it stimulates the generation of new blood vessels which is a prerequisite for the formation new tissue. Dysfunctions of the crosstalk is a major cause of cancer of the kidney, liver, stomach, breast, and brain.

Cell proliferation is activated by formation of complexes between TGFR-β and CD44, very similar to the cooperation between RTK and integrins assembled in adhesion domains (see Figure 20). It has been discovered that the lateral coupling of CD44 and the MET-receptor is mediated by a small peptide sequence of the variable domains v6 of CD44v. Cancer development in pancreas can be stopped by blocking the CD44-RTK linkage with synthetic analogs of the peptide segments responsible for the CD44-MET-c binding peptide [Tremel 2009]. Below we will discuss the role of CD 44 as regulator of cell growth.

A phosphorylation switch controls the interaction of CD44 and the GFR:Two most intriguing functions of CD44 are the stimulation of cell proliferation and its arrest by contact inhibition. These opposing functions are regulated by a complex formation between GFR and the two FERM exposing proteins ezrin and merlin. The FERM protein merlin exhibits several unique properties. It exhibits a FERM domain but no actin binding segment, in contrast to the other FERM proteins. This unique property determines the role of merlin as tumor suppressor. Similar to the other FERM proteins (say ezrin) it can exist in a sleeping conformation by mutual binding of the N-and C-terminal (see inset on the bottom left of Figure "24, CD44/merlin"). The supra-molecular complex of CD44, ezrin and merlin has been proposed to function as sensor of cell density. At low cell density, the growth factor receptor GFR, embedded in the complex, constantly stimulates cell proliferation after binding of the GF. This is assumed to occur by activation of the ERK/MAPK pathway (shown at the bottom right of Figure 24). At high cell density the supramolecular complex dissociates by dismantling of the ezrin-merlin complex and cell proliferation is impeded. The cell density mediated control of cell proliferation by merlin is also strongly suggested by the observation that knock out of merlin in drosophila embryos leads to hyper-proliferation. Two possible models of switching between growth activating and growth inhibiting states are described below and in Figure 24.

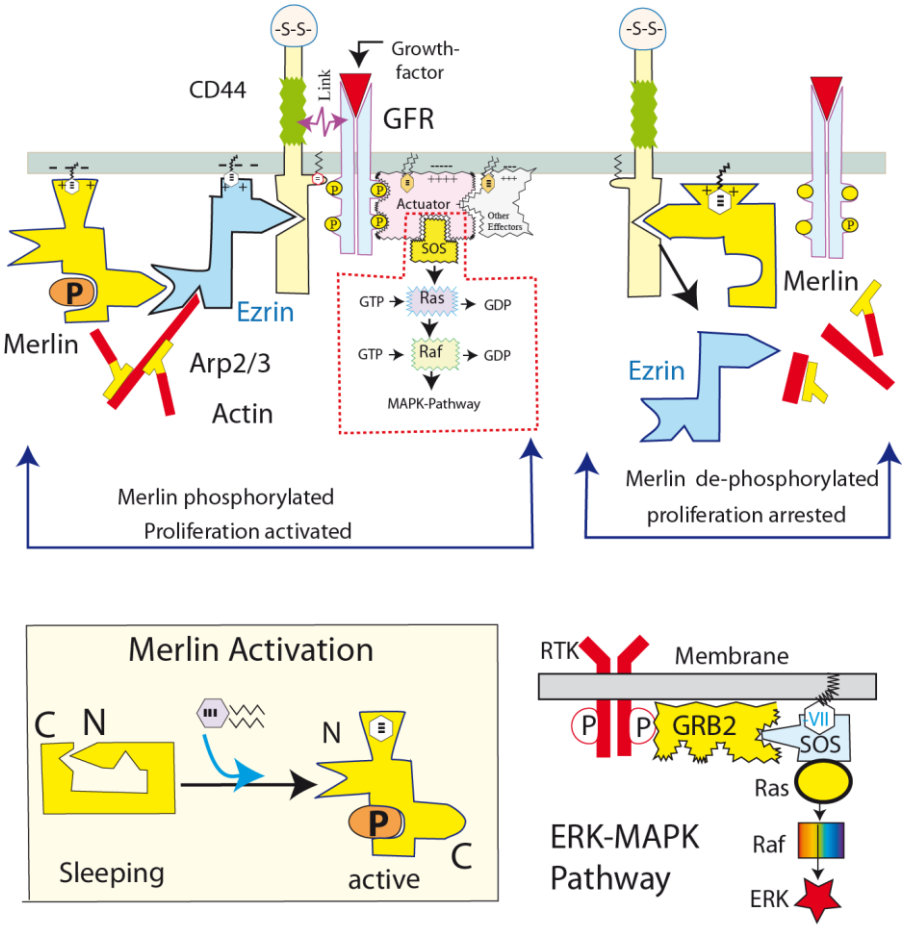

Figure 24 *Schematic view of the transition between growth promoting and growth arresting states of complex between CD44 and the growth factor receptor (GFR). The transition is mediated by switching the merlin state of phosphorylation. Top left side: Growth promoting state established by binding of merlin and ezrin complexes to the FERM binding domain of CD44 which, in addition forms a complex with the growth factor receptor (a RTK). The state is stabilized by phosphorylation of merlin at serine and threonine residues. Cell proliferation is active due to the constituent activation of the RTK within the supramolecular complex. Right side: De-phosphorylation of merlin (by phosphatases) results in the displacement of the ezrin/merlin complex from the CD 44 cytoplasmic tail by direct binding of merlin to the FERM binding domain. The active CD44/GFR/actin assembly dissolves resulting in the arrest of cell proliferation.*
Bottom left side: transition between sleeping and active conformation of merlin by intramolecular complex formation between the N and C termini of FERM domains. Bottom right side: simplified mechanism of cell stimulation by activation of ERK/MAPK pathway through RTK mediated acticvation of scaffolding protein GRB-2 (see E. Sackmann Lecture Notes in Biological Physics accessible via www.biophx.de)

Evidence that the supramolecular complexes of CD44, ezrin and merlin could function as sensor of cell density was provided in elegant experiments by Morrison et al. [Morisson

2004]. They showed first, that the transition from the proliferating to the arrested state is triggered by the de-phophorylation of merlin; second, that the transition sets in above a certain threshold density of cells; and third that the growth arrest is preceded by a 3.5 fold increase of the genetic merlin expression. The de-phophorylated merlin displaces ezrin form the CD44 receptors resulting in the dissolution of the actin gel patches. The model of the phophorylation switch is supported by the finding that the growth can be arrested via dephophorylation of merlin by adding soluble HA, even at very low cell densities (that is within the logarithmic growth regime).

Concluding Remark: The Morrison experiments suggest that cell proliferation by CD44/GFR requires the formation of CD44/GFR microdomains which are assembled by actin gel clusters. Due to the large head group of CD44 the activated GFR could be constantly dephophorylated by CD45 or CD 148, in contrast to the situation in immunological synapses. However, the activation of GFR is generally mediated by mutual phosphorylation of the cytoplasmic tails which act as or bind kinases. Therefore clustering of receptors is essential for their activation (see [Alberts et al 1995 Chapter 15 for an enlightening discussion). The formation of CD44/GF clusters could thus serve the enhancement of the activation of the GFR.

Another question raised by the Morrison experiment concerns the arrest of cell proliferation. As noted above, cell division can be arrested even in the logarithmic growth phase by addition of hyaluronic acid. This can be explained in terms of the steric hindrance of the access of growth factors to the GFR hidden within the glycocalix, as will be described below:

IX.5. Models of growth arrest of endothelial cell monolayers.

The Glycocalix as Selective Filter: Most growth factors are relatively large proteins (radii~5 nm). Examples are the epidermis GF (EGF with 6 kDa) and the hepatocyte GF (10 kDa). Their access to the specific growth factor receptor (GFR) may therefore be impeded at high cell densities due to the tight packing of glycoproteins or by coupling of soluble HA to the cell surface, as observed by Morrison et al [Morrison 2004]. To gain insight into its filter function we consider the glycocalix as an entangled network of polyelectrolytes characterized by the mesh size ξ (see Figure 25 below). Due to the electrostatic repulsion between the charged segments the macromolelcules are considered to be semi-flexible at physiological salt concentrations.

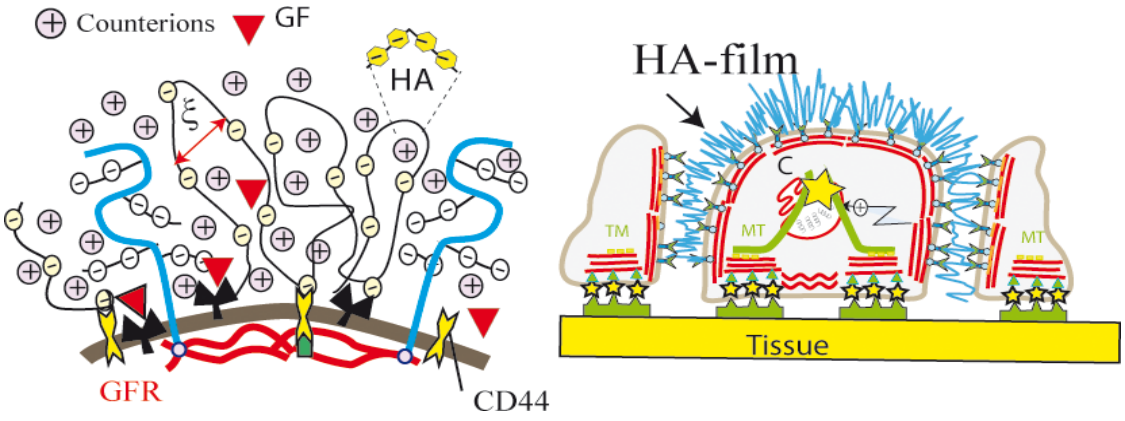

Figure 25 *Left: Schematic view of glycocalix as selective filter that controls access of peptide growth factors. The glycocalix is composed of head groups of membrane bound proteoglycans (CD44, Syndecans) and hyaluronic acid bound to the CD44 receptors. (To simplify the presentation the latter are drawn shorter than their natural length). The fraction of Ha bound to the receptors is increased with growing density of the HA monomers. Right: Simplified view of endothelial cell layer at the onset of growth arrest, with the cell covered by dense layer of polysaccharide composed of head groups of glycoproteins and surface grafted HA (presented as blue coat).*

The diffusion of globular macromolecules of diameter d through the glycocalix can be described in terms of particle diffusion in entangled networks of semiflexible macromolecular. The diffusion is determined by limiting laws:

- First, theoretical consideration based on scaling law arguments suggest that the diffusion coefficient depends of the mesh size ξ as.

$$D(d,\xi) \approx D_o \exp\left\{-\beta\left[\frac{d}{\xi}\right]^2\right\}, \qquad \text{(I)}$$

where ξ is the mesh size of the network (double arrow in Figure 25). This exponential law follows from the assumption that the diffusion of the particle is an activated process (see [de Gennes 1976]). The probability of a diffusional jump is thus determined by $p \propto \exp\{-\Delta G_{ela}/k_B T\}$. If the diameter of the particle is comparable to the mesh size, the diffusion is determined by the elastic energy cost required to expand the network from ξ to d: $\Delta G \approx k_B T\left(d/\xi\right)^2$. Note to physicists: in solid state physics this is often called the Zener model. Equation (I) has been well verified for entangled networks of actin filaments [Schmidt 1989].

- Second, scaling arguments lead to the following relationships between the mesh size and the monomer concentration c, which holds for rod like and flexible polymers, respectively

$\xi \propto c^{-1/2}$ (IIa) $\xi \propto c^{-3/4}$ (IIb)

Combining Eq. (I) and Eq. (IIa) yields

$$D(c,d) = D(0,d)\exp\left[-\beta' c d^2\right] \qquad \text{(III)}$$

where $\beta' \approx 1$. This laws was also verified for entangled actin networks [Schmidt 1989].

We consider HA films as a biologically relevant example. Its molecular weight is typically 1.3 10^6 Da (monomer number N=3100, monomer (Kuhn-) length $\lambda_K \approx 0.8nm$).The correlation between the mesh size and the monomer concentration c within the entangled network can be easily established by assuming that the filaments form a cubic network of lattice constant $a \approx \xi$ and bond length λ. The concentration c of monomers can be expressed as $c = 6.2310^{26}\tilde{c}$ monomers per m^3, where $\tilde{c}$ is the number of moles. By considering a unit cell one can write: $c = 3a\tilde{c}/\lambda a^3$ resulting in $a \approx \xi \approx 2.5/\sqrt{\tilde{c}}\ nm$.

The physiological situation of the Morrison experiment can be mimicked by self-assembly of HA films, anchored on solid supported membranes through the HA binding protein p32 [Schilling 2003]. The thickness of the films varies from $< h > \approx 250nm$ in the absence of salt to $< h > \approx 100nm$ in the presence of 200mM NaCl. The Young modulus increases from E≈ 4Pa to E≈200 Pa. From the values of E the mesh size can be estimated by considering the scaling law $E = \frac{k_B T}{N\xi^3}$.The mesh size for the above salt concentrations is $\xi \approx 7nm$ and $\xi \approx 2nm$. Interestingly, the density of the self-assembled HA-networks does not change remarkably with the density of HA-receptors on the membrane This result predicts that cells covered by a self- assembled HA film at physiological salt concentration blocks the access of the GF of radii >2 nm.

The situation is depicted in Figure 26, were Eq. (1) is plotted as function of the ratio d/ξ.The diffusion coefficient drops by a factor of two for $d/\xi \propto 3/4$, demonstrating the strong impediment of the stimulation of the GFR by the GF at mesh sizes of 5nm.

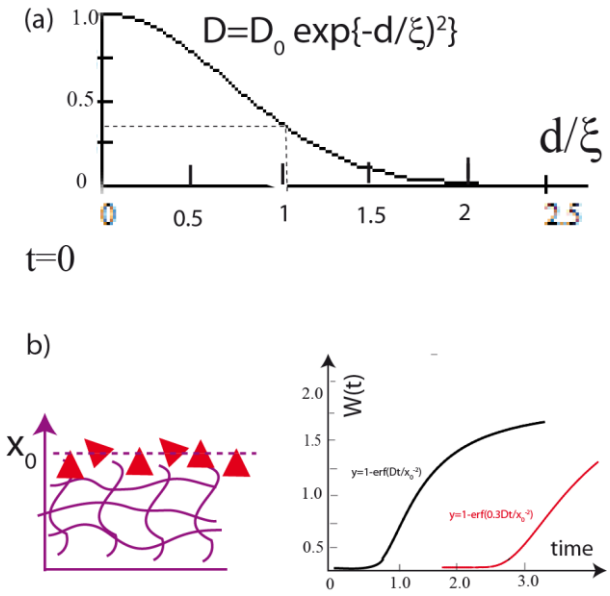

Figure 26 *Cell proliferation arrest by inhibition of growth factor access to the growth factor receptor (GFR). (a) Reduction of diffusivity of molecules in macromolecular network as function of the ratio diameter/mesh size (d/ξ) demonstrating the sharp reduction of D at $d \rightarrow \xi$. (b) Left: Model of growth factors positioned at t= 0 on the surface of the polyelectrolyte film of hyaluronic acid. Right: Plot of probability W(t) of growth factor arriving at cell surface after time t for $D=D_0$ and $D=0.3D_0$.*

The impediment becomes more clearly visible if we consider now the time required for a particle, initially located at t=0 at the surface of the HA-film at position $x=x_0$, to reach the surface of the cell at position x=0. The initial distribution of the GF at the surface of the HA-film can be described by a δ-function. The probability distribution of the particle is then determined by the solution of the diffusion equation (see Exercise 60. I in [Landau VI])

$$w(x,t) = \frac{1}{2\sqrt{\pi Dt}}\left[\exp\left\{\frac{-(x-x_0)^2}{4Dt}\right\} - \exp\left\{\frac{-(x+x_0)^2}{4Dt}\right\}\right] \quad \text{(IV)}$$

Note: at $t \rightarrow 0$ $w(x_0, 0) \rightarrow$ const and $w(0,0) \rightarrow 0$. The time evolution W(t) of the GF at the cell surface is determined by the flux of molecules: $j = D\partial w/\partial x$. W(t) is obtained by integrating j from t=0 to t: $W(t) = D\int_0^t \frac{\partial w}{\partial x}$ .Integration of the diffusion equation leads to the inverse error function

$$W(t) = 1 - erf\left[\frac{x_0}{2\sqrt{Dt}}\right] \quad \text{(V)} \qquad erfx = \frac{2}{\sqrt{\pi}}\int_0^t e^{-t^2} dt \quad \text{(VI)}$$

Fig 22a shows the dramatic delay of the arrival of the GF at the cell surface if the GF size becomes equal to the mesh size $d \rightarrow \xi$.

Tow important conclusions can be drawn from the above consideration:

- First, it shows that that the activation of the GFR by the growth factors

can be strongly delayed at increasing cell density, such as confluent of endothelial cell layers, resulting in the arrest of cell growth.

- Second, it predicts a dramatic change of the behavior of transformed cells. These cells secrete proteases which cleave the glycoproteins, including HA receptors, thus dismantling the growth factor repellant film from the cell surface. This results in the impediment of the arrest of cell proliferation triggered by GFR coupled to CD44.

Growth arrest by Merlin-Ezrin disassembly and cadherin mediated Hippo pathway.We saw above that merlin can act as clutch which controls the coupling of CD44 and growth factor receptors (RTK) to the actin cortex via ezrin. In this activated state cell proliferation starts. If this supra-molecular complex is broken up by partial de-phosphorylation of merlin, cell proliferation is arrested (see Figure25). As noted above, the experiment by Morrison [Morisson 2001] shows that cell proliferation is arrested even in the logarithmic growth phase by binding of HA segments to CD44. Since the binding constant of HA is very low ($K_d \approx$ 10-100 µM, [Richter 2010]) the arrest sets in only at high HA concentrations. For example, a HA polymer of n= 2000 monomers is expected to exhibit a Flory radius of $R_F = \lambda_K R_F^{3/5} \approx 100nm$ (for $\lambda_K \approx 13$ nm) the concentration of HA monomers within the random coil. Therefore the switching of merlin form active to inactive state by HA binding becomes only effective if the HA polymers forms a densely packed solution. Since CD 44 is about 40 nm long this situation arises if the cells approach each other to a distance of smaller than about 100 nm. This limiting state shown is shown in Figure 27. Under this condition the cells start to adhere by formation of cadherin-cadherin bonds which bind optimal if the inter-cell distance ~23 nm. The HA and CD44 are expelled from the contact by a zipper like fashion. In the intermediate state the interface between the cells could decay into tightly bound domains formed by cadherin linkers and zones separated by CD44-HA-CD44 links. When the cells are compressed to such an extent that the intracellular distance becomes ≤ 23 nm the adhesion becomes controlled by the homophilic cadherin receptors which couple to the actin cortex through the α-catenin/β-catenin complex. Now, a new mechanism of contact inhibition based on the Hippo-signaling pathway sets in [Nam_Gyun 2011].

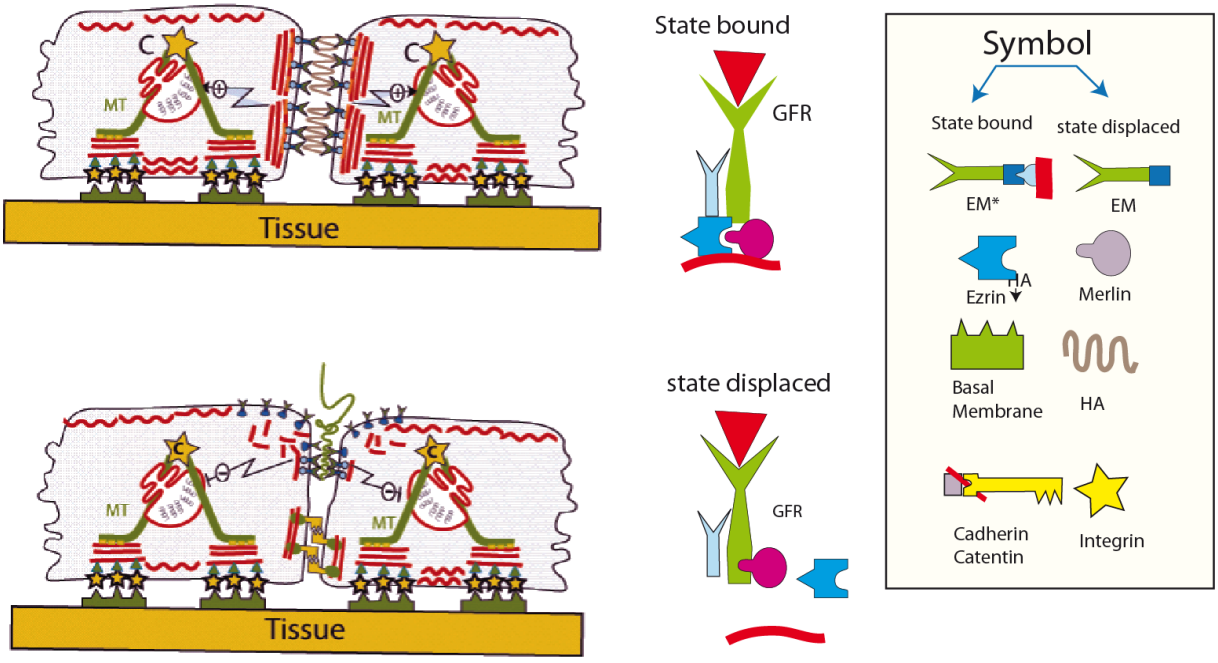

Figure 27 *Model of contact inhibition of endothelial cell growth. The top image shows the low density state with merlin forming a complex with ezrin that links CD44 and its associated RTK to the actin cortex resulting in cell proliferation (see Figure 24). At high densities (intracelluar distance ≈40nm), CD44 and HA are compressed, merlin is de-phosphorylated and displaces ezrin (see Figure 24). Consequently the GFR/CD44 complex dissociates and Cell proliferation arrests. Cell-cell contact is now mediated by cadherin and a new mechanism of contact inhibition, controlled by cadherin/catenin complexes, is switched on. Note that the two mechanism mediating adhesion can coexist by formation of adhesion domains.*

X: Characteristic differences of normal and cancer cell adhesion.

Introductory remarks: In this chapter some examples are presented which demonstrate the role of the glycocalix for the modified adhesion behaviour of cancer cells. Transformed cells are often distinguished from healthy ones by characteristic changes of the glycocalix. One general change is the modification of the oligosaccharide composition of glycoproteins and glycolipids [Hakomori 1985]. Second, the expression of the glycoproteins acting as CAMs, such as syndecans and CD44, is changed together with the molecular structure of the oligosaccharide. Third, the control of adhesion mediated by these

glycoproteins is modified by small debris of proteoglycans generated by a drastic increase in the metal protease activity of cancer cells. Thus, members of the ADAM metal protease family (also called sheddases) release soluble ectodomains which can inhibit adhesion to the external EM by blocking the binding sites for the heparan sulfates. Moreover, the decrease of the packing density of CD 44 and other glycoproteins is expected to facilitate the access of the GFR by growth factors (see Figure 26). Below we summarize some relationships between snydecan modification and cancer cell behavior by concentrating on the modification of cell adhesion (see also review [Beauvais 2004]).

X.1.Correlation between syndecans and cadherins

Down regulation of syndecan-1 has been shown to promote the formation of mesenchyme cells. This switching of the cell state is caused by the loss of E-cadherin from the surface, pointing to a correlation between syndecans and cadherins. This correlation is also revealed by the observation that syndecan-1 plays a key role for the polarization of epithelial cells and their adhesion on the basal membrane. Most intriguing is the observation that the formation of mesenchyme cells occurs below a certain threshold of the syndecan density on the cell surface.

The role of syndecan-2 during cell transformation is complex. Their cell surface density may be decreased (such as in lung melanoma cells) or they may be overexpressed, as in the case of colon cancer. In the first case the reduced level of syndecan-2 may result in the loss of adhesion domain formation on fibronectin below a certain threshold density. In colon cancer cells syndecan-2 is overexpressed by a factor of 2-5. The cells assume a rounded shape and pile-up over confluent monolayers formed on a hard substrate. After seven days the cells detach from the colony which points to the loss of E-cadherins. They start to divide and to migrate, thus assuming typical behaviour of metastatic cells [Xin Tang 2010]. This behavior can be reversed by reducing the syndecan-2 expression [Beauvais 2004].

Interestingly, the cells with enriched syndecan-2 can form adhesion domains on soft, fibronectin exposing substrates and proliferate (see [Beauvais 2010]). This can be explained by the formation of adhesion domains formed by syndecan-2 /integrin-β_1 complexes which can trigger ongoing cell division. According to Figure 21" the binding sites for integrins (the RGD peptides) and syndecan on fibronectin are close together. Therefore the two CAMs mediate adhesion in a cooperative fashion resulting in adhesion domains even at low densities of soft polymer substrates, which are assumed to expose a small density of binding sites.

The cell division can be blocked by adding soluble syndecan-2 extracellular domains [Park et al 2005]. The adherent cells start to round, the G0/G1 cell cycle arrests due to the abolishment of the activation of cell division by EGF growth factors. Interestingly, extracellular fragments of syndecan-4 do not block cell division.

X.2. Control of adhesion by modulation of structure of proteoglycan exposing receptors (CAMs): An interesting observation to be explored

Cancer cells produce enzymes, such as heparanase and hyaluronidase, that degrade the glycocalix of many cells, including endothelial or hematopoetic cells. Heparanase cleaves the heparan sulfate residues of the cell surface glycoproteins (such as syndecans or CD44) and the extracellular matrix (see [Alberts 1996], Chapter 19). An important consequence of these oligosaccharide-cleaving enzymes is the facilitation of transgression of cells through endothelium by degradation of the glycocalices of both the endothelial cell and the blood cells.

The effect of removal of heparin and heparin sulfate from membrane bound proteoglycans (i) on the adhesion strength and migration of endothelial cells during wound healing and (ii) on the their behavior under flow was explored by Moon et al [Moon 2000], by observing endothelial cell layers under sub-confluent conditions. Such experiments can provide direct insights into the control of cell adhesion and migration under shear flow. Cleavage of heparin and heparin sulfate in proteoglycans has several consequences. First, it decreases EC adhesion rates by 40% and adhesion strengths by 33%. Second, the HSPG disruption decreased stress fibers, the size of focal adhesions and enhanced EC migration speed. Most importantly, the cells lost the capacity to migrate in the hydrodynamic stress direction. This loss is paralleled by the observation that the distribution of the focal adhesion kinases was not polarizes and FAK did not accumulate at the focal adhesion sites.

References

[James and Vale 2012] JR. James and RD. Vale Biophysical mechanism of T-cell receptor triggering in a reconstituted system. Nature 2012, **487**: 264-69.

[Townes and Holtfreter 1955] P. L. Townes und J. Holtfreter Directed movements and selective adhesion of embryonic amphibian cells. Journal of Experimental Zoology (1955), 128:53-120

[Fotya and Steinberg 2005] RA. Fotya and MS. Steinberg The differential adhesion hypothesis: a direct evaluation. Developmental Biology 278 255– 263.

[Simson et al 1998] R. Simson, E. Wallraff, J. Faix, J. Niewöhner, G. Gerisch and E. Sackmann. Membrane Bending Modulus and Adhesion Energy of Wild-Type and Mutant Cells of Dictyostelium Lacking Talin or Cortexillins. Biophys. J. (1998) 74: 514-522

[Sackmann 1996] E. Sackmann Supported Membranes: Scientific and Practical Applications. Science (1996) 271: 43-47.

[Sackmann and Tanaka 2000/2005] (a) E. Sackmann and M. Tanaka Supported membranes on soft polymercushions: fabrication, characterization and applications. Trends in Biotechnology 2000**, 18:** 58-64 ; (b) M. Tanaka and E. Sackmann Supported Lipid Membranes as Cell-Tissue Surface Models. Nature, 2005, **437**: 656- 662.
[Gönnenwein et al 2003] S. Goennenwein et al. (2003) Functional incorporation of integrins into solid supported membranes on Ultrathin Films of Cellulose: Impact on Adhesion Biophys. J. **85:** 646–655;

[Hu et al. 2000] B. Hu et al. Interaction between integrin αIIbβ3 and synthesized cyclic hexapeptide containing RGD. Biochemistry , 2000, **39:** 12284-12294

[Albersdörfer 1997]A. Albersdoerfer, T. Feder and E. Sackmann. Adhesion-Induced Domain Formation by Interplay of Long-Range Repulsion and Short-Range Attraction Force: A Model Membrane Study Biophys. J. 1997, **73**: 245-257.

[Guttenberg et al 2000] Z. Guttenberg et al. Measuring Ligand-Receptor Unbinding Forces with Magnetic Beads: Molecular Leverage. Langmuir, 2000, **16:** 8984-8993.

[Bruinsma et al. 2000] R. Bruinsma, A. Behrisch and E. Sackmann Adhesive Switching of Membranes: Experiment and Theory. Phys. Rev. E, 2000, 61: 4253-4267.

[Landau- Lifshitz 1983] ID, Landau and EM. Lifshitz, Theoretical Physics Theory of elasticity . Pergamon Press, 1970

[Helfrich, 1978] W. Helfrich Steric interaction of fluid membranes in multilayer systems. Z. Naturforschung (1978)33a: 305-315.

[Seifert and Lipowsky 1995] U. Seifert and R. Lipowsky Generic interaction of fluid membranes in "Handbook of Biological Physics" Vol I, Ch.VIII, (Eds:. R. Lipowsky und E.Sackmann, Elsevier, Amsterdam 1995.

[Seifert 1997] U. Seifert. Configurations of fluid membranes and vesicles. Advances in Physics,1997, 46:13-137.

[Guttenberg et al 1991] Z. Guttenberg et al First-order transition between adhesion states in a system mimicking cell-tissue interaction Europhysics Letters (2001) 54: 826-932

[Pixley 2012] FJ. Pixley. Macrophage Migration and Its Regulation by CSF-1 Internat. Journal Cell Biology, 2012, 2012: 1-8

[Marx et al 2002] S. Marx et al. Repulsion and Dynamical Phase Separation of Multicomponent Lipid Bilayers Phys. Rev. Letters, 2002, **88** : 138102

[Zidovska and Sackmann 2006] A. Zidovska, and E. Sackmann Brownian Motion of Nucleated Cell Envelopes Impedes Adhesion. Phys. Rev. Letters, 2006, **96:** 048103-07.

[Zemel et al. 2010] Zemel, et al., Optimal Matrix Rigidity for Stress-Fibre Polarization in Stem Cells. Nature Physics, 2010, **6** : 468-473).

[Sackmann 2010] E. Sackmann How cells feel forces Nature Phys. 2010, 6:407-408

[Smith and Seiffert 2005] A. Smith, and U. Seifert, (2005) Effective Adhesion Strength of Specifically Bound Vesicles. Phys, Rev E, 2005, **71**:61902.

[Smith and Sackmann 2009] A. Smith and E. Sackmann, E., 2009 Progress in Mimetic Studies of Cell Adhesion and the Mechanosensing. ChemPhysChem, 2009, **10 :** 66- 78

[Reister Gottfried et al. 2008] E. Reister-Gottfried et al. Dynamics of Specific Vesicle-Substrate Adhesion: From Local Events to Global Dynamics Phys. Rev. Lett. 2008, 101, 208103.

[Häckel et al. 1997] W. Haeckl, U. Seifert and E. Sackmann. Effects of Fully and Partially Solubilized Amphiphiles on Bilayer Bending Stiffnesses and Temperature Dependence of the Effective Tension of Giant Vesicles. J. Phys. II France (1997) 7: 1141-1157.

[Bruisma et al. 1994] R. Bruinsma, M. Goulian, and P. Pincus, Self-assembly of membrane junctions. Biophys. J. ,1994, **67:** 746-750.

[21Sackmann 2006] (a) E. Sackmann, 2006 Thermo-elasticity and adhesion as regulators of cell membrane architecture and function. J. Phys. Condens. Matter , 2006, **18:** R785-R825.

[Weikl and Lipowsky 2004] Th. Weikl and R. Lipowsky Pattern formation during T-cell activation. Biophys. J. 2004, **87** : 3665-3578.

[Cahn 1977] JW. Cahn. Critical point wetting J. Chemical Physics, 1977, **66:** 3667-3672

[Boulbitch et al 2001] A. Boulbitch, A., Guttenberg, Z., Sackmann E. (2001) Kinetics of membrane adhesion mediated by ligand–receptor interaction studied with a biomimetic system. Biophys. J. 2001 **81:** 2743–2751.

[Brochard/de Gennes] F. Brochard and P. de Gennes, P. (2002) Adhesion induced by mobile binders : Dynamics, Proc. Natl. Acad. Sci. USA , 2002, **99**:7854

[Lorz et al. 2007] B. Lorz et al. Adhesion of giant vesicles mediated by weak binding of sialyl-lewisX to E-selectin in the Presence of Repelling Poly(ethylene glycol) Molecules. Langmuir, 2007, 23: 12293-12300.)

[Smith et al 2008] A. Smith et al. Force-induced growth of adhesion domains is controlled by receptor mobility (2008). PNAS, 2008, **105** : 6906–6911.

[Wegener et al.2007] KL. Wegener et al. Structural Basis of Integrin Activation by Talin. Cell. 2007, **128 :** 171-82.
[von Andrian and Mempel 2003] UH. von Andrian and Thorsten R.Mempel. Homing and cellular trafficking in lymph nodes. Nature Rev.s in Immunology 2003**, 3:** 867-878.

[Gunzer et al. 2000] M. Gunzer, A. Schaefer, S. Borgmann, S. et al. Antigen presentation in extracellular matrix interactions of T cells with dendritic cells are dynamic, short lived, and sequential Immunity , 2000, **13 :** 323–332,

[Varma 2006] R. Varma, et al. T-cell receptor proximal signals are sustained in peripheral microclusters and terminated in the central supramolecular activation cluster. Immunity, 2006, 25: 117–127

[Freiberg et al 2002] B. FreibergStaging and resetting T cell activation in SMACs . Nature Immunology, 2002, **3 :** 911-917.

[Sackmann 2011] E. Sackmann. Quantal concept of T-cell activation: adhesion domains as immunological synapses. New Journal of Physics, 2011, **13**: 065013

[Sackmann 2012] E. Sackmann. Physics of cellular immune reaction by immunological synapses. Lecture Notes on Biological Physics www.biophy.de.

[Heinrich and Sackmann 2006] D. Heinrich and E. Sackmann, E. 2006 Ative mechanical stabilisation of the viscoplastic intracellular space of Dictyostelia cells by microtubule actin cross talk. Acta Biomaterialia, 2006, **2 :** 619-631

[Stone et al. 2009] J.D. Stone et al. -Cell receptor binding affinities and kinetics: impact on T-cell activity. Immunology, 2009, **126:** 165–176

[Choudhuri et al. 2005] Choudhuri, K. et al. T-cell receptor triggering is critically dependent on the dimensions of its peptide-MHC ligand. Nature, 2005**, 436:** 578–582

[Combs et al. 2006] J. Combs et al. 2006 Recruitment of dynein to the Jurkat immunological synapse. Proc. Natl. Acad. Sci. USA, 2006, **103 :** 14883–14888

[Stinchcombe et al. 2006] Stinchcombe et al. Centrosome polarization delivers secretory granules to the immunological synapse. Nature, 2006, **443 :** 462-465

[Wülfling and Davis 1998] Ch. Wülfing and MM. Davis, MM. 1998: A receptor/cytoskeletal movement triggered by costimulation during T-cell activation. Science, 1998, **282 :** 2266-2269.

[Tzima et al 2005] E. Tzima, et al. A mechanosensory complex that mediates the endothelial cell response to fluid shear stress. Nature, 2005, **437** : 426-431 .
[Cinamon et al 2001] G. Cinamon, V. Shinder, and R. Alon, R. Shear forces promote lymphocyte migration across vascular endothelium bearing apical chemokines. Nature Immunology. Nat. Immunol. 2001, **2** :515-22.

[Atherton and Born 1973] A. Atherton and VR. Born Relationship Between the Veocity of Rolling Granuloctes and the Blood Flow in Venules. J. Physiology 1973, **233:** 157-165

[Newman 1997] PJ. Newman. Biology of PECAM-1. J. Clin. Invest. 1997, **99** : 3–8

[Grabham et al.] P. Grabham et al. Microtubule and Rac 1-dependent F-actin in growthcones. Journal of Cell Science 2003, 116: 3739-3748,

[Watanabe et al 2010]} Watanabe, TM., et al. (2010) Myosin-X Induces Filopodia by Multiple Elongation Mechanism. J. Biol. Chem. 2010, **285:** 19605-19614.

[Faix and Rottner 2006] J. Faix and K. Rottner. 2006. The making of filopodia. Curr. Opin. Cell Biol. 2006, **18:** 18-25.

[Lan and Papoian 2008] YH. Lan and GA. Papoian. The Stochastic Dynamics of Filopodial Growth. Biophys J. 2008, **94**:3839-3852.

[Wahl 2000] S. Wahl et al. [2000] Ephrin-A5 Induces Collapse of Growth Cones by Activating Rho and Rho Kinase

[Luo 2002] L. Luo. Rho GTPases in neuronal morphogenesis. Nature Review neuroscience, 2003, **1** : 173.180

[Mc Hugh 2009] B. McHugh et al. Integrin activation by Fam38A uses a novel mechanism of R-Ras targeting to the endoplasmic reticulum. J Cell Sci. 2009, 123, 51-66

[Faroudi et al. 2003] M. Faroudi M, Zaru R, Paulet P, Müller S and Valitutti S J 2003 Cutting edge: T lymphocyte activation byrepeated immunological synapse formation and intermittent signaling. J. Immunology, 2003, **171:** 1128–3

[Nam-Gyun et al 2011] Nam-Gyun Kim et al. E-cadherin mediates contact inhibition of proliferation through Hippo signaling-pathway components PNAS, 2011, **108:** 11930–11935

[Cannon et al 2011] JL. Cannon et al. CD43 interaction with ezrin-radixin-moesin (ERM) proteins regulates T-cell trafficking and CD43 phosphorylation. Mol Biol Cell 2011, 22: 954–963.

[Ly 2003] DP. Ly et al. De Novo Expression of the Integrin {alpha}5{beta}1 Regulates {alpha}v{beta}3-Mediated Adhesion and Migration on Fibrinogen. J Biol. Chem. 2003, 278: 21878-21885.

[Bache et al. 2004] KG. Bache, T. Slagsvold and H. Stenmark. Defective Downregulation of Receptor Tyrosine Kinases in Cancer EMBO J. 2004, **23:** 2707–2712.

[Morrison et al.2004] H. Morrison et al. The NF2 tumor suppressor gene product, merlin, mediates contact inhibition of growth through interactions with CD44. Genes and Development 2001, **15:** 968–980 2001

[Gundersen 1988] G. Gundersen and J, Bulinski Selective stabilization of microtubules oriented toward the direction of cell migration. Proc. Natl. Acad. Sci. USA, 1998, **85:** 5946–5950

[Faroudi 2003] M. Faroudi et al. T lymphocyte activation byrepeated immunological synapse formation and intermittent signaling J. Immunology, 2003, **171:** 1128–3

[Mannville et al 2010] Manneville X. et al. Dlg1 binds GKAP to control dynein association with microtubules, centrosome positioning, and cell polarity J. Cell Biol. 2010 191: 585–598

[Sackmann 2006] E. Sackmann. Thermo-elasticity and adhesion as regulators of cell membrane architecture and function. J. Phys. Condens. Matter, 2006, 18: R785-R825.

[Hendrickson et al. 2008] Hendrickson S. et al. T-cell sensing of antigen dose governs interactive behaviour with dendritic cells and set the threshold for T-cell activation. Nature Immunology, 2008, **9:** 282 291

[Kaufmann et al. 1992] S. Kaufmann, S. et al. Talin anchors and nucleates actin filaments at lipid membranes: A direct demonstration FEBS Letters, 1992**, 314:** 203-205.

[Sackstein2008] Sackstein, R. (2011) The Biology of CD44 and HCELL in Hematopoiesis: The "Step 2-bypass Pathway" and other Emerging Perspectives. Curr. Opinion Hematol. 2011, **18:** 239–248.

[Tremel et al. 2009] M. Tremel et al. (2009) A CD44v6 peptide reveals a role of CD44 in VEGFR-2 signaling, 2009, **114:** 5236-5244.

[Stone 2009]J.D. Stone, TD. Stone, AS. Chervin and DM. Kranz -Cell receptor binding affinities and kinetics: impact on T-cell activity. Immunology, (2009) 126: 165–176

[Woods 2001] H. Woods (2001) Syndecans : transmembrane modulators of adhesion and matrix assembly matricellular proteins. J Clinical Invest. 2001:935–941.

[Okamoto et al. 1999] Okamoto I. et al. Metal proteases CD44 cleavage induced by a membrane-associated metalloprotease plays a critical role in tumor cell migration. Oncogene, 1999, 18: 1435-1446

[Gooddison et al. 1999] S. Goodison, et al. CD44 cell adhesion molecules. J. Clin. Pathol: Mol Pathol, 1999, **52:**189–196

[Knutson et al. 1996] JR. Knutson et al. CD44/Chondroitin Sulfate Proteoglycan and a2b1 Integrin Mediate Human Melanoma Cell Migration on Type IV Collagen and Invasion of Basement Membranes. Molecular Biology of the Cell 1996 **7**: 383-396,

[Elkin 2001] M. Elkin, M., , et al. Heparanase as mediator of angiogenesis: mode of action. FASEB J.2001**, 15:** 1661–1663.

[Van Sluis 2010] Van Sluis, G. et al (2010) A Low Molecular Weight Heparin Inhibits Experimental Metastasis in Mice Independently of the Endothelial.PLoS ONE , 2010 e1120

[Beauvais, 2004] Beauvais, M., Rapraeger, A. (2004) Syndecans in tumor cell adhesion and signaling. Reproductive Biology and Endocrinology 2004, 2:3

[Kusano 2000] Kusano Y et al (2000) Participation of syndecan 2 in the induction of stress fiber formation in cooperation with integrin alpha5beta1: structural characteristics of heparan sulfate chains with avidity to COOH-terminal heparin-binding domain of fibronectin. Exp Cell Res. 256: 434-44.

[Park 2002] H. Park et al. Syndecan-2 mediates adhesion and proliferation of colon carcinoma cells. J Biol Chem. 2002, **277:** 29730-29736.

[Pixley 2012] Pixley, FJ. (2012) MacrophageMigration and Its Regulation by CSF-1 Internat. J. Cell Biology Article ID 501962.

[Lee and Marchant 2001] Lee, I., Marchant, RE. (2001). Force measurements on the molecular interactions between ligand (RGD) and human platelet aIIBb3 receptor system. Surf. Sci. 2001, 491:433–443.

[Wolny et al. 2010] PM. Wolny et al. Analysis of CD44-Hyaluronan Interactions in an Artificial Membrane System. J. of Biol. Chem. 2010, **285:** 30170–3018

[Watanabe et al. 2004] T. Watanabe, S. Noritake, J. Sato K, et al Interaction with IQGAP1 links APC to Rac1, Cdc42, and actin filaments during cell polarization and migration .Dev Cell. 2004, 7: 871-83.

[Lum et al. 2002] AF. Lum et al. Dynamic regulation of LFA-1 activation and neutrophil arrest on intercellular adhesion molecule. J. Biol Chem. (2002) **277:** 20660-70.

[Zidovska 2011] A. Zidovska and E. Sackmann On the Mechanical Stabilization of Filopodia Biophys. J. 2011, **100**: 1–10

[Auth and Gov2007] T. Auth S.A. Safran and N. S. Gov, Fluctuation of coupled fluid and solid membranes with application to red blood cells. Phys. Rev. E 2007, **76:** 051910-1-18.

[Zilker 1992) A. Zilker, M. Ziegler and E. Sackmann, 1**992**, Spectral analysis of erythrocyte flickering in 0.3–4mm−1 regime by micro interferometry combined with fast image processing, Phys. Rev. A 1992, 46: 7998-8001.

[Nardi 1998] J. Nardi, R. Bruinsma and E. Sackmann Adhesion-Induced Reorganization of Charged Fluid Membranes. Phys. Rev. E 1998, **58:,** 6340-6354

[Hendrickson 2008] Hendrickson S. et al. (2008) T-cell sensing of antigen dose governs interactive behaviour with dendritic cells and set the threshold for T-cell activation. Nature Immunology 9:282 291

[Bell et al 1984] GI. Bell, M. Dembo, P. Bongrand, Cell adhesion Competition Between Nonspecific Repulsion and Specific Bonds Biophys. J. 1984, **45:** 1051; b) M.

.Rädler, J O et al (1995) Fluctuation analysis of tension-controlled undulation forces between giant vesicles and solid substrates Physical Review E 514526-4536

[Boulbitch 2001] A. Boulbitch, Z. Guttenberg, E. Sackmann (2001) Kinetics of membrane adhesion mediated by ligand–receptor interaction studied with a biomimetic system. Biophys. J.2001, **81:** 2743–275

[Pierres et al. 2008] A. Pierres et al. How cells tiptoe on adhesive surfaces before sticking Biophys. J. 2008, **94:** 4114-4122.

Critchley 2008]. Critchley D, Gingras A. 2008. Talin at a glance. J. Cell Sci. 121:1345-47

[Smith et al. 2009] (a) Smith, A., Sackmann, E., (2009) Progress in Mimetic Studies of Cell Adhesion and the Mechanosensing. ChemPhysChem 10: 66- 78

Critchley 2008]. Critchley D, Gingras A. 2008. Talin at a glance. J. Cell Sci. 121:1345-47

[Smith 2009] (a) Smith, A., Sackmann, E., (2009) Progress in Mimetic Studies of Cell Adhesion and the Mechanosensing. ChemPhysChem 10: 66- 78

[Sackmann 2012] E. Sackmann "Biophysics of Immunology" in Sackmanns Lecture Notes in Biological Physics www.biophy.de.

[Elkin 2001] M. Elkin, M. et al. (2001) Heparanase as mediator of angiogenesis: mode of action. FASEB J. 15: 1661–1663.

[van Sluis 2010] G. van Sluis et al (2010) A low molecular weight heparin inhibits experimental metastasis in mice independently of the endothelial. PLoS ONE 2010, **5**, e1120

[Beauvais, 2004] Beauvais, M., Rapraeger, A. (2004) Syndecans in tumor cell adhesion and signaling. Reproductive Biology and Endocrinology 2004, 2:3

[Woods] Woods,A.[2001], Syndecans: transmembrane modulators of adhesion and matrix assembly. Clin Invest.107: 935–941.

[Kusano 2000] Kusano Y et al (2000) Participation of syndecan 2 in the induction of stress fiber formation in cooperation with integrin alpha5beta1: structural characteristics of heparan sulfate chains with avidity to COOH-terminal heparin-binding domain of fibronectin. Exp Cell Res. 256: 434-44.

[Moon] J.M.Moon Role of Cell Surface Heparan Sulfate Proteoglycans in Endothelial Cell Migration and Mechanotransduction

[Morrisonet al 2007] H. Morrison et al Merlin/Neurofibromatosis Type 2 Suppresses Growth by Inhibiting the Activation of Ras and RacCancer Res 2007; 67: (2). January 15, 2007

[Grabham et al. 2003] P. Grabham et al. Microtubule and Rac 1-dependent F-actin in growthcones. Journal of Cell Science 2003, 116: 3739-3748,

[Watanabe et al. 2010]} Watanabe, TM., et al. (2010) Myosin-X Induces Filopodia by Multiple Elongation Mechanism. J. Biol. Chem. 285:19605-19614.

[Tremel 2009] M. Tremel et al. A CD44v6 peptide reveals a role of CD44 in VEGFR-2 signaling 2009 114: 5236-5244

[Stone et al 2009] J.D. Stone et al.-Cell receptor binding affinities and kinetics: impact on T-cell activity. Immunology, 2009, **126:** 165–176

[Woods 2001] **[**Okamoto 1999] Okamoto I. et al (1999) Metal proteases CD44 cleavage induced by a membrane-associated metalloprotease plays a critical role in tumor cell migration Oncogene 1999, Volume 18, Number 7, Pages 1435-1446

[Bai et al 2007] Y. Bai Y. Inhibition of the hyaluronan-CD44 interaction by merlin contributes to the tumor-suppressor activity of merlin Oncogene 2007, **26**: 836–850.
[Gooddison et al. 1999] Goodison, S. et al. CD44 cell adhesion molecules J Clin Pathol: Mol Pathol 1999, **52:**189–196

[Knudsen 1996] Knutson, JR. et al. (1996) CD44/Chondroitin Sulfate Proteoglycan and a2b1 Integrin Mediate Human Melanoma Cell Migration on Type IV Collagen and Invasion of Basement Membranes. Molecular Biology of the Cell 7: 383-396,

[Elkin 2001] Elkin, M., , et al. (2001) Heparanase as mediator of angiogenesis: mode of action. FASEB J. 15: 1661–1663.

[Van Sluis 2010] Van Sluis, G. et al (2010) A Low Molecular Weight Heparin Inhibits Experimental Metastasis in Mice Independently of the Endothelial.PLoS ONE 5: e1120

[Beauvais, 2004] Beauvais, M., Rapraeger, A. (2004) Syndecans in tumor cell adhesion and signaling. Reproductive Biology and Endocrinology 2004, 2:3

[Woods 2001] A. Woods Syndecans: transmembrane modulators of adhesion and matrix assembly. J. Clin Investigation, 2001, **107:** 935–941.

[Kusano 2000] Kusano Y et al. Participation of syndecan 2 in the induction of stress fiber formation in cooperation with integrin alpha5beta1: structural characteristics of heparan sulfate chains with avidity to COOH-terminal heparin-binding domain of fibronectin. Exp Cell Res. 2000, **256**: 434-44.

[Park 2002]Park H et al. (2002) , Syndecan-2 mediates adhesion and proliferation of colon carcinoma cells. J Biol Chem. 277: 29730-29736.

[Pixley 2012] Pixley, FJ. (2012) MacrophageMigration and Its Regulation by CSF-1 Internat. J. Cell Biology Article ID 501962.

[Lee and Marchant 2001] L. Lee and RE. Marchant. Force measurements on the molecular interactionsbetween ligand (RGD) and human plateletaIIbb3receptor system. Surf. Sci. 2001, **491,** 433-441..

[Wolny et al. 2010] PM. Wolny et al. Analysis of CD44-Hyaluronan Interactions in an Artificial Membrane System J. Biol. Chem. 2010, 285: 30170–3018

[Watanabe 2004] T. Watanabe et al. Interaction with IQGAP1 links APC to Rac1, Cdc42, and actin filaments during cell polarization and migration. Dev. Cell.(2004) 7:871-83.

[Lum et al 2002] AF. Lum et al. Dynamic regulation of LFA-1 activation and neutrophil arrest on intercellular adhesion molecule. J. Biol Chem. 2002 **277:** 20660-70.

[Zidovska 2011] A. Zidovska and E. Sackmann On the Mechanical Stabilization of Filopodia Biophys. J. (2011) 100: 1–10

[Auth et al 2007] T. Auth, SA. Safran and N, Gov, Fluctuation of coupled fluid and solid membranes with application to red blood cells. Phys.Rev.E 2007**, 76:** 051910-1-18.

[Zilker et al 1992] A. Zilker, ., M. Ziegler and E. Sackmann, Spectral analysis of erythrocyte flickering in 0.3–4mm−1 regime by micro interferometry combined with fast image processing, Phys. Rev. A, 1992 **46:** 7998-8001 (1992)

[Nardi 1998] J. Nardi, R. Bruinsma and E. Sackmann Adhesion-Induced Reorganization of Charged Fluid Membranes.Phys. Rev. E 1998, 58, 6340-6354

[Hendrickson 2008] Hendrickson S. et al. T-cell sensing of antigen dose governs interactive behaviour with dendritic cells and set the threshold for T-cell activation. Nature Immunology 2008, **9:**282 291

[Raedler et al 1995] JO. Rädler et al. Fluctuation analysis of tension-controlled undulation forces between giant vesicles and solid substrates. Physical Review E 1995, **51:** 4526-4536

[Boulbitch 2001] Boulbitch, A., Guttenberg, Z., Sackmann E. Kinetics of membrane adhesion mediated by ligand–receptor interaction studied with a biomimetic system. Biophys. J. 2001, **81:** 2743–275

[Sackmann 2012] E. Sackmann "Biophysics of Immunology" in Sackmanns Lecture Notes in Biological Physics www.biophy.de.

Appendix

Appendix A: Generic attraction and repulsion forces.

The adhesion is determined by three generic forces: (i) the Van der Waals interaction, (ii) the disjoining pressures mediated by membrane bending excitations and (iii) the steric repulsion by repeller molecules. The gravity will be considered in Appendix B.

The Van der Waals interaction between a lipid bilayer (M) of thickness d_m and a solid surface (S) at distance h is given by

$$V_{VdW}(h) = \frac{H_{MG}}{12\pi}\left\{\frac{1}{h^2} - \frac{1}{(h+d_m)^2}\right\} \qquad \text{(A.1a)}$$

and between two free membranes with minimal distance h by:

$$V_{VdW}(h) = \frac{H_{MM}}{12\pi}\left\{\frac{1}{h+2d_m)^2} - \frac{1}{h^2} + \frac{2}{(h+d_m)^2}\right\} \quad \text{(A.1b)}$$

where H_{IJ} are the (material dependent) Hamaker constants. The first equation is obtained by considering the interaction of the glass plate first with the lipid bilayer at distance d and then with the aqueous phase at distance $d+d_m$ .The second equation is obtained in a similar way by replacing the glass plate by a bilayer of thickness d_m embedded in water. Note finally that the interaction potential between two half planes at a distance z is $V_{Ij} = H_{IJ}/12\pi z^2$

The Hamaker constants for the first case is $H_{MG} \approx 8.0\ 10^{-21}$J and for the second $H_{MM} \approx 5x10^{-21}$ J and are both about equal to k_BT. For a distance of 10 nm the Van der Waals attraction is about $1.5\ 10^{-6}$ Jm^{-2}.

The repulsion between membranes can be mediated by three contributions (i) the electrostatic double layer potential, (ii) The steric forces mediated by repeller molecules and (iv) an entropic disjoining pressure generated by thermally excited bending undulations which was discussed in the main text (ChapterIV). The control of adhesion by the electrostatic interaction between two equally charged membranes (mediated by counterions) is a subtle problem which has been studied in detail in a specific model system [Nardi et al. 1998] and will be addressed again at the end. Under physiological conditions (salt concentrations > 10 mM) the Debye length is smaller than 1 nm. The electrostatic potential is short ranged compared to the repulsion potential mediated by the glycocalix of cell surfaces and is not considered further.

The steric interaction potential is determined by the compression of the extracellular domains of the proteins forming the glycocalix, such as the glycoproteins CD43, CD44, CD 45 and syndecanes. By assuming that the head groups of these repellers behave mechanically as a flexible macromolecule this compression corresponds to the situation of macromolecules

confined between two plates. Following [Bruisma et al 2000] the interaction potential can be approximated by the Dolan-Edwards potential for which an analytical expression exists for two limiting situations. For distances larger that the Flory radius of the macromolecule ($h>R_g$) it can be expressed as

$$V_P \approx k_B T \rho_L \left(\frac{R_g}{h}\right)^2 \exp\left\{-\frac{3}{2}\left(\frac{h}{R_g}\right)^2\right\} \qquad \text{(A.2)}$$

ρ_L is the lateral concentration of repeller molecules. This situation holds if the inter-membrane distance within the adhesion domains (h in Figure 5) is comparable to the extension R_g (equal to the Flory radius) of the repeller head groups into the extracellular space. For shorter distances ($h<<R_g$) the repellers are expelled from the domains of tight adhesion one obtains

$$V_p \approx k_B T \rho_L \qquad \text{(A.3)}$$

This is a very important result. It tells us that for $h << R_g$ the contribution of the repellers to the repulsive pressure between the membranes is equal to the lateral osmotic pressure exerted by the repeller molecules on the adhesion domains. Below we present several examples showing that this entropic effect plays a key role for the control of the adhesion strength.

The elastic energy costs come into play if the formation of a bond is associated with the reduction of the inter-membrane distance (from H to h_o). The elastic free energy W_{ela} is obtained by minimizing the free energy functional (Eq. (1)) yielding [Bruinsma et al. 1994]

$$W_\zeta \approx 8V'' (H-h)^2 \zeta_p^2 = 8\sqrt{\kappa V''}(H-h)^2 \qquad \text{(A.4)}$$

Eq (A7) has a simple meaning. W_{ela} is about equal to the energy cost required to squeeze the glycocalix by (H-h) over a disc of radius ζ_p. For vesicles containing 30% cholesterol V'' is of the order V'' ~ 10^{14} Jm^{-4} and $\kappa \approx 50\ k_BT$. With h ≈15 nm and H≈ 45 nm one finds $W_\xi \approx 5k_BT$ which is a moderate value. The elastic energy divided by the circumference $U \approx \pi\zeta_p$ of the disc is a measure for the line tension: $\Gamma \approx 3V''(H-h)^2\zeta_p$. For typical values: (H-h) ≈20nm V''=10^{12} Jm^{-4} and $\varsigma_p \approx 50nm$, it is of the order $\Gamma \approx 1pN$.

Electrostatic interfacial forces mediated by the charge of the glycocalix:

The repulsive disjoining pressure of neutral polymer films or brushes can be accounted for by the Dolan-Edwards potential [Bruinsma et al 2000]. The situation is much more complex for cell surfaces covered by negatively charged glycoproteins, such as membrane bound proteoglycans and glycolipids exposing sialic acids. It is helpful to consider two limiting case. First, at physiological salt concentrations (400 mM) and not too high packing densities of the glycoproteins, the anions and cations of the salt and the counterions provided by the glycoproteins, are expected to distribute equally within the polymer film and compensate the charges. A second situation is encountered if two cell start to adhere and the salt of the extracellular fluid is expelled from the interface. In this case the electrostatic

interaction is determined by the osmotic pressure generated by the counterions that are dissociated from the glycocalix generating constituents. Such a situation may occur in nature if the glycoproteins are removed from the cell surface and the electrostatic force is determined by the charged glycolipids. Unfortunately, the composition of the glycocalix is very complex and generally not known. We therefore consider in the following the case of erythrocytes as the best characterized cell to estimate the effect of electrostatic forces on cell adhesion. The major glycoproteins acting as repellant CAMs are Glycophorins A, B and C which function also as blood group antigens and which extends about 10 nm into the extracellular space. The cells expose also a rather high density of glycoproteins (about 7 mole %) containing one negative charge and some mole% blood group antigens exposing 4-6 sialic acid groups. The head groups extend only 1-2 nm into the extracellular space.

To estimate the electrostatic disjoining pressure between two cells or cells and tissue surfaces and to compare it with the Van der Waals attraction we consider two limiting cases. We first assume that the repulsion is determined by the osmotic pressure generated solely by the counterions provided by the polyelectrolyte. Here we consider the situation of a cell surface densely covered by glycolipids. In the second case we assume that the polyelectrolyte density is low and is saturated with electrolyte. Several models of this situation were developed in connection with theory of the stabilization of colloids by charged polymer brushes. For the complex situation of cell surfaces a model of colloid stabilization by Ph. Pincus is applied [Pincus 1991]. More sophisticated theories can be found in this reference.

We start with the estimation of the electrostatic disjoining pressure for the case of surfaces covered by glycolipids. The osmotic pressure of the counterions provided by the polyelectrolyte is generally given by $\Pi(h) = \rho(h) k_B T$, where $\rho(h)$ is the counterion charge density (charges per unit volume). To calculate $\rho(h)$ we assume that the two dimensional charge density of the polyelectrolyte is $e\sigma$ (charges m^{-2}). $\rho(h)$ is obtained from the Poisson Boltzmann equation which can be expressed as (in the cgs system):

$$\Delta\varphi(z) = 4\pi\varepsilon l_B \sigma^{-2} \exp\left\{\frac{e\varphi}{k_B T}\right\}\rho(z) \qquad \text{(A4.a)}$$

Where $\varphi(h)$ is the electrical potential. As can be verified by insertion, this nonlinear differential equation can be solved by the counterion concentration

$$\rho(x) = 2\pi\rho_0\left\{l_B (x+\lambda)^2\right\}^{-1} \qquad \text{(A4.b)}$$

This equation tells us that the counterion distribution extends over a length λ into the z direction, where λ is the so called Gouy-Chapman length and l_B the Bijerrum length defined as follows:

$$\lambda = \frac{\sigma^{-1}}{2\pi l_B} \qquad \text{(A4c)} \qquad ; \qquad l_B = \frac{e^2}{\varepsilon k_B T} \quad \text{(A4d);}$$

l_B is a measure for the distance over which two elementary charges exhibit an interaction energy $k_B T$. For water and 25°C is $l_B \approx 0.7$ nm. The Bijerrum length is related to the more familiar Debye screening length κ^{-1} by $\kappa^2 = 4\pi n l_B$, where n is the density (ions/m^2) of dissolved ions (assumed to be monovalent).

We are now interested in the disjoining pressure p_{disj} between two charged cell surfaces (of interfacial distance 2h). The counterions can be considered to form an ideal gas confined within a layer of thickness 2d. For this situation p_{disj} is determined by the osmotic pressure Π of the counterions (which is k_BT times the counterion concentration). Π can be easily calculated for the interaction of two identical charged surfaces [Hiemenz 1986], [Israelachvili 1984]. For the case of two interacting cell surfaces covered with polyelectrolyte brushes the situation is more complex. To calculate the osmotic pressure by application of the equation $\Pi(h) = \rho(h) k_B T$, we have to consider the two limiting cases: namely $h >> \lambda$ and $h << \lambda$. The osmotic pressures are (in Π units of Pa)

for $h >> \lambda$: $\Pi = k_B T\, \rho(h) = \dfrac{k_B T}{2\pi l h^2}$ (A.5a) ; for $h << \lambda$ $\Pi = \dfrac{k_B T}{\sigma^{-1} h}$ (A5.b)

In the context of cell adhesion we are interested in the balance between the electrostatic repulsion, mediated by the glycoproteins or glycoprotein assemblies and the van der Waals (vdW) attraction which is expressed in terms of the Hamaker constant H

$$P_{VdW} = \frac{H}{4\pi h^3} \qquad \text{(A.6)}$$

P_{VdW} is determined by the plasma membrane, since the contribution of the polyelectrolyte brushes is small due to the low monomer density. For two opposing bilayers $H \approx 2k_BT$ [Raedler 1995]. To compare the relative contributions of the electrostatic and vdW pressure we calculate the distance d* at which the two disjoining pressures compensate. From Eq. (A.5b) and Eq.(A.6) we obtain:

$$h^* = \sqrt{1/2\pi\sigma} \quad \text{(A.7)}$$

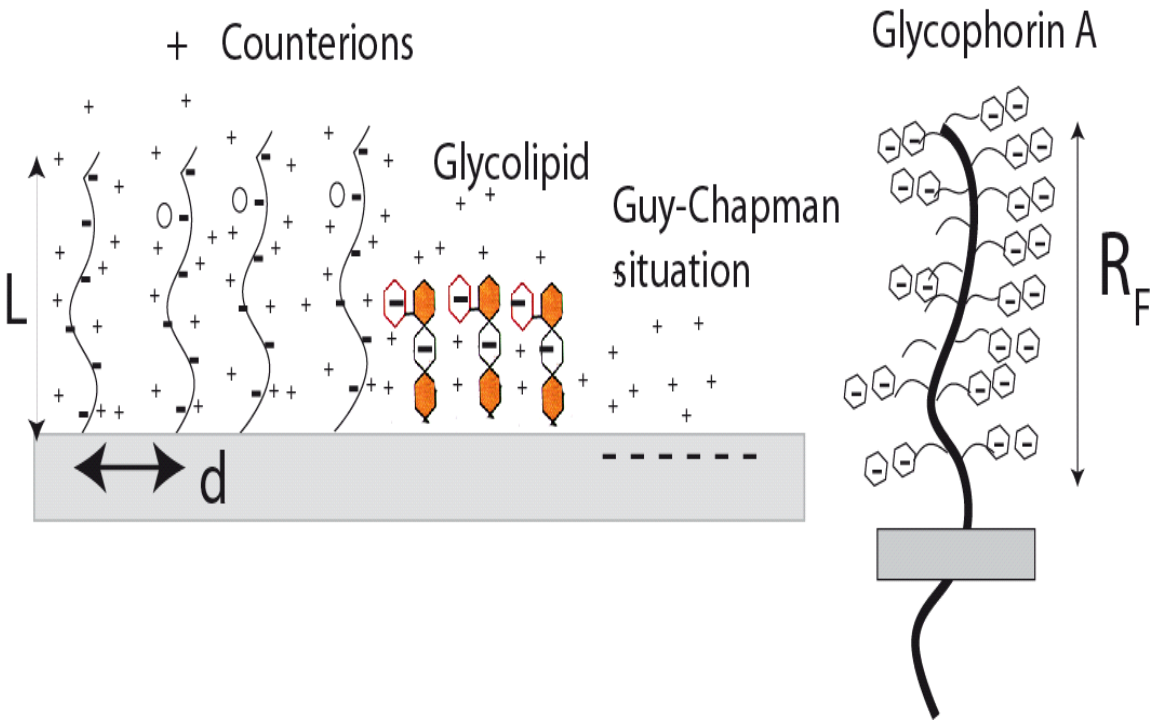

Figure A.1 *Left: Three situations of charged surfaces : Right. Structure of gycophorin as an example of a glycoprotein exposing charged sugar groups The extracellular domain is composed of 50 amino acids and exposes up to 32 sialic acid groups.*

We consider first the interaction of two erythrocytes depleted of glycophorins. Most of the 7% of glycolipids are gangliosides (GD1 and GM1) with one negative charge (from a sialic acid isoform). We ignore a smaller fraction of glycolipids acting as blood group antigen which expose 4-6 negative charges. The Guy-Chapman length is about $\lambda \approx 20nm$ and we therefore deal with the situation given by Eq. (S2.xd). The osmotic pressure is given by $\Pi \approx 5x10^{-5} h^{-1} Pa$. The distance at which the electrostatic and the vdW pressures compensate is h*≈1.5 nm. This result shows that even in the case of membranes covered only by glycolipids the disjoining pressure is determined by the electrostatic repulsion. This result is important for our model of myelin formation introduced in Chapter VIII.

Consider now the situation that the interaction between the cells is determined by the glycophorins based on the assumption that the disjoining pressure is determined by the counterions provided by the polyelctrolyte and the salt. Several models have been proposed for this case in connection with the stabilization of colloids by polyelectrolyte brushes. For the estimation of the strength of the glycophorin mediated repulsion we use an equation proposed by Pincus (see Equation II.9 in [Pincus, 1991]):

$$\Pi = p_{disj} = \frac{k_B T\, N}{2c_s\, d^4} \frac{1}{h^2}$$

The surface of erythrocytes is A~ 100μm and the number of glycophorins N~3x10^5 copies per cell, corresponding to an intermolecular distance of 20 nm. About 50 peptides of the 134 amino acid long protein point into the extracellular space-and expose 16 sugar residues. Most of these are tetra-saccharides Thus the total number of monomers is N ≈ 110. The salt concentration (400mM) is c_s= 2.5 10^{26} Ions m^{-2} and d^4≈16 10^{-32} m^4. Therefore, $\Pi = \frac{6x10^{-15}}{h^2}$.

It is interesting to compare the result with the Flory radius of the glycophorin head group. We assume that the molar volume of the 110 monomers is 0.5 nm^3 (the average of the molar volume of sugar (1.2 nm^3) and amino acids (0.12 nm^3)).We find for the Flory radius $R_F \approx \sqrt[3]{0.5} N^{\frac{3}{5}}$ =0.8x16=17 nm. The disjoining pressure at this distance is $\Pi = 20Pa$ and is orders of magnitude larger that the vdW repulsion $p_{disj} = 2k_B T / 4\pi h^2 \approx 10^{-5}$Pa.

In summary, the consideration in the present section shows that the electrostatic disjoining pressure of the glycocalix dominates the cell-cell interaction In Chapter XXX we will show how the repulsion can be overcome in order to wrap myelin sheets around axons.

[Hiemenz 1986] P.Hiemenz Principle of colloid and surface chemistry. Marcel Dekker New York. 1986

[Israelachbvili 1985] J Israelachvili Intermolecular and Surface Forces. Academic Press. New York 1985

[Manabe et al] MJ, Manabe et al . Structure of the major O-glycosidic oligosaccharide of monkey erythrocyte glycophorin. Glycoconj J. 1989;6(4):499-510.

[Pincus 1991] Ph Pincus Colloid stability owith grafted polyelactrolytes Macromolecules 1991, **24**, 2912-2919

[Rädler et al 1995] J. Rädler, H. Strey and E. Sackmann. Fluctuation analysis andof tension controlled undulations forces between giant vesicles and solid surfaces. Phys. Rev.E. 1995, 51, 4526-4536.

[Tomita and Marchesi 1975] Tomita and Marchesi 1975 Amino-acid sequence and oligosaccharide attachment sites of human erythrocyte glycophorin. Proc Natl Acad Sci U S A. 1975 A72(8):2964-8.

Appendix B: The "boundary stress analysis" Model.

The following model allows us to measure the adhesion strength and other pertinent parameters by analyzing the contour at the rim of adhesion discs in terms of the balance of elastic boundary stresses ([Guttenberg et al 2001] See also [Landau and Lifshitz], § 16 exercise 4), while the global deformation of the cells can be neglected. If a shell adheres it is flattened within the adhesion zone resulting in a strong local deformation of the shell along a small band of width d running around the contact line. The membrane is stretched perpendicular to this band while the bending deformation extends over the whole shell. The following consideration shows that the energy cost of this locally stretched band is much larger than the bending energy associated with the local and global deformation of the shell . The local stretching can be characterized in terms of the deformations ξ according to $\varepsilon = \frac{\partial \xi}{\partial s} \approx \frac{\xi}{d}$. The local change in curvature is: $\delta \frac{1}{R} = \frac{\partial^2 \zeta}{\partial s^2} \approx \frac{\xi}{d^2}$. With the bending modulus $\kappa \sim Eh^3$ and the 2D compression modulus $\kappa \sim Eh^3$, the elastic energy contributions of the local deformation become:

$W_\kappa \sim \frac{Eh^3 \xi^2}{d^4}$ and $W_K \sim \frac{Eh\,\xi^2}{d^2}$.

The ratio of the bending energy to the stretching energy is thus $W_\kappa / W_K \approx h^2 / d^2 \approx h^2 / R^2 \sim 10^{-2}$, showing that the major energy is stored in the membrane stretching. This approximation can be easily verified by assuming that the radius R of a spherical shell (say the earth crust) is increased by an increment r. By calculating the stretching energy and by using the relationship $K = \kappa h^2$ one arrives at the above equation.

For the rigorous determination of the state of adhesion and the evaluation of the phase diagram of adhesion we have to consider also the global bending energy. For this purpose we consider the whole cell as a sphere of radius R the radius of which is expanded to $R+\xi$ .The change in bending energy per unit area is then

$$\delta W_{\kappa} \sim \frac{Eh^3 \xi^2}{R^4}$$

as can be easily verified. The total elastic energy can then be expressed as

$$F = 2\pi r \int_0^{\infty} ds \left\{ \kappa \left(\frac{\partial^2 \xi}{\partial s^2} \right)^2 + \Sigma_0 \left(\frac{\partial \xi}{\partial s} \right)^2 + 4K \frac{\xi^2}{R^2} \right\} \qquad (3)$$

Here κ, σ and K are the bending modulus, the membrane tension and the compression modulus (with $K \approx \kappa h^2$), ds is the line element in the radial direction d the width of the deformation stripe and r the radius of the adhesion disc. The first term accounts for the bending, the second for the stretching and the third for the global bending deformation estimated above. The shape of the contour can now be determined by solving the Euler Lagrange equation for the above energy functional. One can account for the gravitational force $F_{grav} = \Delta\rho\, gV$ ($\Delta\rho$ density difference, g gravity constant, V shell volume) by considering the boundary conditions that the F_{grav} must be balanced by the deformation of the shell (see [Guttenberg et al 2001]) . The deformations in the has the form

$$\xi = const \exp\{-s/a\} \qquad \text{and} \qquad \eta = const \exp\{-s/a\}$$

The exponential decay shows that the deformation near the contact line is indeed restricted to a narrow band.

The state of adhesion and the free adhesion energy Δg_{ad} of the adhering zones can be determined by fitting the calculated deformations ξ to the deflections measured by the RICM technique for different molar fractions x_L and x_R. A μ_L-μ_R phase diagram has been established for the model system shown in Figure 2. As can be seen good agreement is achieved by the procedure.

(a)

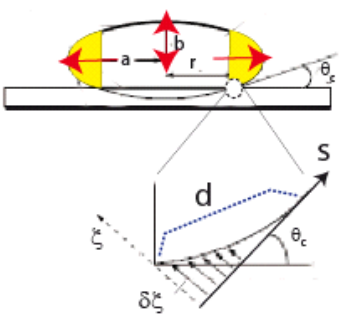

(b)

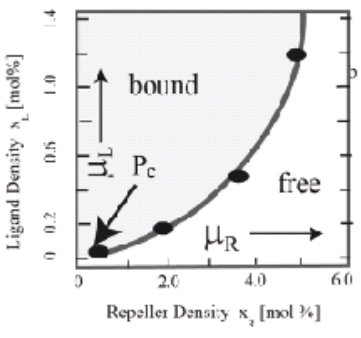

Figure A.2 *Boundary stress model based on the classical shell theory and the assumption that the adhesion-induced deformation is restricted to a narrow band of width d running around the contact line (for an enlightening justification see see [Landau and Lifshitz , Volume VII § 16, exercise 4]). The parallel arrows at the inset at the bottom indicate the strain field within the deformed band. The edges of the ellipsoid indicated by yellow color mark the regions that determine the gravitational force. Bottom: phase diagram represented in chemical potential space (μ_L-μ_R) of repeller and receptor. Dots represent measured data and the line the calculated phase boundary separating free (f) and bound (b) states. P_c marks the critical point. Image modified after [Guttenberg et al 2001]*

In summary, the boundary-stress model provides a powerful analytical albeit complicated tool to characterize the state of adhesion and to measure local adhesion energies. On the other side these data can also be obtained by considering the boundary conditions according to figure "Boundary". On the other side the good agreement between experiment and theory shows that the adhesion of soft shells can be described quantitatively by the classical theory of shells. It is a justification for the analysis of the adhesion strength in terms of the boundary conditions alone.

References:

[Guttenberg et al 2001] Z. Guttenberg, et al. Europhysics Letters (2001) 54: 826-932

[Landau/Lifshitz 1970] ID. Landau and EM. Lifshitz, Theoretical Physics Vol7, Theory of Elasticity, Pergamon Press 1970

Appendix C: Relationship between the specific adhesion free energy per CAM-CAM pair and equilibrium binding constants.

An unsolved question is how to relate the specific binding energy per CAM-CAM pair measured by the present method with unbinding forces obtained by force spectroscopy [Merkel-Evan 1999], [Weissel et al. 2003]. The unbinding forces measured by the second method depend on the rate of force application. Typical values for integrin-RGD linkages are 50 pN for force rates of 50 nN sec^{-1} which corresponds to a binding energy of the order of 10 k_BT. This value agrees quite well with that determined by the contour analysis [Gönnenwein 2003] and is about equal to the binding energy of RGD-Integrin at thermodynamic equilibrium.

Traditionally, the binding strength of linker pairs (A and B) is characterized in terms of the dissociation constants K_d of the equilibrium A+B=C. which are frequently known from chemical equilibrium studies. The specific binding energies can be estimated from dissociation constants, by application of the Van't Hoff equation

$$K_D = \frac{1}{v}\exp\left\{\frac{-\Delta G}{k_B T}\right\} \qquad \text{with} \qquad v = \frac{v_A v_B}{v_C} \qquad (1)$$

where v_i is the molar volumes of the molecules i. The molecular volumes of proteins are all of the order of $1nm^3$ which provides a simple method to estimate the binding energies. A dissociation constant $K_d \approx 10^{-6}$ M ltr^{-1} (or 10^{-9} M ltr^{-1}) would thus correspond to a binding energy of $\Delta G = k_B T \ln v K_d \approx 10\, k_B T$ (or 20 k_BT) in good agreement with the value obtained by contour analysis [Gönnenwein 2003]. Considering the fact that the adhesion strength of cells is determined by many forces, including the 2D osmotic pressure exerted by non-bound receptors and repellers or bending deformations it is obvious that single molecule measurements can only give a rough estimate of the binding strength under physiological conditions

[Weissel et al 2003] JW. Weisel, et al. Curr. Opin. Struct. Biol. 2003, **13:**227–235.

[Gönnenwein et al 2003] S. Goennenwein et al. Biophys. J. 2003, **85:** 646–655;

[Merkel et al 1999] R. Merkel et al. Nature. 1999, **397:**50–53.

Appendix D: A remark on 2D and 3D matrices

Most studies on the control of cell adhesion and locomotion are performed with cell lines adhering on solid supports,sometimes functionalize by adsorbed films of EM proteins. Cell adhesion and migration in biological or biomimetic 3D network may differ drastically from behavior on solid surfaces. Thus fibroblast on solid surfaces form large focal complexes comprising some hundred different functional proteins as shown in numerous elegant experiments by Geiger et al. (see [Geiger et al XXX]). However, it cannot be excluded that some of these proteins bind to focal complexes by nonspecific adsorption. In contrast, no large focal contacts but only small adhesion domains are formed in collagen matrices or tissue, unless the collagens form bundles [Rhee et al 2007], including FAK The stiffness of substrates can also affect the distribution of regulatory proteins. One example exemplifying the problem is the focal complex kinase FAK. which plays a key role for the survival and proliferation of cells (see . In developing tissue, FAK is not distributed at the basal side of epithelial cells, as observed in cell layers adhering on solid substates but at the apical side. Another prominent example is the growth of axons. On solid supports, the several 10 µm broad axon growth cones are formed by the growth of actin networks cross-linked by Arp2/3. In tissue or on solid supports covered by laminin one observes thin protrusion with the microtubules penetrating to the tip of the protrusions where they stimulate the formation of small veils of actin networks.

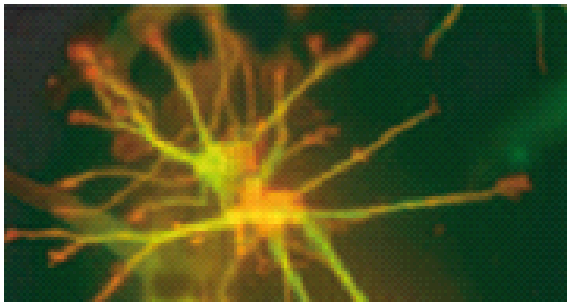

[Geiger et al] B. Geiger et al. Nat. Rev., Mol. Cell. Biol. 2001, 2: 793–805
[Rhee at al. 2007] Rhee S. et al. PNAS 2007**, 104**: 5425–5430

Appendix E: On the Tension-Induce Switching of Cell Adhesion

An important consequence of the tension-induced reduction of the dynamic membrane roughness is the tension-induced switching of cell adhesion by a first order transition of membranes from the free to the bound state. Figure D1 shows an example of such transitions (cf. [Albersdörfer 1997], Figure 812]). The area of the vesicle shell is increased by raising the temperature. This results in the formation of buds which is accompanied with an abrupt increase in membrane tension and a decrease in contact area.

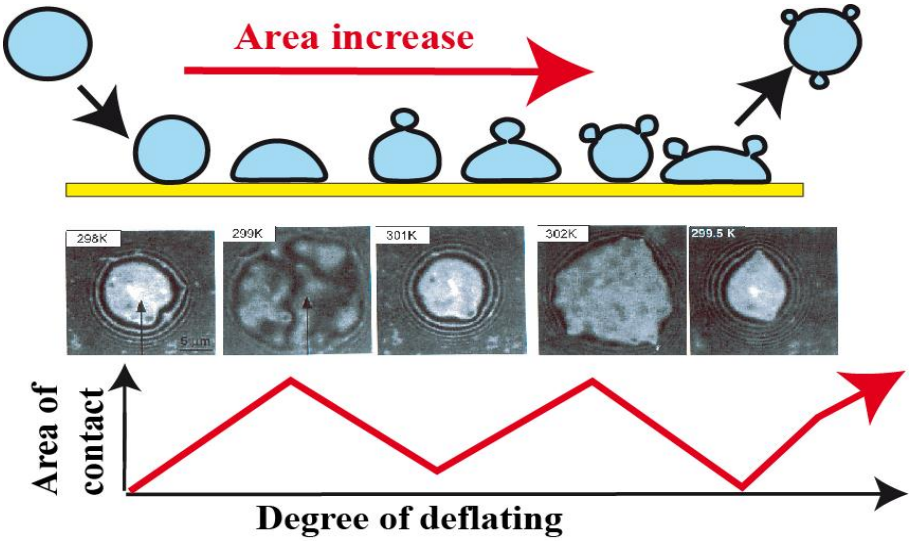

Figure D.1 *The middle row shows the change of the contact area of an vesicle (doped with lipid coupled biotin adhering on a streptavidin-coated supported membrane) caused by increasing the excess area of the vesicle by increasing the temperature from 298 K to 304 K. Note the sudden drops in contact area between 299 and 299.5 K and between 303.5 and 304 K which are attributed to the membrane tension induced by budding of small bud (diameter*

[Albersdörfer et al 1997] A. Albersdoerfer, T. Feder and E. Sackmann. Biophys. J. 1997, 73: 245-257;

Glossary to lecture note Physics of Cell Adhesion:

ADAP: (synonym for **a**dhesion and **d**egranulation-**p**romoting **a**dapter **p**rotein). The coupling of actin to MTs is frequently mediated by dynein through the linker ADAP. This enables the generation of tensile forces between the centrosome and the actin cortex resulting in the mechanical polarisation of cells. Knock-out of ADAP results in the loss of cell polarisation by centrosome.

Calpains: Cytosolic residing proteases, activated by a rise in intracellular Ca^{2+} level through cell activation, triggering cell differentiation, proliferation and death. Calpains work on many membrane bound proteins, including membrane-bound receptor-tyrosine kinases (RTK) and cell adhesion molecules. Calpains proteolyse many signaling-related substrates, such as protein kinase C (PKC), the G□ of heterogeneous G□□□ GTPases, protein tyrosine phosphatases and talin. The decomposition of talin plays an essential role for the uncoupling of adhesion domains at the trailing end of migrating cells

CAS: a highly phosphorylated 130 kDa scaffolding protein that associates with v-Src. It can rapidly change the state of phosphorylation. Cas plays a critical role for cell adhesion, migration, proliferation and survival of normal cycling cells.

CD43: plays a key role as repellent CAM in hematopoietic cells (T-cells) (together with CD 45 and Cd44). Owing to the attachment of charged oligosaccharide to the extracellular protein sequence is stretched and extends about 45 nm into the extracellular space. Depending on the situation CD 43 can act as inhibitor or activator of adhesion. It prevents the tight binding of lymphocytes to endothelial cells (ENC) but it mediates weak linkages to cells exposing E-selectins such a blood vessels or L.selection such as lymph vessels (see also CD44). Most importantly,its cytoplasmic tail is essential for the transport of CD 43 to the uropod during cell polarisation (Walker and Green J. Immunol. (1999) 162: 4109. CD 43 and CD45 occupy about 30% of the surface of lymphocytes.

CD44 cell-surface glycoprotein (or antigen) and hyaluronic acid binding domain: This multi purpose glycoprotein is involved in cell–cell interactions, cell adhesion and migration**.** It exhibits a lectin-like domain at the N-terminus (residues 21-178) which recognizes hyaluronic acid, but it also binds to osteopontin, collagens, and matrix metallo proteinases.

The CD44 function is controlled by posttranslational modifications. An important modification is the sialofucosylations (attachment of sialic acid residues via fucose). This CAM is called HCELL-receptor. It is a major cell surface receptor for hyaluronan (HA).

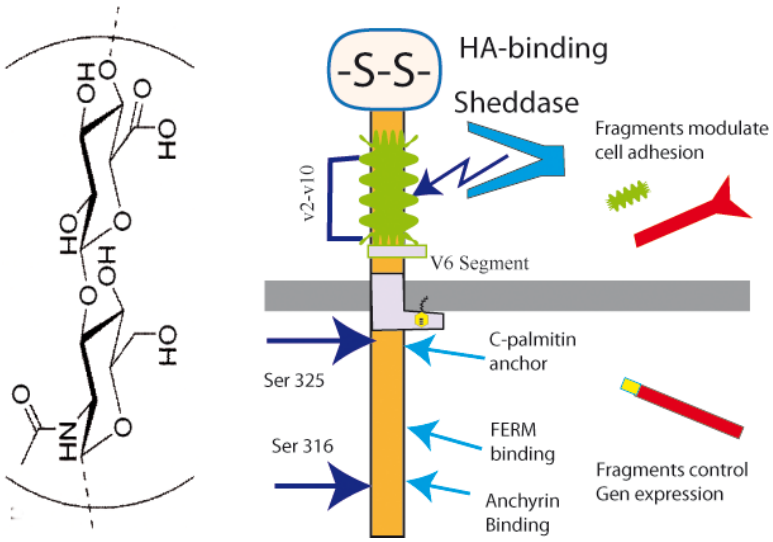

Domains structure of CD 44
Left: Molecular structure of disaccharide forming HA-polymers. The contour length is about 1nm.
Right: Domain structure of CD44 receptor. The extracellular domain comprises the HA binding head group (stabilized by S-S-bonds) and the variable domain v2-v10 indicated by the green corrugated mantle. The segment v6 mediates the formation of CD44/RTK complexes. The cytoplasmic domain exposes a PIP2 binding domain which is assumed to stabilize the membrane binding by electro-hydrophobic forces and a binding pocket for FERM domains FERM. The extracellular domains are cleaved by metal proteases (sheddases) and the fragments control the cell adhesion (see Chapter VI.2). The intracellular segment can be cleaved by specific proteases and control the expression of various proteins including CD44 itself.

CLIP 170: This family acts as MT-capturing protein. It plays a key role as nucleator of microtubules by linking the plus end to the F-actin via the scaffolding protein IQGAP. After phosphorylation it can bind to dynein/dynactin complexes which is important for spindle association.

Chondroitin sulfat proteoglycans (CSPGs): Proteoglycans composed of core protein filament exposing chondroitin sulfate side chain. They are involved in the adhesion, growth and migration of cells. CSPGs interact with laminin, fibronectin, tenascin, and collagen.

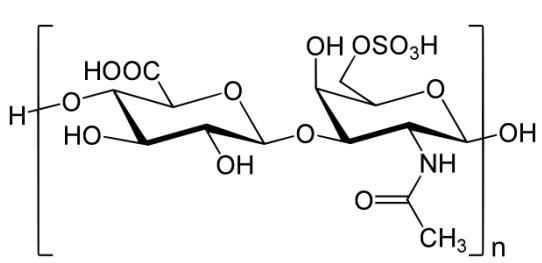

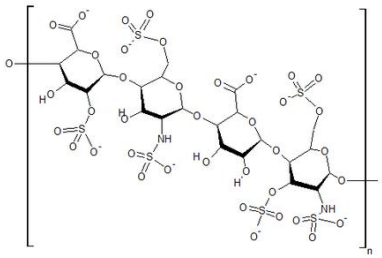

Chondroitin sulfate Heparan sulfate

Effector (Activator). In cell biology effectors are functional proteins which act as transducer between cell signals and cell functions. In the terminology of control systems robotics it would be called activator.Their activation is often triggered by binding to scaffolding proteins which are excited by phosphorylation of tyrosine groups or by direct binding to membranes through the electro-hydrophobic effect. Examples are phopholipase-C, protein kinase C, Guanine exchange factors (GEF). See Sackmann Lecture Notes www.biophy.de/ Hydrophobic-electrostatic membrane coupling of proteins.

FAK (Focal adhesion kinase) is an "integrin-responsive tyrosine kinase". It exhibits a FERM homology domain, a binding site for Src kinase (near tyrosine 397), for CAS (a scaffolding protein) and one for paxilin (mediating the coupling to focal adhesion complexes). Moreover, FAK is also a scaffolding protein. FAK can reside in the cytoplasm in a sleeping conformation which is stabilized by complex formation between the C- and N-terminus. It is activated by binding of activators to its FERM domain. Activated FAK exhibits the capacity of auto-phosphorylate. It then binds Src kinase which in turn phosphorylates other sites on FAK and the FAK-binding proteins, such as CAS and paxillin. Some important functions of FAK are: (i) Regulation of cell proliferation and survival through activation of PI3K/PKB (Akt) and Grb2/SOS/Ras/Raf-1/MEK/ERK pathways (see Chapter VII.1 Figure 10c). (ii) Control of cells motility and adhesion turnover through regulation of the Rho GTPases, especially RhoA, Rac-1 and Cdc42. One important function is the down-regulation of stress fiber formation mediated by RhoA. This occurs by activating RhoA-GAP, which de-activates Rho * by GTP hydrolysis. Reference: Frame, MC. et al. (2010) The FERM domain: organizing the structure and function of FAK. Nat Rev Mol Cell Biol. 11: 802-14.

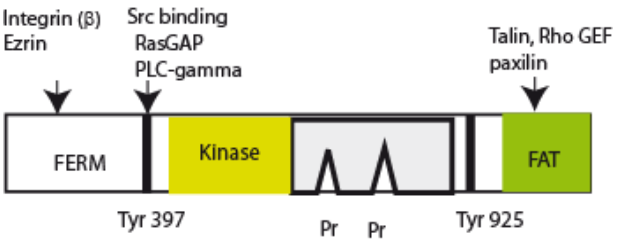

Domain structure of FAK an integrin-responsive tyrosine kinase.

Filiopodia and Fascin: Filopodia are semi-ordered bundles with one bound fascin per 25-60 actin monomers, corresponding to a distance of 30-60 nm Phosphoryleted fascin (at Serin 39) is inactive. Phosphorylation of fascin by protein kinase C in vitro reduced its actin-binding constant from $3.5 \times 10^6\ M^{-1}$ to $<0.5 \times 10^5\ M^{-1}$, Dephosphorylated fascin mediates actin bundling in filopodia. FRAP revealed that fascin dissociates from filopodial filaments with an off-rate of $0.12\ s^{-1}$ and that it undergoes diffusion at moderate rates with a coefficient of 6 $\mu m^2\ s^{-1}$. Reference: Vignjevic, D. J Cell Biol.**174**, 2006 863–875. (see Sackmann: Exploring the environment by filopodia).

Grb2 stands for growth factor receptor-bound protein. It is a scaffolding protein involved in signal transduction and cell communication. Inhibition of Grb2 abolishes the proliferation of many cell types. The protein couples to receptors of RTK family, such as the epidermal growth factor receptor. It contains one SH2 domain and two SH3 domains. Its two SH3 domains form complexes with proline-rich regions of other proteins. Its SH2 domain binds tyrosine phosphorylated sequences. An example: Grb2 links the epidermal growth factor receptor to the activation of Ras which triggers cell proliferation via the ERK/MSAPK pathway

Growth factors: small peptides (~5nm) that trigger the cell proliferation and differentiation after binding to specific growth factor receptors (GFR). Growth factors include both cytokines and hormones (insulin). Examples are epidermal growth factor (EGF) and hepatocyte growth factor (HGF). HGF regulates cell growth, cell motility, and morphogenesis by activating a tyrosine kinase signalling cascade after binding to the c-Met receptor. HGF is secreted by mesenchymal cells and stimulates mainly endothelial and epithelial cells. It consists of a dimer (a and b chains), but becomes only active after protease induced cleavage into a 69-kDa and 34-kDa chain. This results in the formation of a a,b-dimer connected by a disulfide bond. The GF dimer connects two GFR monomers which enables the mutual phosphorylation of the cytoplasmic chains of the GFR (see Alberts et al, 1996, chapter 15). In connection with adhesion, most important is the clustering of the GFR by adhesion induced domain formation. An example is the activation of the GFR of membrane bound ephrins (see Chapter VII.5 of this review and [Alberts 1996] chapter 15)

Hyaluronic acid (HA): A linear polysaccharide made up of sugar dimers shown below. HA often acts as buffer between cells. HA filaments can reach lengths of a few µm (10^4 kDa) and form Random coils with radii $R_F \approx 500$ nm. It binds mainly to standard CD44s.

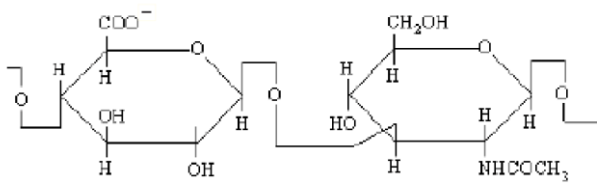

ICAM-1 is a member of the immunoglobulin superfamily. ICAM-1 is a transmembrane protein possessing an amino-terminus extracellular domain, a single transmembrane domain, and a carboxy-terminus cytoplasmic domain. IgIt recognizes specifically the integrin LFA-1.The structure of ICAM-1 is characterized by heavy glycosylation. The protein's extracellular domain is composed of multiple loops (up to 9) stabilized by disulfide bridges. Note that a small population of ICAMs is constantly exposed by many cells. However, the density is greatly increase by cytokine stimulation of macrophages acting as APC (such as by interleukin-1). The extracellular head group of ICAM is composed of 453 amino acid forming five immunoglobuline-like domains (of about 290 nm length).

The cytoplasmic tail of some ICAMs, such as ICAM-2, exhibit a FERM binding domain

IQGAP-1 (cooperation with CLIP170 and cell polarization and GTPase activation): The multifunctional scaffolding protein IQ-GAP exhibits several binding sites for different activators (effector).Two activators involved in cell polarization are Cdc42 and Rac. They are transiently coupled to MT plus ends by binding in their activated state to CLP170/IQGAP complexes [Gundersen 2002]. The function is described in Chapter VII.4. Most importantly, Clip 170 links the MT plus end to the actin cortex thus generating traction forces in the MT. Moreover, it prevents the deactivation of the GTP-GTPases by guanine activation proteins (GAP) thus maintaining the GTPases Cdc42 and Ras in the activated state for some time. Most important is the capacity of IQGAP to bind beta-Catenin to E-cadherin.
[Gundersen 2002] GG. Gundersen Current Biology, 2002, 12, R645–R647,

Integrins (and their activation): The major CAMs mediating cell tissue interaction. They simultaneously play a key role for the signal transduction from the EM to the cytoplasm. It is generally mediated by coupling of the cytoplasmic beta1 chain to numerous effector proteins, such as FAK, the src family kinases, Rho-GTPases and PI3-K.

The Integrin-affinity is controlled by several Ras-GTPases: H-Ras, K-Ras and N-Ras suppress high integrin affinity (see [Hughes et al 1997]), whereas R-Ras generally activates integrin affinity (Zhang et al 1996). Most importantly, R-Ras can also down-regulate adhesion strength through decomposition of talin by the protease calpain. R-Ras activates the effector Fam 38A (located in ER-membranes) which stimulates the calcium release form the ER.vesicles.
In connection with adhesion, two aspects are important: (1).The activation of all Ras occurs by membrane binding which is mediated by electro-hydrophobic interaction (see Supplements Chapter 9 www. biophy.de). For that purpose some of the Ras are modified post-translationally by coupling of different lipid chains to the C-end. In particular, H-Ras and R-Ras are modified by coupling of farnesyl and geranylgeranyl groups, recspectively (see "GTPases")
[Zhang et al 1996] Z. Zhang Integrin Activation by R-ras Cell, 1996, **85**, 61–69.
[Mc Hugh et al.2009] B. McHugh et al. J Cell Sci. 2009, **123**, 51-60
[Svensson et al 2010] L. Svensson et al. PLoS ONE 2010, **5,** e15090

LFA-1 (Lymphocyte function-associated antigen) LFA-1 is a distinct integrin with beta2 and alpha-L chains. It is activated in leucocytes after stimulation by cytokines as described in chapter VII.3. LFA-1 integrins recognize the CAM ICAM-1.
timulation of macrophages acting as APC (such as by interleukin-1).

LAT (Linker for activation of T-cells). LAT (a 36 kDa integral protein) is a membrane bound scaffolding protein which can recruit several actuators which are involved in the control of genetic transcription. LAT is also linked to membranes by palmitoyl lipid anchors and exhibits several tyrosin-residues. Phosphorylation of these groups by the ZAP-kinase results in the attraction of the actuators. Of primary importance is the recruitment of the phospholipase PCL-Cg mediating the liberation of Ca from storage vesicles. Ca triggers the opening of the Ca- mediated pathway of genetic transcription (see E. Sackmann www.biophy.de / Biophysics of the immune response.

MHC: The major histocompatibility complexes (MHC) classes I and II are glycoproteins that present antigens (small oligopeptides of ~ 10 monomers) to T lymphocytes. They are integral membrane proteins composed of heterodimers. The antigens may consist of fractions of proteins of the organism itself (self- peptides), or may stem from foreign sources ("nonself"-peptides), originating from bacteria or viruses. Properly functioning immune systems ignore self-peptides while foreign peptides stimulate the T-cells,

LAT (Linker for activation of T-cells). LAT (a 36 kDa integral protein) is a membrane bound scaffolding protein which can recruit several actuators which are involved in the control of genetic transcription. LAT is also linked to membranes by palmitoyl lipid anchors and exhibits several tyrosin-residues. Phosphorylation of these groups by the ZAP-kinase results in the attraction of the actuators. Of primary importance is the recruitment of the phospholipase PCL-Cg mediating the liberation of Ca from storage vesicles. Ca triggers the opening of the Ca- mediated pathway of genetic transcription (see E. Sackmann www.biophy.de / Biophysics of the immune response.

Lck-activation: The kinase Lck is a member of the so called Src family of non-receptor tyrosine kinases which is anchored in the plama membrane by fatty acid anchors . When the T cell receptor is engaged by the APC, Lck acts to phosphorylate the ζ-chains of the CD3 complex. This allows another cytoplasmic tyrosine kinase called ZAP-70 to bind to them. The activated ZAP in turn phosphorylates another molecule in the signalling cascade called LAT (short for Linker of Activated T cells), a trans-membrane protein that serves as a docking site for a number of other proteins, such as , PI-3K, and phospholipase Cγ. Note that Lck is anchored in the membrane via palmitoyl chains and diffuses in cells with $D \approx 0.26\ \mu m^2 s^{-1}$.

MHC: The major histocompatibility complexes (MHC) classes I and II are glycoproteins that present antigens (small oligopeptides of ~ 10 monomers) to T lymphocytes. They are integral membrane proteins composed of heterodimers. The antigens may consist of fractions of proteins of the organism itself (self- peptides), or may stem from foreign sources ("nonself"-peptides), originating from bacteria or viruses. Properly functioning immune systems ignore self-peptides while foreign peptides stimulate the T-cells,

Merlin: A member of the FERM-carrying proteins. Encoded by neuro-fibromatosis-2 (NF2) gene, such as ezrin, radixin, moesin. An essential role is growth inhibition (see Chapter IX.4 Figure 23). Cells lacking functional merlin hyperproliferate [Morrison2001]. Therefore Merlin plays a critical role for cell division by controlling contact inhibition. Morrison, H. (2001) Genes and Development,2001, 15:968–980

Microtubule plus end binding proteins (MBP): This class of proteins binding to the plus end of MT include: EB1, dynactin, APC, and CLIP-170.

Microtubule-actin cross talk. There are several candidates mediating the coupling of the MT to actin. For the present review on cell adhesion we have to consider two mechanisms:

1) Coupling via end binding proteins (EB1) with the help of the actin growth pomotor formin (and Dial 1). In many undifferentiated cells the microtubules are highly flexible and are not bound to the actin cortex. However, crosslinking between MT and the actin network comes into play if cells adhere to surfaces or migrate in the tissue. Then a fraction of the MT is fixed with their plus end at the leading edge. The tubulin of these stable MT is modified (post-translationally). In the resting state of the cells these proteins exist in a sleeping conformation and have to be activated. This is mediated by the GTPase Rho which acts through the GDP→GTP exchange protein ROCK. Although EP 1 is called end-binding-protein, it mediates the MT binding over large lengths as well as the formation of MT bundles which can mutually slide over each other. For references see A. Reilein A and W. Nelson W. 2005. Nature Cell Biol. **7:** 463 – 473); Rodriguez OC. et al. 2003. Nature Cell Biol**. 5:** 599-609.

2) Coupling via Dynactin:. The rod-like supramolecular complex (of~ 1.1-MDa) is about 37 nm long and 10 nm thick. Its major constituents are (i) the actin-like filament arp 1, (ii) capping proteins determining the length of the rod (iii) a constituent mediating the binding of the motor protein dynein. (iv) vareous regulatory proteins. The thickness of the complex (together with the dynein motor) is about 50 nm (After Hodgkinson J L.2005. Proc. Natl. Acad. Sci USA 102: 3667-3672). For direct visualisation of MT-actin Crosstalk see Heinrich Acta Biomat

PLC-gamma splits phosphatidylinositol-(4, 5)-bisphosphat (PIP2) into diacylglycerol (DAG) und inositol-1,4,5-triphosphate (IP3). DAG activates the signal cascade mediated by protein-kinase C (PKC). IP3, librates Ca-ions from the ER and thus triggers the activation of the transcription factor NFAT by calcineurin mediated dephosphorylation.

Phorbolesters: have important biological properties. The most notorious is the capacity to act as tumor promoters through activation of protein kinase C". This is due to the fact that phorbol esters can mimick the function of Diacylglycerols (DAG) as membrane anchors for proteins such as Protein Kinase C which is activated by recruitment to the membrane mediated by specific binding to DAG anchors.

Phosphatases/Kinases: Phophatases are enzymes that remove phosphate groups. Together with conjugate kinases they control the activity of proteins by phosphorylation-dephosphorylation. Major examples and important properties:

1. Slingshot phosphatase forms a tandem with LIM kinase which regulates actin polymerisation dynamics. LIM-kinase de-activates the F-actin depolymerisation factor cofilin (and thus impedes actin growth) by phosphorylation while slingshot restores the activity.
2. The phophatase PTEN forms a tandem with PI-3Kinase (PI-3K). It removes phosphate groups from phophoinositols, thus reducing the number of phosphate groups by one. An important example is the control of the locomotion of Dictyostelia cells or the engulfment of bacteria by these cells. (see E. Sackmann New Journal of Physics 13 (2011) 065013)
CD148: The tyrosine phosphatases is a single chain membrane protein exposing a very large extracellular domain. It thus acts simultaneously as repellent CAM. It is involved in cell growth and mitosis of T-cells. It is expressed at low levels in resting cells but is up-regulated during immune reactions.
CD45: This tyrosine kinase is also characterized by a very large extracellular domain. It plays a key role for the control of the stimulation of naïve T-cells by immunological synapses (see E. Sackmann www.biophy.de/ Biophysics of immune reactions).

Note: The glycosyl groups of the extracellular domain of CD45 and CD148 are constantly changed during the life of T-cells and with aging [see Earl 2008]. For a summary see phosphorylation and dephosphorylation in http/bioweb.wku.edu/courses/biol566 /117phosphorylationdephoisphaorylation. [Earl 2008] LA. Earl CD45 glycosylation controls T-cell life and death. Immunol Cell Biol. 2008, 86: 608-15.

Proteoglycanes: A subset of glycoproteins which are secreted by cells into the EM or act as repellant cell adhesion molecules (CD43, CD 44, PSLG-1). The covalently attached poly- or oligo-saccharides are called glcosaminoglycanes (GAG).

Ras super-family of GTPases (Ras Rho/Rac Rab Rap Raf Arf): Biochemical switches that can switch between an inactive state (with GDP bound) and an active state (with GTP bound). The switches are generally activated by membrane binding through electro-hydrophobic forces. Lipid anchors are attached post-translationally by attachment of highly unsaturated fatty accid chains (called prenylation). Some species, H-Ras, N-Ras, and K-Ras are farnesylated and others, such as RhoA, Rap1, and R-Ras are geranylgeranylated

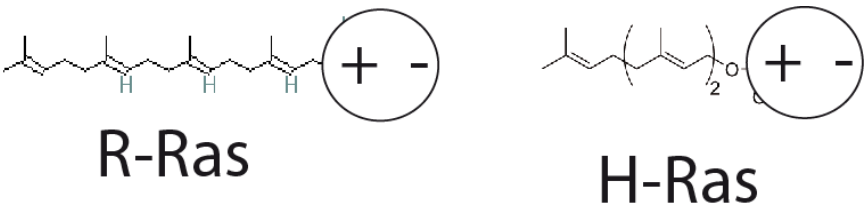

The GTPases exhibit lipid anchors mediating their membrane coupling. But they reside in the cytoplasm in sleeping conformations, which is often stabilize by binding of a specific protein: „guanine nucleotide dissociation inhibitors“(GDI). The GTPase is activated by exchange of GTP for GDP: a process mediated by a GDP→GTP exchange factor (GEF) shown in the Figure below. The lipid chain of the GTPase is now exposed. It can bind to the membrane and interact with actuators of the cytoskeleton

A second important regulation mechanism is the following. The intrinsic GTPase activity of the switches is rather weak resulting in a long lifetime of the activated switch. In order to accelerate this low rate of hydrolysis (which is about 0.01/min), and to switch-off the GTPase rapidly, another regulatory proteins has to come into play, namely the "GTPase activating proteins "(GAP). They stimulate the Rho-GTPases to hydrolyse the GTP resulting in a rapid de-activation of the molecular switch. GEF and GAP thus control their net activity.

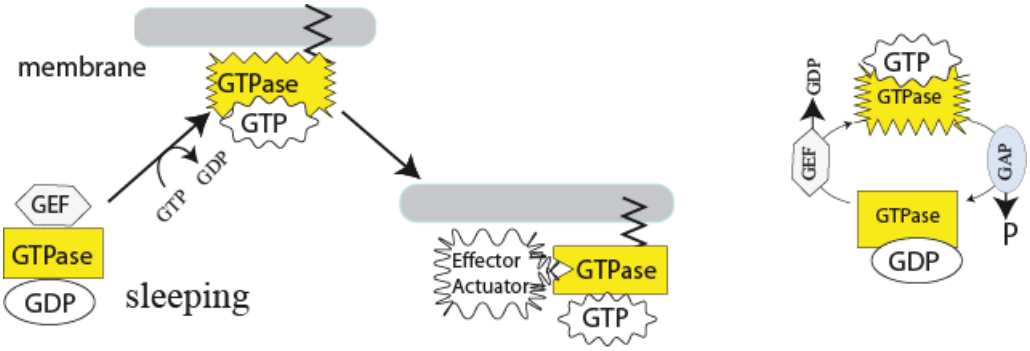

Activation of the effectors (actuators) by molecular switches of the Ras super-family.The super-family comprises over 100 members, including Ras, Rho, Rap Raf Arf. Left: activation and membrane binding of a GTPase by exchange of GTP for GDP. After membrane binding the switch controls the activity of a specific actuator. Right: control of the activity of the molecular switches by the tandem GEF↔GAP (described in the text).

Rho-associated protein kinase (ROCK): A (158 kDa) serine-threonine kinase. It is mainly involved in the regulation of cell shape by reorganization of the cytoskeleton. ROCK resides in the cytoplasm in a sleeping conformation and is activated by binding of activated GTP-Rho. One essential function of ROCK is to induce the formation of stress fibers coupled to focal adhesions, which occurs by phosphorylating myosin light chain (MLC).

Rho-associated protein kinase (ROCK): A (158 kDa) serine-threonine kinase. It is mainly involved in the regulation of cell shape by reorganization of the cytoskeleton. ROCK resides in the cytoplasm in a sleeping conformation and is activated by binding of activated GTP-Rho. One essential function of ROCK is to induce the formation of stress fibers coupled to focal adhesions, which occurs by phosphorylating myosin light chain (MLC).

Syndecans 1-4: universal and specific features. The 30 amino acid long membrane-spanning domain is conserved during evolution. The cytoplasmic domains are composed of a conserved segment which exhibits a FERM binding pocket and a variable domain which can

bind various effector proteins involved in cell signalling. The intracellular C-terminal contains an AA sequence EFYA. It binds proteins exposing PDZ-homology domains, including the post-synaptic density 95 protein (abundant in presynaptic ends) and the calcium/calmodulin-dependent serine protein kinase (CASK). The extracellular domains of the syndecans are highly divergent: They differ in the number and distribution of CS and HS side chains. Syndecan-1 and -3 expose both types of sulfonated oligosugars (CS and HS) while syndecan-2 and syndecan- 4 exhibit only HS side chains. . Since all members of the syndecan family expose FERM domains they can mediate the transduction of external cues (mechanical forces or growth factor binding) into cell signals or reorganization of the intracellular actin scaffold.

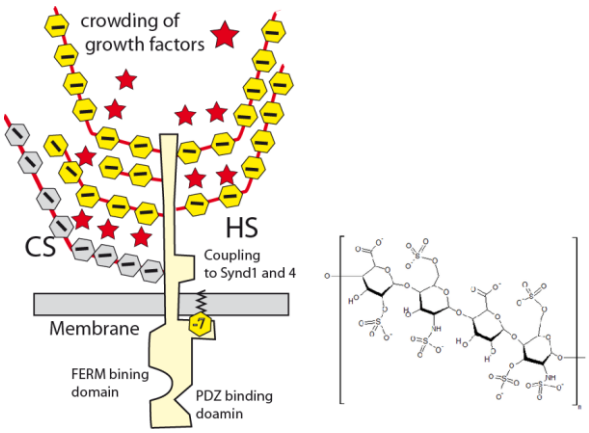

Figure "syndecan I": The outer domain (the N-terminal) exposes negatively charged oligosaccharides composed of heparin sulfate and chondroitin sulfate. They may comprise 10 to 50 di-saccharides, each with a length of about 1nm. Segments of the core protein can mediate the syndecan self-assembly. The image at the bottom right shows the structure of the heparan sulfate which binds to many extracellular matrix molecules. The sugar dimers CS and HS can weakly bind growth factors (GF, red stars) and can thus accumulate these signal molecules at the cell surface.

Specific features of the syndecans:

Syndecan-1 (synd-1) is an important regulator of cell-cell and cell-EM interactions. The extracellular domain is 210 AA long and exhibits 3 heparan sulfate groups near the N terminal (at AA 37,45, 47) and 2 chondroitin sulfate attachment (AA 210, 220). It tends to interact with $\alpha x \beta 3$ integrins and it is accumulated on the basal side of epithelial cells. Down regulation of its expression in epithelial cells results in loss of basal-apical cell polarity associated with a reduced level of E-cadherin on the cell surface. This points to the involvement of synd-1 in the epithel-mesenchyme switching during wound healing.
Syndecan-2 is the predominant syndecan expressed during embryonic development and wound healing. Its extracellular domain is relatively short (comprising 145 AAs) It cooperates often with beta1-integrins and promotes actin stress fibre formation [Kusano 2000]. However, this is attributed to an indirect mechanism through the binding of the heparan sulfat groups to the COOH-end of fibronectin (see Figure above). This can lead to the formation of fibronectin fibrilles in the EM, The consequence is a dramatic increase in integrin binding sites and a dramatic enhancement of integrin clustering, [Woods 2000}.
Syndecan 3: plays an important role in regulation of skeletal muscle differentiation and development. This syndecan binds poorly to EM components. It is assumed to be mainly involved in modulating the effect of growth factors. It plays, however, an important role for

the extension of axons.A specific feature is that it binds to integrins with beta3 and beta 5 chains but not to $\alpha x \beta 1$ pairs.

Syndecan 4: shares some common properties with syndecan-2, such as the relatively short extracellular domain and the cooperative interaction with beta1 integrins. It regulates cell adhesion and migration together with these integrins in a positive way. The variable cytoplasmic segment can bind protein kinase C and PIP2 lipids.

Src-kinases: a family of non-receptor tyrosine kinases including nine members, such as: Lck, Src, Fyn. Src family kinases interact with many cellular cytosolic, nuclear and membrane proteins, modifying these proteins by phosphorylation of tyrosine residues. Src was the first kinase member discovered.

Talin (FERM-proteins): Talin is a major constituent of the composite cell envelopes of most mammalian cells or amoebae. It mediates the direct coupling of actin to the intracellular domains of glycoproteins (via its head group exhibiting a FERM domain) and to other major cell adhesion molecules such as integrins (via its tail domain). The FERM domain is the same as that found in many other actin membrane couplers, such as the red blood cell 4.1 protein, ezrin, radixin and moesin. As all FERM proteinms talin can exist in an inactive and an active state. In the former the binding site for the membrane protein is shielded. Similar to the situation for band IV.1, (shown in Fig 1), the FERM domain becomes activated by phosphorylation.

Talin plays also a key role for the control of cell adhesion mediated by integrins. It stimulates or stabilizes its activated state by binding with its FERM domain to the intracellular domain of the beta-chains (see Figure 7 for a model). The binding affinity of talin is increased by binding of PIP2 and PIP3 to talin (see [Moore et al 2010]). The binding constant of talin to lipid membranes containing 10% PIP2 and 10 % phosphatidylserin is about 0.55µM and 0.9 µM.

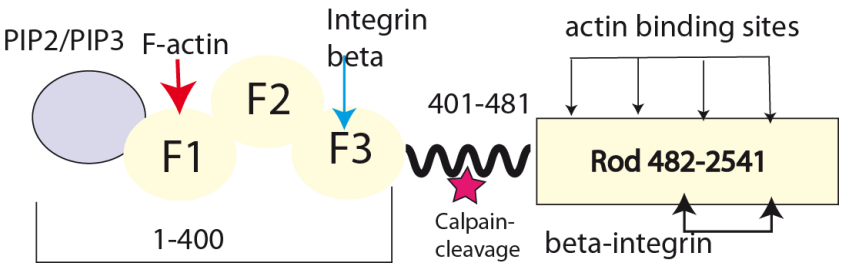

(I)

(I) Domain structure of talin. To retract adhesion domains Talin is decomposed by the protease calpain which is activated by intracellular Ca-bursts.

[Moore et al 2010] DT Moore et al. Affinity of talin-1 for the β3-integrin cytosolic domain is modulated by its phospholipid bilayer environment. PNAS 2011 early edition.
[Gritchley] Critchley D and Gingras A. 2008. J. Cell Sci.121: 1345-1347). a comprehensive review of the role of talin.

Tumor necrosis factor (TNF), This cytokine is mainly produced by activated macrophages. Its primary role is the regulation (stimulation) of immune cells and to induce apoptotic cell death.

Selectins (E,L,P) are vascular CAMs expressed which bind ligands exposing sialic acid carrying groups (such as Lewis X) and fucosylated glycanes, (such as CD44) is involved in the slow leukocyte rolling of WBC on endothelial cells lining the inner wall of blood vessels:

E-selectin is expressed only on inflamed endothelium (That is after the action of cytokines) and cooperates with P-selectin. The outer chain is composed of five consensus repeat domains. In non-activated endothelial cells, it is stored in granules. The extracellular chain exposes nine consensus domains and is about 40 nm long. Minutes after Inflammation or stimulation by histamine, thrombin, or phorbol esters, P-selectin appears at the cell surface by secretion, but only for ~10 min Afterwards it is slowly expressed by cytokines (interleukin-1 (IL-1)) or tumor necrosis factor a (TNF-a)). It binds first to the ligand PSGL-1) which is always present on all WBC. The transient interactions between P-selectin and PSGL-1 mediates cell rolling along the venular; together with E-selectin.

P-selectin functions as a cell adhesion molecule (CAM) on the surfaces of activated endothelial cells. It appears first at the cell surface by secretion, but but after 10 minutes it is slowly expressed by cytokines (interleukin-1 (IL-1)) or tumor necrosis factor a (TNF-a)).

L-selectin: belongs to the selectin family of proteins, which recognize sialylated carbohydrate groups. It acts as"homing receptor" for lymphocytes to enter secondary lymphoid tissues via high endothelial venules. It is cleaved by ADAM.

SELL, is a cell surface component acting as adhesion/homing which mediates lymphocyte-endothelial cell interactions and serves the homing of lymphocytes. The molecule is composed of multiple domains: one homologous to lectins, one to epidermal growth factor, and two to the consensus repeat units found in selesctins

Sialyl LewisX, also known as sialyl LeX and SLeX, is a tetra-saccharide carbohydrate that is usually attached to cell surface glycoproteins (CD43) and glycolipids. An important feature is the attachment of a sialic acid group. Sialic acids are a class of sugars with COO- acid groups and differ by additional side groups. It is known to play a vital role in cell-to-cell recognition processes. It is also one of the most important blood group antigens and is displayed on the terminus of glycolipids that are present on the cell surface. Major receptors are selectins. The sialic acids are typically found at the outermost ends of many N-glycans, O-glycans, and glycosphingolipids (as in the case of Lewis X-factor shown below.

TGF-beta growth factor: secreted by macrophages and many other cells, The GF is released after inflammational stimuli of cells. The activated receptor triggers the genetic pathway mediated by the transcription factor SMAD. TGF-β plays a crucial role in the regulation of the cell cycle. It induces the synthesis of p15 and p21 proteins, which block the advance through the G1 phase of the cell cycle. TGF-β suppresses expression of c-myc, a gene which is involved in G1 cell cycle progression.

Uropod pseudopod: Terms to characterize the polarisation of cells during cell locomotion, such as of leucocytes and killer cells. The cells assume an elongated shape with the leading edge (or pseudopod) and the trailing end. The polarized state is mechanically stabilized by crosstalk between the actin and microtubule scaffolds. (see Also integrin activation) S. Fais and W. MalorniLeukocyte uropod formation and membrane/cytoskeleton linkage in immune interactionsJournal of Leukocyte Biology *vol. 73 no. 5 556-563*

VCAM-1 (Vascular cell adhesion molecule-1) is a integrin receptor located on endothelial cells. It binds to the integrin VLA-4 (a4b1) normally expressed on leukocyte plasma membranes. They only adhere to their appropriate ligands when leukocytes are activated (such as by chemotactic agents or cytokines) and the integrins undergo a transition from the low to the high affinity state. They then bind strongly to cell adhesion molecules I-CAM-1 and V-CAM,